MHD Flows in Compact Astrophysical Objects

Accretion, Winds and Jets

Bearbeitet von
V.S. Beskin

1. Auflage 2012. Taschenbuch. xviii, 425 S. Paperback
ISBN 978 3 642 26177 0
Format (B x L): 15,5 x 23,5 cm
Gewicht: 682 g

Chapter 2
Force-Free Approximation—The Magnetosphere of Radio Pulsars

Abstract The general view of the radio pulsar activity seems to have been established over many years. On the other hand, some fundamental problems are still to be solved. It is, first of all, the problem of the physical nature of the coherent radio emission of pulsars. In particular, as in the 1970s, there is no common view of the problem of the coherent radio emission mechanism of a maser or an antenna type. Moreover, there is no common view of the pulsar magnetosphere structure. The point is that the initial hypothesis for the magnetodipole energy loss mechanism is, undoubtedly, unrealistic. Therefore, the problem of the slowing-down mechanism can be solved only if the magnetosphere structure of neutron stars is established. However, a consistent theory of radio pulsar magnetospheres has not yet been developed. Thus, the structure of longitudinal currents circulating in the magnetosphere has not been specified and, hence, the problems of neutron star braking, particle acceleration, and energy transport beyond the light cylinder have not been solved either. The theory of the inner structure of neutron stars is also far from completion. Naturally, it is impossible to dwell on all these problems here and, therefore, we discuss in detail only the problems directly associated with the main theme of this book, viz., the theory of radio pulsar magnetospheres. The first two sections consider the basic physical processes in neutron star magnetospheres and the secondary plasma generation mechanism. Then we formulate a pulsar equation, i.e., the force-free Grad–Shafranov equation in flat space providing the correct determination of the energy losses of radio pulsars. Further, the exact analytical solutions obtained for radio pulsar magnetospheres are also discussed in detail. It is demonstrated that, within the force-free approximation, a self-consistent theory cannot be formulated. Finally, the current pulsar magnetosphere models are analyzed.

2.1 Astrophysical Introduction

It would be no exaggeration to say that the discovery of radio pulsars at the end of the 1960s—sources of cosmic pulse radio emission with characteristic period $P \sim 1$ s (Hewish et al., 1968)—can be called one of the most important events in astrophysics in the 20th century. Indeed, the new class of space sources connected with neutron stars was first discovered, the existence of which was even predicted

V.S. Beskin, *MHD Flows in Compact Astrophysical Objects,* Astronomy and Astrophysics Library, DOI 10.1007/978-3-642-01290-7_3,

in the 1930s (Baade and Zwicky, 1934; Landau, 1932). Most of the other compact objects discovered later [X-ray pulsars, X-ray novae (Giacconi et al., 1971)] showed that neutron stars, even if they are not the richest ones, are really one of the most active populations in Galaxy. It is not surprising, therefore, that A. Hewish was awarded the Noble Prize for this discovery in 1974.

Neutron stars (mass M of the order of solar mass $M_\odot = 2 \times 10^{33}$ g with the radius R of only 10–15 km) are to evolve from the catastrophic compression (collapse) of ordinary massive stars at the later stage of their evolution or, for example, from white dwarves that exceeded, due to the accretion, the Chandrasekhar limit of mass $1.4\,M_\odot$. The simplest interpretation of both the small rotation periods P (the smallest known period $P = 1.39$ ms) and the superstrong magnetic fields $B_0 \sim 10^{12}$ G is based on exactly this generation mechanism (Kardashev, 1964; Pacini, 1967). Indeed, if the neutron star is supposed to evolve from a normal star (radius $R_\mathrm{s} \sim 10^{11}$ cm, the rotation period $P_\mathrm{s} \sim$ 10–100 years) with the magnetic field $B_\mathrm{s} \sim 1$ G, from the laws of angular momentum and magnetic flux conservation

$$M R_\mathrm{s}^2 \Omega_\mathrm{s} = M R^2 \Omega, \tag{2.1}$$

$$R_\mathrm{s}^2 B_\mathrm{s} = R^2 B_0, \tag{2.2}$$

it follows that, when compressed to the sizes R, the rotation period P and the magnetic field B_0 of the neutron star are of order

$$P \sim \left(\frac{R}{R_\mathrm{s}}\right)^2 P_\mathrm{s} \sim (0.01 - 1)\,\mathrm{s} \tag{2.3}$$

and

$$B_0 \sim \left(\frac{R_\mathrm{s}}{R}\right)^2 B_\mathrm{s} \sim 10^{12}\,\mathrm{G}. \tag{2.4}$$

It is interesting to note that the basic physical processes specifying the observed radio pulsar activity were actually identified immediately after their discovery. Thus, it was clear that the extremely regular pulsations of the observed radio emission are connected with the neutron star rotation (Gold, 1968). In some pulsars, the frequency stability on the scale of a few years is even larger than that of the atomic standards; therefore, work is underway on the development of a new pulsar timescale (Ilyasov et al., 1998). Further, the energy source of radio pulsars is due to the rotational energy, and the energy release mechanism is connected with their superstrong magnetic field $B_0 \sim 10^{12}$ G. Indeed, when estimated by the simple magnetodipole formula (Pacini, 1967), the energy losses

$$W_\mathrm{tot} = -I_\mathrm{r} \Omega \dot{\Omega} \approx \frac{1}{6} \frac{B_0^2 \Omega^4 R^6}{c^3} \sin^2 \chi, \tag{2.5}$$

where $I_r \sim MR^2$ is the moment of inertia of the star, χ is the inclination angle of the magnetic dipole axis to the rotation axis, and $\Omega = 2\pi/P$ is the angular velocity, amount to 10^{31}–10^{34} erg/s for most pulsars.

This energy release is just responsible for the observed slowdown $\dot{P} \sim 10^{-15}$, which corresponds to the dynamical age $\tau_D = P/2\dot{P} \sim$ 1–10 mln years. The radio pulsars are thus the only space objects whose evolution is fully specified by the electrodynamic forces. Recall that the intrinsic radio emission is only 10^{-4}–10^{-6} of the total energy losses. For most pulsars, this corresponds to 10^{26}–10^{28} erg/s, which is 5–7 orders less than the luminosity of the Sun. Moreover, the extremely high brightness temperature $T_{br} \sim 10^{25}$–10^{28} K uniquely shows that the radio emission of pulsars is generated by a coherent mechanism (Ginzburg et al., 1969; Ginzburg, 1971).

As was noted, the possibility for existence of these objects has already been the subject for study since the 1930s. Moreover, since the early 1960s, the possibility of superfluidity and superconductivity in the interior regions of neutron stars has been actively discussed (see, e.g., Ginzburg and Kirzhniz 1968). Nevertheless, it was believed that because of their small size, neutron stars were actually impossible to detect. Accordingly, in spite of a number of papers (Kardashev, 1964; Pacini, 1967), before the discovery of radio pulsars it was not understood that neutron stars must rotate so fast that the main source of radiated energy is their kinetic rotational energy. As a result, no attempts were actually made to detect the pulsating radiation of the known objects. This was in spite of the fact that by that time an unusual optical star coinciding with an unusual radio source had already been detected in the Crab Nebula. The activity of this star was exactly responsible for the energy release $W_{tot} \approx 5 \times 10^{38}$ erg/s needed to supply the Crab Nebula with relativistic electrons (Rees and Gunn, 1974). Otherwise, the Crab Nebula would have ceased to glow long ago.

Only when it was clear that this unusual source is really connected with a rotating neutron star, the analysis of variability of its optical flux was made (Wampler et al., 1969). It turned out that the optical radiation also reaches us in the form of separate pulses, the period of which ($P \approx 0.033$ s) exactly coincides with the period specified by the data in the radio band. The truth was found after the rotational slowdown $\dot{P}$ of the pulsar in the Crab Nebula was measured, and it was clear that

1. the rate of the energy loss of the rotating neutron star, which was determined by the slowdown of the angular rotational velocity $W = -I_r\Omega\dot{\Omega}$, coincides with $W_{tot} \approx 5 \times 10^{38}$ erg/s;
2. the dynamical age of the radio pulsar $\tau_D = \Omega/2|\dot{\Omega}| \approx 1000$ years coincides with that of the Crab Nebula that came into existence, as is known, during the explosion of the historical supernova AD 1054.

Most radio pulsars are single neutron stars. Of over 1800 pulsars discovered by mid-2008, only about 100 of them belong to binary systems. However, in all these cases, it is known with certainty that in these binary systems there is not any substantial flux of matter from a star-companion onto the neutron star. Since, as we noted, the radio luminosity of pulsars is not high, the present-day receivers'

accuracy allows one to observe pulsars only up to distances of order 3–5 kpc, which is less than the distance to the center of Galaxy. Therefore, we have the possibility to observe only a small part of all "working" radio pulsars. The total number of neutron stars in our Galaxy is 10^8–10^9. This large number of extinct neutron stars is naturally connected with their short lifetime mentioned above.

The discovery of neutron stars was, undoubtedly, an upheaval in astrophysics. Besides the emergence of new purely theoretical problems [magnetosphere structure and the coherent radio emission mechanism (Michel, 1991; Beskin et al., 1993; Lyubarskii, 1995; Mestel, 1999), the theory of accreting sources in close binary systems (Shapiro and Teukolsky, 1983; Lipunov, 1992), the theory of the inner structure and the surface layers of neutron stars (Baym and Pethick, 1979; Sedrakyan and Shakhabasyan, 1991; Liberman and Johansson, 1995; Kirzhnits and Yudin, 1995)], which gave impetus to theoretical research, the radio pulsars are used for concrete astrophysical measurements. This was possible due to the unique properties of the impulse emission of radio pulsars that make it possible, in particular, to control not only the frequency but also the signal phase. Here we can mention, for example,

- the determination of the electron density in the interstellar medium by the time delay of the arrival of pulses at different frequencies (Lyne and Graham-Smith, 1998; Johnston et al., 1999);
- the determination of the galactic magnetic field by the polarization plane rotation at different frequencies (Lyne and Graham-Smith, 1998; Brown and Taylor, 2001);
- the refined diagnostics of the GR effects in close binary systems (Taylor and Weisberg, 1989);
- the search for relic gravitational waves (Sazhin, 1978).

Thus, the general pattern of the radio pulsar activity seems to have been established over many years. On the other hand, some fundamental problems are still to be solved. It is, first of all, the problem of the physical nature of the coherent radio emission of pulsars. In particular, as in the 1970s, there is no common view of the problem of the coherent radio emission mechanism of a maser or an antenna type (Blandford, 1975; Melrose, 1978; Beskin et al., 1988; Lyubarskii, 1995; Usov and Melrose, 1996; Lyutikov et al., 1999). Besides, there is no common viewpoint on the structure of the pulsar magnetosphere (Michel, 1991; Beskin et al., 1993; Lyubarskii, 1995; Mestel, 1999). The point is that the initial hypothesis for the magnetodipole energy loss mechanism (2.5) is, undoubtedly, unrealistic. Strictly speaking, this chapter primarily deals with the proof of this assertion. We only stress here that low-frequency waves with frequency $\nu = 1/P$ cannot propagate in the interstellar medium for which the plasma frequency is, on average, several kilohertz (Lipunov, 1992). Therefore, the problem of the slowing-down mechanism can be solved only by determining the magnetosphere structure of the neutron star. However, the consistent theory of the radio pulsar magnetosphere has not been constructed yet. Thus, the structure of the longitudinal currents circulating in the magnetosphere is not specified and, hence, the problem of the neutron star braking, particle acceleration, and energy transport beyond the light cylinder still remains

unsolved. The theory of the inner structure of neutron stars is also far from completion. Naturally, it seems impossible to discuss all these problems here. Therefore, we discuss in detail only the problems directly connected with the main theme of this book, viz., the theory of the pulsar magnetosphere. The main problems to be discussed are the following:

1. the magnetosphere structure of a rotating neutron star;
2. the determination of the energy loss mechanism of radio pulsars;
3. the energy transport from the rotating neutron star within the magnetosphere; and
4. the determination of the particle acceleration mechanism in the pulsar wind.

2.2 Basic Physical Processes

2.2.1 Vacuum Approximation

Before proceeding to the discussion of the consistent theory of radio pulsars, we consider the basic physical processes taking place in the magnetosphere. We should make a reservation that in this chapter we do not actually discuss the GR effects, the exception is one of the particle generation mechanisms. Though the GR effects on the neutron star surface can amount to 20% (Kim et al., 2005), they are not, generally, taken into account in the development of the pulsar magnetosphere theory. The point is that the electromagnetic force $F_{\rm em} \sim eE$ acting on a charged particle near the neutron star surface turns out to be many orders greater than the gravitational force $F_{\rm g} = GMm/R^2$. This condition allows us to disregard the electromagnetic field distortion connected with the space curvature in the vicinity of the neutron star.

We first discuss the simplest vacuum model which, even if very far from reality, gives an insight into the key properties of the real magnetosphere of the neutron star. Thus, we consider a homogeneous magnetized star rotating in vacuum. The basic parameters defining the properties of the magnetosphere are the magnetic field B_0, the star radius R, and the angular rotational velocity Ω. For a well-conducting star, we find that in its interior

$$\mathbf{E}_{\rm in} + \frac{\mathbf{\Omega} \times \mathbf{r}}{c} \times \mathbf{B}_{\rm in} = 0. \tag{2.6}$$

In this chapter, we, as usual, restore the dimension. The condition (2.6) simply implies that the electric field in the coordinate system rotating with the star is zero: $\mathbf{E}' = 0$.

Suppose now that the star rotation axis is parallel to the magnetization axis. Then the problem is stationary and, therefore, the electric field is fully defined by the potential $\Phi_{\rm e}$ ($\mathbf{E} = -\nabla\Phi_{\rm e}$), which inside the star can be written as

$$\Phi_{\rm e}(r < R, \theta) = \frac{1}{2}\,\frac{\Omega B_0}{c}\, r^2 \sin^2\theta. \tag{2.7}$$

Hence, on the star surface

$$\Phi_{\rm e}(R, \theta) = \Phi_0(\theta) = -\frac{1}{3}\,\frac{\Omega B_0}{c} R^2 \mathcal{P}_2(\cos\theta) + \text{const}, \tag{2.8}$$

where $\mathcal{P}_2(x) = (3x^2 - 1)/2$ is the Legendre polynomial. The electric potential beyond the star can be found from the solution of the Laplace equation $\nabla^2 \Phi_{\rm e} = 0$ with the boundary conditions

1. $\Phi_{\rm e}(R, \theta) = \Phi_0(\theta)$;
2. $\Phi_{\rm e}(r, \theta) \to 0$ for $r \to \infty$.

The solution corresponding to the zero total electric charge of the star has the form

$$\Phi_{\rm e}(r > R, \theta) = -\frac{1}{3}\,\frac{\Omega B_0}{c}\,\frac{R^5}{r^3}\mathcal{P}_2(\cos\theta). \tag{2.9}$$

As shown in Fig. 2.1, the rotation of homogeneously magnetized star gives rise to a quadrupole electric field beyond it. As to the magnetic field, for an axisymmetric rotator, it is exactly equal to the dipole magnetic field

$$\mathbf{B}(r > R) = \frac{3(\mathbf{mn})\mathbf{n} - \mathbf{m}}{r^3}, \tag{2.10}$$

where $\mathbf{n} = \mathbf{r}/r$, and $|\mathbf{m}| = B_0 R^3/2$ is the star magnetic moment.

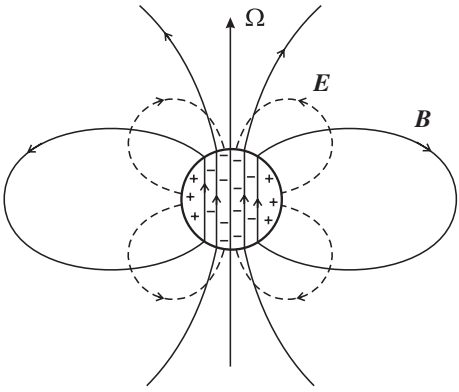

Fig. 2.1 The structure of the axisymmetric vacuum magnetosphere of the neutron star. The rotating homogeneously magnetized star generates the dipole magnetic field (*solid lines*) and the quadrupole electric field **E** (*dashed lines*)

Problem 2.1 Show that the surface charge density $\sigma_{\rm s}$ defined by the jump of the normal electric field component $4\pi\sigma_{\rm s} = \{E_n\}$ has the form (Mestel, 1971)

$$\sigma_s(\theta) = \frac{1}{8\pi}\frac{\Omega R}{c} B_0(3 - 5\cos^2\theta). \tag{2.11}$$

Explain why the total surface charge is different from zero

$$Q_* = \int \sigma_s(\theta) \mathrm{d}o = \frac{2}{3}\frac{\Omega B_0}{c} R^3 \neq 0. \tag{2.12}$$

Using the simplest vacuum model, we can make a number of general conclusions.

- The longitudinal electric field $E_\parallel = (\mathbf{E}\cdot\mathbf{B})/B$ in the vicinity of the star surface can be estimated as

$$E_\parallel \sim \frac{\Omega R}{c} B_0. \tag{2.13}$$

- In the axisymmetric case (and for the zero total electric charge), the sign of the product $(\mathbf{E}\cdot\mathbf{B})(\mathbf{B}\cdot\mathbf{n})$ remains the same over the neutron star surface.

The latter conclusion is very important. The particles in the strong magnetic field can move along the magnetic field only (see below). This implies that for the axisymmetric rotator, particles of the same sign are ejected from both magnetic poles of the neutron star. As we will see, this important property retains in the case of the plasma-filled magnetosphere.

For an arbitrary inclination angle χ, the problem was solved by Deutsch (1955) long before the discovery of pulsars. In this case, the electromagnetic fields are a sum of the fields of the rotating magnetic dipole and the electric quadrupole, and the quadrupole moment can be represented as

$$Q_{ik} = \frac{R^2}{c}\left[m_i\Omega_k + m_k\Omega_i - \frac{2}{3}(\mathbf{m}\cdot\mathbf{\Omega})\delta_{ik}\right]. \tag{2.14}$$

The electromagnetic fields for the arbitrary distance r in the limit $R \to 0$ for $\chi = 90^\circ$ are described by the known expressions (Landau and Lifshits, 1989)

$$B_r = \frac{|\mathbf{m}|}{r^3}\sin\theta\,\mathrm{Re}\left(2 - 2\mathrm{i}\frac{\Omega r}{c}\right)\exp\left(\mathrm{i}\frac{\Omega r}{c} + \mathrm{i}\varphi - \mathrm{i}\Omega t\right), \tag{2.15}$$

$$B_\theta = \frac{|\mathbf{m}|}{r^3}\cos\theta\,\mathrm{Re}\left(-1 + \mathrm{i}\frac{\Omega r}{c} + \frac{\Omega^2 r^2}{c^2}\right)\exp\left(\mathrm{i}\frac{\Omega r}{c} + \mathrm{i}\varphi - \mathrm{i}\Omega t\right), \tag{2.16}$$

$$B_\varphi = \frac{|\mathbf{m}|}{r^3}\,\mathrm{Re}\left(-\mathrm{i} - \frac{\Omega r}{c} + \mathrm{i}\frac{\Omega^2 r^2}{c^2}\right)\exp\left(\mathrm{i}\frac{\Omega r}{c} + \mathrm{i}\varphi - \mathrm{i}\Omega t\right), \tag{2.17}$$

$$E_r = E_r^Q, \tag{2.18}$$

$$E_\theta = \frac{|\mathbf{m}|\Omega}{r^2 c}\,\mathrm{Re}\left(-1+\mathrm{i}\frac{\Omega r}{c}\right)\exp\left(\mathrm{i}\frac{\Omega r}{c}+\mathrm{i}\varphi-\mathrm{i}\Omega t\right)+E_\theta^Q, \tag{2.19}$$

$$E_\varphi = \frac{|\mathbf{m}|\Omega}{r^2 c}\cos\theta\,\mathrm{Re}\left(-\mathrm{i}-\frac{\Omega r}{c}\right)\exp\left(\mathrm{i}\frac{\Omega r}{c}+\mathrm{i}\varphi-\mathrm{i}\Omega t\right)+E_\varphi^Q. \tag{2.20}$$

Here $\mathbf{E}^Q$ is the quadrupole static electric field

$$\mathbf{E}^Q = -\nabla\Phi_\mathrm{e}^Q, \quad \Phi_\mathrm{e}^Q = \frac{Q_{ik}n_i n_k}{2r^3}. \tag{2.21}$$

At distances much smaller than the wavelength $r \ll c/\Omega$, the electromagnetic fields are close to the sum of the fields of the magnetic dipole and the electric quadrupole at rest, and at large distances $r \gg c/\Omega$, they correspond to a spherical wave. Since, according to (2.13), the quadrupole electric field on the star surface is much smaller than the magnetic field and, on the other hand, the quadrupole electric field decreases with distance faster than the dipole magnetic field, the electric quadrupole does not make a real contribution to the energy loss of the rotating star. Consequently, the energy losses are determined, with adequate accuracy, by the standard expression (2.5). Therefore, we restrict ourselves in (2.18), (2.19), and (2.20) to the static part of the electric quadrupole field only.

One should stress here that the magnetodipole radiation turned out to result in the change of not only the rotation period $P = 2\pi/\Omega$ but also the evolution of the inclination angle χ, since, for the magnetodipole losses the invariant $\mathcal{I}_\mathrm{md}$ remains constant (Davis and Goldstein, 1970)

$$\mathcal{I}_\mathrm{md} = \Omega\cos\chi. \tag{2.22}$$

Hence, for the magnetodipole losses, the inclination angle of the rotating magnetized star must decrease with the characteristic time τ_χ coinciding with the dynamical lifetime $\tau_\mathrm{D} = P/2\dot{P}$. As a result, a decrease in the energy release is due not only to an increase in the rotation period but also to a decrease in the inclination angle χ.

Unfortunately, the only direct observational channel permitting us to judge the radio pulsar energy release mechanism is the so-called braking index

$$n_\mathrm{br} = \frac{\ddot{\Omega}\Omega}{\dot{\Omega}^2} = 2-\frac{\ddot{P}P}{\dot{P}^2}, \tag{2.23}$$

which, as is easily checked, coincides with the exponent in the slowing-down dependence on the angular velocity, viz., $\dot{\Omega} \propto \Omega^{n_\mathrm{br}}$. As we see, to determine the braking index, we must know the second derivative of the period $\ddot{P}$. However, for most radio pulsars, we fail to identify the second derivative of the noise background associated with faster (than the slowing-down time) variations of the rotation period of the neutron star (Johnston and Galloway, 1999). Therefore, it is possible to determine the breaking index only for the fastest radio pulsars. As seen from Table 2.1, in all

Table 2.1 Braking index $n_{\rm br}$ for fast radio pulsars

PSR	P (s)	$\dot{P}(10^{-15})$	$n_{\rm br}$
$B0531+21$	0.033	421	2.51 ± 0.01
$B0540-693$	0.050	479	2.14 ± 0.01
$J1119-6127$	0.408	4022	2.91 ± 0.05
$B1509-58$	0.150	1490	2.84 ± 0.01
$J1846-0258$	0.324	7083	2.65 ± 0.01

cases, the braking index is less than 3, whereas the dipole slowing-down law (2.5) yields $n_{\rm br} = 3$.

Problem 2.2 Show that in a more realistic model taking into account the evolution of the inclination angle χ (2.22), the braking index is even larger than 3 (Davis and Goldstein, 1970)

$$n_{\rm br} = 3 + 2\cot^2\chi\,. \tag{2.24}$$

Problem 2.3 Integrate the evolution equation (2.5), with account taken of the integral of motion (2.22), and show that the period of the pulsar $P(t)$ exponentially fast (with characteristic time $\tau_{\rm D} = P_0/2\dot{P}_0$) approaches the maximum value of $P_{\max} = P_0/\cos\chi_0$ and the angle χ approaches 0°.

Thus, we can conclude from the analysis of the braking index that the simple magnetodipole mechanism cannot, evidently, be responsible for the observed slowing down of the radio pulsar rotation. Therefore, there were numerous attempts to correct relation (2.24) for example, by the magnetic field evolution (Blandford and Romani, 1988; Chen et al., 1998) or the interaction of the superfluid component in the neutron star nucleus with its hard crust (Allen and Horvath, 1997; Baykal et al., 1999) (see also Melatos, 1997; Xu and Qiao, 2001). It turned out, however, that most of the similar effects can lead to insignificant corrections only and cannot change the value appreciably (2.24). In any event, the determination of the braking index of other neutron stars and also the second-order braking index $n_{\rm br}^{(2)} = \Omega^2\dddot{\Omega}/\dot{\Omega}^3$ [this parameter is now known only for Crab pulsar (Lyne and Graham-Smith, 1998)] would make it possible to greatly clarify the nature of the radio pulsar slowing down. On the other hand, almost immediately after the discovery of the radio pulsars, it was obvious that the vacuum model is not a good zero approximation to describe the neutron star magnetosphere. And the reason, strange as it may seem, is that a superstrong magnetic field exists.

2.2.2 Particle Generation in the Strong Magnetic Field

The superstrong magnetic field $B \sim 10^{12}$ G leads to a number of important consequences.

- The synchrotron lifetime (Landau and Lifshits, 1989)

$$\tau_{\rm s} \approx \frac{1}{\omega_B}\left(\frac{c}{\omega_B r_{\rm e}}\right) \sim 10^{-15}\,{\rm s} \tag{2.25}$$

  ($\omega_B = eB/m_{\rm e}c$—electron cyclotron frequency, $r_{\rm e} = e^2/m_{\rm e}c^2$—the classical electron radius) appears much smaller than the time it takes for a particle to escape the magnetosphere. Consequently, the charged particle motion in the neutron star magnetosphere includes the motion along the magnetic field lines and the electric drift in a transverse direction.
- Since the dipole magnetic field lines are curved, the relativistic particle motion along a curved trajectory gives rise to the emission of hard γ-quanta due to the so-called curvature radiation (Zheleznyakov, 1996). This process is quite analogous to the ordinary synchrotron radiation, because the nature of the accelerated motion is unessential and for relativistic particles the formation length $\delta r \sim R_{\rm c}\gamma^{-1}$ is much smaller than the curvature radius $R_{\rm c}$. Therefore, all formulae for the synchrotron radiation can be used to describe the curvature radiation with the only change, viz., the Larmor radius $r_B = m_{\rm e}c^2\gamma/eB$ is to be replaced by the radius of curvature of the magnetic field line $R_{\rm c}$. In particular, the frequency corresponding to the maximum radiation now looks like

$$\omega_{\rm cur} = 0.44\frac{c}{R_{\rm c}}\gamma^3. \tag{2.26}$$

  The extra degree γ as compared to the synchrotron radiation case $\omega_{\rm syn} = 0.44\omega_B\gamma^2$ is associated here with the fact that for the synchrotron losses the Larmor radius r_B itself is proportional to the particle energy.
- Finally, the importance of the one-photon generation of electron–positron pairs in the superstrong magnetic field $\gamma + B \to e^+ + e^- + B$ was understood, which occurs when photons in their motion cross the magnetic field lines (Sturrock, 1971). Indeed, the probability (per unit length) of the conversion of a photon with energy $\varepsilon_{\rm ph}$ propagating at an angle of θ to the magnetic field **B** far from the threshold (i.e., for $\varepsilon_{\rm ph} \gg 2m_{\rm e}c^2$) is (Berestetsky et al., 1982)

$$w = \frac{3\sqrt{3}}{16\sqrt{2}}\frac{e^3 B\sin\theta}{\hbar m_{\rm e}c^3}\exp\left(-\frac{8}{3}\frac{B_\hbar}{B\sin\theta}\frac{m_{\rm e}c^2}{\varepsilon_{\rm ph}}\right). \tag{2.27}$$

  Here the value

$$B_\hbar = \frac{m_{\rm e}^2c^3}{e\hbar} \approx 4.4\times 10^{13}\,{\rm G} \tag{2.28}$$

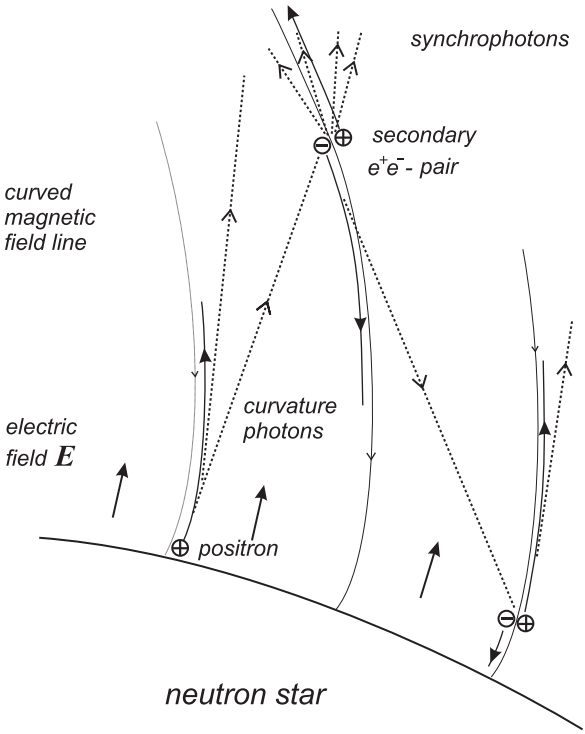

Fig. 2.2 Structure of the acceleration region and particle generation in the vicinity of the neutron star surface. The primary particles that penetrated the nonzero longitudinal electric field region are accelerated along the curved magnetic field lines and begin to radiate hard γ-quanta. These curvature photons (*dotted lines*) propagating in the curved magnetic field reach the particle generation threshold and create electron–positron pairs. Secondary particles radiate synchrophotons and, after acceleration, start to radiate new generation of curvature γ-quanta

corresponds to the critical magnetic field for which the energy gap between two Landau levels reaches the rest energy of an electron, viz., $\hbar\omega_B = m_e c^2$. Recall that, unlike the electric field, the magnetic field itself cannot generate particles. However, it can act as a catalyst that ensures the fulfillment of the laws of energy and momentum conservation for the process studied.

As we see, the characteristic magnetic fields of neutron stars are not much smaller than the critical magnetic field $B_\hbar$. Therefore, the neutron star magnetosphere appears nontransparent even to low-energy photons with energy $\varepsilon_{\rm ph} \sim$ 2–3 MeV, i.e., in the vicinity of the particle generation threshold. We thus have the chain of processes (see Fig. 2.2).

1. The primary particle acceleration by the longitudinal electric field existing, as was shown, in the vacuum approximation.
2. The emission of curvature photons with characteristic frequencies $\omega \leq \omega_{\rm cur}$ (2.26).
3. The photons propagation in the curved magnetic field up to the generation of the secondary electron–positron pairs.
4. The acceleration of secondary particles, the emission of curvature photons, which, in turn, give rise to the generation of new secondary particles.
5. The screening of the longitudinal electric field by the secondary plasma.

Thus, we can conclude that the vacuum magnetosphere of the neutron star with magnetic field $B_0 \sim 10^{12}$ G proves unstable to the charged particle generation.

Some comments for correcting the above-formulated pattern are necessary. Note first that though the curvature photons are actually emitted parallel to the magnetic field lines, due to the same curvature of the magnetic lines a γ-quantum in its propagation starts moving at an increasingly greater angle of θ to the magnetic field. On the other hand, for the small, as compared to the curvature radius, photon free path l_γ, we can take $\sin\theta \approx l_\gamma / R_\mathrm{c}$. Therefore, the γ-quantum free path l_γ can be estimated as (Sturrock, 1971)

$$l_\gamma = \frac{8}{3\Lambda} R_\mathrm{c} \frac{B_\hbar}{B} \frac{m_\mathrm{e} c^2}{\varepsilon_\mathrm{ph}}, \tag{2.29}$$

where $\Lambda \approx 20$ is a logarithmic factor.

Further, for not too strong magnetic fields $B < 10^{13}$ G, the secondary particles are generated on the nonzero Landau levels (Beskin, 1982; Daugherty and Harding, 1983). Because of the short synchrotron lifetime τ_s (2.25), all the "transverse" energy is radiated actually instantaneously due to the synchrotron emission. It turns out that the energy of these synchrophotons is high enough for these photons to be absorbed by the strong magnetic field and generate secondary particles. As to primary particles, they can be generated by the cosmic background radiation. A comprehensive analysis showed (Shukre and Radhakrishnan, 1982) that the cosmic γ-ray background leads to the generation of 10^5 primary particles per second. This is quite enough for the neutron star magnetosphere to be effectively filled with an electron–positron plasma.

Problem 2.4 Having determined the free path length l_γ as $\int_0^{l_\gamma} w(l)\mathrm{d}l = 1$, show that

$$\Lambda \approx \ln\left[\frac{e^2}{\hbar c}\frac{\omega_B R_\mathrm{c}}{c}\left(\frac{B_\hbar}{B}\right)^2\left(\frac{m_\mathrm{e}c^2}{\varepsilon_\mathrm{ph}}\right)^2\right]. \tag{2.30}$$

Problem 2.5 Show that if a photon of energy $\varepsilon_\mathrm{ph} \gg m_\mathrm{e}c^2$ generates a pair moving at an angle of θ to the magnetic field, after the secondary particles descend to the lower Landau level, their Lorentz factors are

$$\gamma \approx \frac{1}{\theta} \approx \frac{R_\mathrm{c}}{l_\gamma}. \tag{2.31}$$

Problem 2.6 Using the law of motion of a relativistic particle

$$\frac{\mathrm{d}\varepsilon_\mathrm{e}}{\mathrm{d}l} = eE_\parallel - \frac{2}{3}\frac{e^2}{R_\mathrm{c}^2}\gamma^4, \tag{2.32}$$

where the first term on the right-hand side corresponds to the acceleration in the electric field and the second one to the radiation reaction, show that for the standard radio pulsar ($B_0 = 10^{12}$ G, $P = 1$ s) the primary electron energy ε_e (and the positron one) can amount to 10^8 MeV, and the energy of curvature photons to 10^7 MeV.

2.2.3 Magnetosphere Structure

Thus, the important conclusion is that the plasma-filled magnetosphere model rather than the vacuum model is a more natural zero approximation. This implies that in the zero approximation the longitudinal electric field can be considered to be zero

$$E_\parallel = 0. \tag{2.33}$$

Physically, this condition implies that light electrons and positrons can always be redistributed so as to screen the longitudinal electric field. The occurrence of the longitudinal field in some magnetosphere region immediately leads to an abrupt plasma acceleration and to the explosive generation of secondary particles.

As a result, we can determine the main features defining the pulsar magnetosphere.

Corotation. Due to the presence of plasma in the pulsar magnetosphere, the frozen-in condition (2.6)

$$\mathbf{E} + \frac{\boldsymbol{\Omega} \times \mathbf{r}}{c} \times \mathbf{B} = 0 \tag{2.34}$$

is, with adequate accuracy, satisfied not only in the interior of the neutron star but also in the whole magnetosphere. As a result, the drift velocity

$$\mathbf{U}_\mathrm{dr} = c\frac{\mathbf{E} \times \mathbf{B}}{B^2} = \boldsymbol{\Omega} \times \mathbf{r} + j_\parallel \mathbf{B} \tag{2.35}$$

($j_\parallel$—a scalar function) consists of the motion along the magnetic field and the rigid corotation with the neutron star. This corotation is present in the magnetosphere of the Earth and large planets.

Light cylinder. It is clear that the rigid corotation becomes impossible at large distances from the rotation axis $\varpi > R_\mathrm{L}$, where the light cylinder radius R_L is defined as

$$R_{\mathrm{L}} = \frac{c}{\Omega}. \tag{2.36}$$

Actually, this scale defines the magnetosphere boundary. For the ordinary pulsars $R_{\mathrm{L}} \sim 10^9$–10^{10} cm, i.e., the light cylinder is at distances several thousand times larger than the neutron star radius.

Light surface. As we see in the following, of great importance in the radio pulsar magnetosphere structure is the so-called light surface—the surface on which the electric field becomes equal to the magnetic one, viz., $|\mathbf{E}| = |\mathbf{B}|$. In the presence of longitudinal currents, this surface does not coincide with the light cylinder but is at larger distances and extends to infinity for rather high longitudinal currents. The light surface defines the magnetosphere boundary more correctly, because the drift approximation (2.34) and (2.35) becomes inapplicable beyond its boundaries and so does the MHD approximation.

Polar cap. Since in the polar coordinates r, θ the dipole magnetic field lines are described by the relation $r = r_{\max} \sin^2 \theta_m$, where $r_{\max}$ is the maximum distance of the given field line from the star center, we can estimate the polar cap radius at the pulsar magnetic pole $R_0 = R \sin \theta_0$ from which the magnetic field lines extend beyond the light cylinder. Substituting for $r_{\max}$ the light cylinder radius R_{L}, we get

$$R_0 = R \left(\frac{\Omega R}{c} \right)^{1/2}, \tag{2.37}$$

where the factor

$$\varepsilon_{\mathrm{A}} = \left(\frac{\Omega R}{c} \right)^{1/2} \sim 10^{-2} \tag{2.38}$$

is, as we will see, the main small parameter in the theory of the pulsar magnetosphere. Thus, for ordinary radio pulsars the polar cap size is only several hundreds of meters. And on this extremely small, on a cosmic scale, area comparable with the stadium size, the basic processes responsible for the observed activity of radio pulsars occur.

Open and closed field lines. As shown in Fig. 2.3, the magnetic field lines going beyond the light cylinder can diverge and extend to infinity. Since, as was noted, the particle motion is possible only along the magnetic field, two groups of magnetic field lines stand out in the magnetosphere. One group passing through the polar cap intersects the light cylinder and extends to infinity. The other group located far from the magnetic axis is closed within the light cylinder. The plasma located on the closed magnetic lines turns out to be captured, whereas the plasma filling the open magnetic lines can escape the neutron star magnetosphere.

Critical charge density. Finally, it is very important that the charge density in the magnetosphere of the rotating neutron star must be different from zero. Indeed, using relation (2.34), we find $\rho_{\mathrm{e}} \approx \rho_{\mathrm{GJ}}$ where

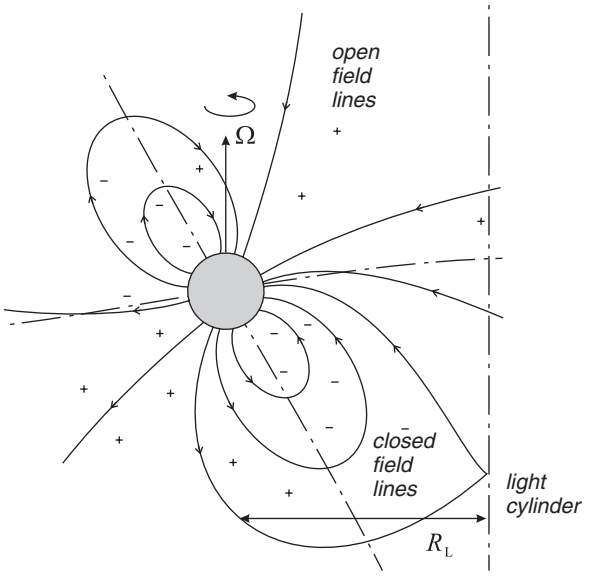

Fig. 2.3 The magnetosphere structure of radio pulsars. The open field lines coming out from the magnetic poles cross the light cylinder (*dashed and dotted line*). The charge density ϱ_{GJ} (2.39) changes the sign on the surface on which the magnetic lines are orthogonal to the angular velocity vector $\mathbf{\Omega}$

$$\rho_{GJ} = \frac{1}{4\pi}\mathrm{div}\mathbf{E} \approx -\frac{\mathbf{\Omega}\cdot\mathbf{B}}{2\pi c}. \tag{2.39}$$

This expression was first obtained in P. Goldreich and P. Julian's pioneer paper (Goldreich and Julian, 1969). Therefore, the critical charge density (2.39) is, generally, called the Goldreich–Julian (GJ) charge density. For ordinary pulsars, the appropriate concentration $n_{GJ} = |\rho_{GJ}|/e$ near the star surface is 10^{10}–10^{12} 1/cm^3. Accordingly, the characteristic value of the current density can be written as $j_{GJ} = \rho_{GJ}c$. Finally, the characteristic value of the total electric current in the magnetosphere can be estimated as a product of the polar cap area, the GJ charge density, and the velocity of light:

$$I_{GJ} = \pi R_0^2 \rho_{GJ} c. \tag{2.40}$$

The physical meaning of the GJ charge density is simple—it is the charge density needed to screen the longitudinal electric field. The perpendicular electric field occurs and its value, as we saw, turns out to be exactly the value of the electric drift in the crossed fields to generate the plasma corotation.

Problem 2.7 Show that for the case of the total corotation (i.e., when the poloidal currents are absent in the neutron star magnetosphere and, therefore, the total current $\mathbf{j}$ can be written as $\mathbf{j} = \rho_e \mathbf{\Omega} \times \mathbf{r}$), the exact expression for the GJ charge density has the form

$$\rho_{\rm GJ} = -\frac{\mathbf{\Omega}\cdot\mathbf{B}}{2\pi c\left(1-\dfrac{\Omega^2\varpi^2}{c^2}\right)}. \tag{2.41}$$

How can the singularity on the light cylinder be explained?

Problem 2.8 Show that the total electric charge of the neutron star for the plasma-filled magnetosphere is

$$Q_* = \frac{1}{3}\,\frac{\Omega B_0}{c}\,R^3 \neq 0. \tag{2.42}$$

Compare it with the charge Q_* (2.12) obtained by integrating the surface charge density for the vacuum magnetosphere.

Some explanation is also necessary here. First of all, as is evident from relation (2.35), the light cylinder is the real boundary of the magnetosphere only for the zero toroidal magnetic field, i.e., for the zero longitudinal electric current. As we will see, for the sufficiently large longitudinal current (and, hence, for the large enough toroidal magnetic field), the drift motion can occur at distances much larger than the light cylinder radius $R_{\rm L}$. However, as shown in Fig. 2.4, in this case, there is almost the full compensation of the corotational velocity $\mathbf{\Omega}\times\mathbf{r}$ and the toroidal slip velocity along the magnetic field $j_\parallel B_\varphi$, so that the drift velocity $\mathbf{U}_{\rm dr}$ is directed radially from the star. Therefore, beyond the light cylinder, in spite of the validity of the drift approximation, the particle motion is actually perpendicular to the magnetic field lines.

Further, relation (2.37) for the polar cap radius is only an estimate in order of magnitude. The point is that the electric currents connected with electric charges filling the pulsar magnetosphere in the vicinity of the light cylinder begin to disturb the dipole magnetic field. Therefore, the exact form of the polar cap can be found together with the solution of the complete problem of the neutron star magnetosphere. On the other hand, expression (2.37) allows us to estimate the maximum value of the voltage drop in the vicinity of the magnetic poles $\psi_{\max} = E(R_0)R_0$:

$$\psi_{\max} = \left(\frac{\Omega R}{c}\right)^2 R B_0. \tag{2.43}$$

For ordinary pulsars, it yields $\psi_{\max} \sim 10^7$–10^8 MeV.

Finally, important consequences follow from expression (2.39) for the GJ charge density. As shown in Fig. 2.3, in the vicinity of the neutron star, the charge density $\rho_{\rm GJ}$ changes sign on the surface, where $\mathbf{\Omega}\cdot\mathbf{B} = 0$. Therefore, except for the

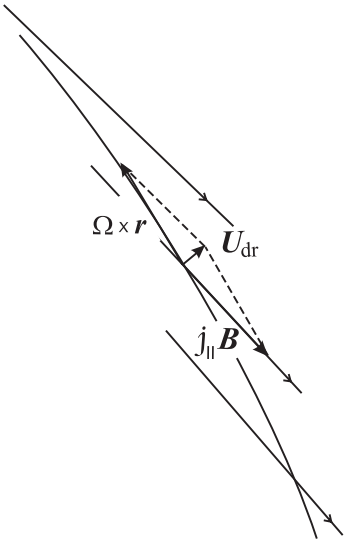

Fig. 2.4 The drift motion of a charged particle beyond the light cylinder in the presence of the strong toroidal field $B_\varphi \gg B_\mathrm{p}$ is nearly in a radial direction. The velocity $\mathbf{U}_\mathrm{dr}$ (which is, naturally, smaller than the velocity of light) can be formally resolved into the corotation velocity $\boldsymbol{\Omega} \times \mathbf{r}$ and the slip velocity along the magnetic field $j_\parallel \mathbf{B}$, each of them can be much larger than the velocity of light. The rotation axis is perpendicular to the figure plane

orthogonal rotator $\chi = 90^\circ$, the GJ charge density has the same sign in the vicinity of both magnetic poles (in fact, this property is directly associated with the already mentioned property of the vacuum magnetosphere—the radial electric field in the region of the magnetic poles is identical). This implies that an inverse current flowing in the vicinity of the boundary of the closed and open magnetic field lines is sure to occur—only, in this case, the total charge of the neutron star does not change. We should call attention to this property since it is the key property in the development of the theory of the neutron star magnetosphere.

Problem 2.9 Show that the light cylinder (where the corotation velocity approaches the velocity of light) is just the scale on which

- the electric field is compared in magnitude with the poloidal magnetic field;
- the toroidal electric currents flowing in the magnetosphere begin to disturb the poloidal magnetic field of the neutron star;
- the toroidal magnetic field connected with the longitudinal GJ current is compared in magnitude with the poloidal magnetic field.

2.3 Secondary Plasma Generation

2.3.1 "Inner Gap"

Thus, in the radio pulsar magnetosphere, two substantially different regions must develop, viz., the regions of open and closed magnetic field lines. The particles

located on the field lines which do not intersect the light cylinder turn out to be captured, whereas the plasma on the field lines intersecting the light cylinder can extend to infinity. Consequently, the plasma must be continuously generated in the region of the magnetic poles of a neutron star.

The necessity to take into account the secondary plasma generation in the magnetic pole region was indicated by Sturrock (1971) and then this process was studied in more detail by Ruderman and Sutherland (1975), and also by V.Ya. Eidman's group (Al'ber et al., 1975). It is based on the above one-photon particle generation in the strong magnetic field. The longitudinal electric field is generated by a continuous escape of particles along the open field lines beyond the magnetosphere. As a result, the longitudinal electric field region forms in the vicinity of the magnetic poles, the height of which is determined by the secondary plasma generation condition. Otherwise, the chain of processes is (see again Fig. 2.2)

1. the primary particle acceleration by the longitudinal electric field induced by the difference of the charge density ρ_e from the GJ charge density ρ_{GJ};
2. the emission of curvature photons with characteristic frequency $\omega \leq \omega_{cur}$ (2.26);
3. the photons propagation in the curved magnetic field up to the secondary electron–positron pair generation;
4. the secondary particles acceleration, the emission of curvature photons, which, in turn, give rise to the new generation of secondary particles.

It is important that a greater part of secondary particles is generated already over the acceleration region, where the longitudinal electric field is rather small, so that the secondary plasma can escape the neutron star magnetosphere.

To estimate the longitudinal electric field we consider, for simplicity, only the one-dimensional equation

$$\frac{\mathrm{d}E_\parallel}{\mathrm{d}h} = 4\pi(\rho_e - \rho_{GJ}), \tag{2.44}$$

which can be used if the gap height H is much smaller than the size of the polar cap R_0 (2.37). Unfortunately, this approximation is valid for the fastest pulsars only. Nevertheless, it contains all information concerning the inner gap structure. In spite of its outward simplicity, Eq. (2.44) comprises a number of substantial uncertainties. The main uncertainty is, undoubtedly, in the expression for the charge density ρ_e, which depends on the particle generation mechanism, which, in turn, is defined by the value of the longitudinal electric field.

We discuss the basic properties of Eq. (2.44). Thus, for the models with the non-free particle escape from the neutron star surface, which are, generally, called the Ruderman–Sutherland model (see the next section), we can take $|\rho_e| \ll |\rho_{GJ}|$ in the zero approximation, and the electric field on the star surface can be different from zero. As a result, we have (Ruderman and Sutherland, 1975)

$$E_\parallel \approx E_{RS}\frac{H-h}{H}, \tag{2.45}$$

where

$$E_{\mathrm{RS}} = 4\pi\rho_{\mathrm{GJ}} H, \tag{2.46}$$

and H is the height of the longitudinal electric field region. Its value should just be determined from the condition for the onset of the secondary plasma generation. Indeed, for $H < H_{\mathrm{cr}}$ the longitudinal electric field is not strong enough to effectively generate particles, whereas for $H > H_{\mathrm{cr}}$, the secondary plasma results in the fast screening of the acceleration region. Besides, for the solid star surface, this event can occur for the antiparallel directions of the magnetic and rotation axes, when near the polar caps $\rho_{\mathrm{GJ}} > 0$, and positively charged particles are to be ejected from the surface. Within this model, the longitudinal current I, generally speaking, can be arbitrary, but, certainly, not larger than the GJ current I_{GJ}.

Problem 2.10 Using expression (2.46) connecting the longitudinal electric field with the gap height H and relations (2.26) and (2.29) for the characteristic energy and the free path of curvature photons, find the expressions for gap height H and potential drop $\psi = E_{\parallel} H$ (Ruderman and Sutherland, 1975)

$$H_{\mathrm{RS}} \sim \lambda_{\mathrm{C}}^{2/7} R_{\mathrm{c}}^{2/7} R_{\mathrm{L}}^{3/7} \left(\frac{B}{B_{\hbar}}\right)^{-4/7}, \tag{2.47}$$

$$\psi_{\mathrm{RS}} \sim \frac{m_{\mathrm{e}} c^2}{e} \lambda_{\mathrm{C}}^{-3/7} R_{\mathrm{c}}^{4/7} R_{\mathrm{L}}^{-1/7} \left(\frac{B}{B_{\hbar}}\right)^{-1/7}. \tag{2.48}$$

Here $\lambda_{\mathrm{C}} = \hbar/m_{\mathrm{e}}c$ is the Compton wavelength.
(Hint: the gap height H can be estimated as a sum of primary particle acceleration length l_{acc} and free path of emitted curvature photon l_{γ}. For small acceleration lengths l_{acc}, the primary particle energy $\varepsilon_{\mathrm{e}} = eE_{\parallel} l_{\mathrm{acc}}$ and, therefore, the emitted photon energy $\varepsilon_{\mathrm{ph}}$ are low, and the free path of such low-energy photons appears significant. The short free paths can be realized only for the sufficiently high energy of photons, for the emission of which a primary particle is to pass a large distance. Therefore, the minimum value of the sum $l_{\mathrm{acc}} + l_{\gamma}$ is the scale on which the secondary plasma generation starts, which can screen the longitudinal electric field. This value is taken as an estimate of the gap height H.)

On the other hand, if particles can freely escape from the neutron star surface, it is logical to take here

$$E_{\parallel}(h = 0) = 0, \tag{2.49}$$

and the charge density ρ_{e} is close to ρ_{GJ}. The longitudinal electric field must also be zero on the upper boundary of the acceleration region

$$E_{\parallel}(h = H) = 0. \tag{2.50}$$

Otherwise, the secondary particles of one of the signs would fail to extend to infinity. As we see, in this model the longitudinal electric current I is to be very close to GJ current $I_{\rm GJ}$. As a result, in the free particle escape model, the longitudinal electric field is specified only by a small difference between the charge density $\rho_{\rm e}$ and the critical density $\rho_{\rm GJ}$. Indeed, the GJ charge density can be written as

$$\rho_{\rm GJ} = -\frac{\Omega B \cos\theta_b}{2\pi c}, \tag{2.51}$$

where θ_b is an angle between the magnetic field and the rotation axis. On the other hand, for the relativistic plasma moving with velocity $v \approx c$, we have within the same accuracy

$$\rho_{\rm e} = C(\Psi)B, \tag{2.52}$$

where $C(\Psi)$ is constant along the magnetic field lines. As we see, the charge densities (2.51) and (2.52) change differently along the magnetic field line. Thus, the GJ charge density (2.51), besides the factor B, also contains the geometric factor $\cos\theta_b$. As a result, the charge-separated relativistic plasma in its motion fails to satisfy the condition $\rho_{\rm e} = \rho_{\rm GJ}$, which gives rise to the particle acceleration in the longitudinal electric field. The longitudinal electric field gives rise to particle acceleration, to hard photon emission, and, hence, to secondary electron–positron plasma generation. Therefore, beyond the acceleration region, the field must already be close to zero.

Note that the conditions (2.49) and (2.50) can be satisfied simultaneously only if the electric charge density on the acceleration region boundaries does not coincide with the GJ density, i.e., when the derivative $\mathrm{d}E_{\parallel}/\mathrm{d}h$ is different from zero here (see Fig. 2.5). As a result, Eq. (2.44) can be rewritten as

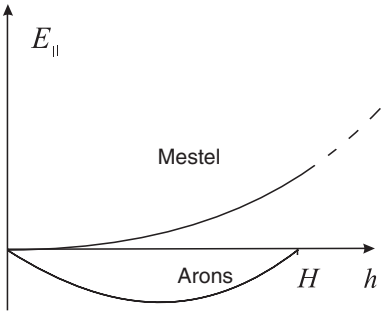

Fig. 2.5 The longitudinal electric field on the "preferable" magnetic field lines $A_a > 0$ in the Arons (1981) and Mestel (1999) models for $\mathbf{\Omega} \cdot \mathbf{B} > 0$. In the Mestel model, the plasma charge density $\rho_{\rm e}$ on the star surface is equal to the GJ charge density $\rho_{\rm GJ}$ (and, hence, $\mathrm{d}E/\mathrm{d}h = 0$), whereas in the Arons model, the charge density for $h = 0$, due to the presence of a particle backflow, differs from $\rho_{\rm GJ}$. As a result, though in both cases the electric field is zero on the star surface, the electric field direction and, hence, the particle acceleration appear different

$$\frac{\mathrm{d}E_{\parallel}}{\mathrm{d}h} = A_a \left(h - \frac{H}{2} \right), \tag{2.53}$$

where

$$A_a = 4\pi \left. \frac{\mathrm{d}(\rho_{\mathrm{e}} - \rho_{\mathrm{GJ}})}{\mathrm{d}h} \right|_{h=H/2}. \tag{2.54}$$

Finally, we have for $\chi > \varepsilon_{\mathrm{A}}$

$$A_a = \frac{3}{2} \frac{\Omega B_0}{cR} \theta_{\mathrm{m}} \cos\varphi_{\mathrm{m}} \sin\chi. \tag{2.55}$$

Here $\theta_{\mathrm{m}} \sim \varepsilon_{\mathrm{A}}$ is the polar angle and φ_{m} is an azimuthal angle relative to the magnetic dipole axis. The solution to Eq. (2.53) has the form

$$E_{\parallel} = -E_{\mathrm{A}} \frac{h(H-h)}{H^2}, \tag{2.56}$$

where

$$E_{\mathrm{A}} \approx \frac{3\pi}{2} \, |\rho_{\mathrm{GJ}}| \, \frac{H^2}{R} \theta_{\mathrm{m}} \cos\varphi_{\mathrm{m}} \tan\chi \sim \varepsilon_{\mathrm{A}} \frac{H}{R} E_{\mathrm{RS}}, \tag{2.57}$$

so that $|E_{\mathrm{A}}| \ll |E_{\mathrm{RS}}|$. Therefore, for this solution to exist, a particle backflow is needed; the value of which can be determined from Eq. (2.44):

$$\frac{j_{\mathrm{back}}}{j_{\mathrm{GJ}}} \approx \varepsilon_{\mathrm{A}} \frac{H}{R} \sim 10^{-4}. \tag{2.58}$$

This model was first studied by J. Arons' group (Fawley et al., 1977; Scharlemann et al., 1978; Arons and Scharlemann, 1979).

Note that the acceleration regime (when the generated longitudinal electric field accelerates particles from the star surface) can occur only on the northern half of the polar cap $-\pi/2 < \varphi_{\mathrm{m}} < \pi/2$ ($A_a > 0$), for which the magnetic field lines bend in the direction of the rotation axis and, hence, $\cos\theta_b$ increases with distance from the star surface. In this case, the generated longitudinal electric field accelerates particles from the star surface. These field lines were called the "preferable" lines. In the domain $\pi/2 < \varphi_{\mathrm{m}} < 3\pi/2$ ($A_a < 0$), where the magnetic field lines, on the contrary, tend to be perpendicular to the rotation axis, the generated longitudinal electric field would lead to the deceleration of particles rather than to their acceleration. As a result, within this model, the acceleration and the generation of the secondary particles occur only in one-half of the region of the open field lines and, accordingly, the radiation directivity pattern should also have the form of a semicircle (Arons and Scharlemann, 1979). However, this conclusion contradicts the observational data (Lyne and Graham-Smith, 1998).

If the bulk particle backflow is absent, Eq. (2.44) yields the completely different solution

$$E_{\parallel} \approx \frac{3\pi}{2} \, |\rho_{\mathrm{GJ}}| \, \theta_{\mathrm{m}} \cos\varphi_{\mathrm{m}} \tan\chi \, \frac{h^2}{R} \sim E_{\mathrm{A}} \frac{h^2}{H^2}, \tag{2.59}$$

in which the longitudinal electric field turns out to be in the opposite direction. Clearly, relation (2.59) can be used only up to distances $h \ll R_0$; at larger distances the longitudinal electric field tends to zero. Consequently, the particle acceleration is possible only on the "unpreferable" magnetic field lines. Exactly this model, in which the particle backflow must naturally be rather small, had been developed for many years by L. Mestel (Mestel and Wang, 1979; Fitzpatrick and Mestel, 1988; Mestel and Shibata, 1994; Mestel, 1999). Thus, only the consistent kinetic model can choose between these two realizations [the thorough investigation of this problem can be found in Shibata (1997) and Shibata et al. (1998)].

2.3.2 Neutron Star Surface

The problem of the neutron star surface structure, which is of interest by itself, is directly associated with the theory of the radio pulsar magnetosphere. Indeed, as was mentioned, the inner gap structure greatly depends on the work function φ_{w} for electrons (the cohesive energy for nuclei) on the neutron star surface. Recall that in the 1970s, the nonfree particle escape model was mainly developed. It was based on a series of theoretical papers on the matter structure in the superstrong magnetic field, in which the work function had a rather large value $\varphi_{\mathrm{w}} \sim$ 1–5 keV (Kadomtsev and Kudryavtsev, 1971; Ginzburg and Usov, 1972; Chen et al., 1974; Hillebrandt and Müller, 1976; Flowers et al., 1977). However, from the early 1980s, when due to the more accurate computations the work function reduced to $\varphi_{\mathrm{w}} \sim 0.1$ keV, the free particle escape models grew in popularity (Müller, 1984; Jones, 1980; Neuhauser et al., 1986).

We stress that the problem remains unsolved. The point is that the accuracy of determination of work function and cohesive energy is not high enough yet (Usov and Melrose, 1996). It turned out that even the chemical composition of the neutron star surface layers is not known—possibly, they do not consist of iron atoms, as was supposed in most papers. The point is that the chemical composition of the surface layers on the polar caps can greatly change because of their bombardment by energetic particles accelerated by the longitudinal electric field in the gap. Besides, and it is the subject of wide speculation now, iron atoms (which, being the most stable nuclei, are, undoubtedly, copiously produced) could have been "sunk" by the action of the gravitational field within the first few years after the formation of the neutron star when its surface was not solid yet (Salpeter and Lai, 1997). It is not improbable, therefore, that, in reality, the neutron star surface layers consist of much lighter atoms rather than iron atoms—hydrogen and helium ones. Since the melting temperature roughly estimated by the formula (Shapiro and Teukolsky, 1983)

$$T_{\mathrm{m}} \approx 3.4 \times 10^7 \, \mathrm{K} \left(\frac{Z}{26}\right)^{5/3} \left(\frac{\rho}{10^6 \mathrm{g/cm^3}}\right) \tag{2.60}$$

depends on the atomic number Z, the neutron star surface at temperature $T \sim 10^6$ K characteristic of ordinary radio pulsars should be liquid and, in any event, must not prevent the free particle escape. The radio pulsar thermal radiation models are just based on this pattern (Zavlin and Pavlov, 2002; Haensel et al., 2007).

2.3.3 Propagation of γ-Quanta in the Superstrong Magnetic Field

We now proceed with a brief discussion of the effects of the propagation of high-energy photons in the superstrong magnetic field in the vicinity of the neutron star surface. This problem is directly associated with the particle generation mechanism in the polar regions of radio pulsars. The quantum effects in the magnetic field, the value of which is close to the critical value $B_\hbar = 4.4 \times 10^{13}$ G (2.28), were known long ago (Berestetsky et al., 1982), but only after the discovery of radio pulsars there was hope of their direct observation. These may include, for example, the photon splitting process $\gamma + B \to \gamma + \gamma + B$ (Bialynicka-Birula and Bialynicka-Birula, 1970; Adler, 1971), the change in the cross-section of the two-photon pair generation $\gamma + \gamma \to e^+ + e^-$, especially near the generation threshold (Kozlenkov and Mitrofanov, 1986), the quantum synchrotron cooling connected with the fast particle transition to the lower Landau level (Mitrofanov and Pozanenko, 1987), as well as the propagation effects due to both the vacuum refraction (Bialynicka-Birula and Bialynicka-Birula, 1970) and the peculiarities of the photon trajectories in the vicinity of the generation threshold of secondary electron–positron pairs (Shabad and Usov, 1984, 1985, 1986). As a result, in the 1970s, the possibility of the direct detection of the effects connected with a quantizing magnetic field (2.28) seemed absolutely real (Mészaros, 1992). Nevertheless, these effects for most radio pulsars appeared rather weak. The point is that, for example, the expression for the refraction index in the strong magnetic field (the formula corresponds to one of the linear polarizations)

$$n = 1 + \frac{7\alpha_{\text{fin}}}{90\pi}\left(\frac{B}{B_\hbar}\right)^2 \tag{2.61}$$

comprises the fine structure constant $\alpha_{\text{fin}} = e^2/\hbar c \approx 1/137$; therefore, we can expect the occurrence of considerable quantum effects only in the fields $B > 10^{14}$ G. For most neutron stars observed as radio pulsars, we can, with adequate accuracy, suppose that γ-quanta propagate rectilinearly.

However, in the context of the discovery of magnetars (pulsating X-ray sources, the periods of which amount to a few seconds and the magnetic field estimated by formula (2.5) reaches 10^{14}–10^{15} G (Thompson and Duncan, 1993; Kouveliotou et al., 1998)), this problem has recently become an urgent one. Therefore, the new thorough computations of both the secondary particle generation process (Weise and Melrose, 2002) and the photon splitting (Baring and Harding, 1997; Chistyakov et al., 1998), and the determination of the trajectories of hard γ-quanta near the

particle generation threshold (Shaviv et al., 1999) were carried out. In particular, it was shown that for sufficiently large magnetic fields $B \sim 10^{14}$–10^{15} G, the process of the γ-quanta conversion due to the photon splitting can be considerably suppressed (Baring and Harding, 1998). Consequently, the secondary plasma generation process can be considerably suppressed as well. It is not surprising, therefore, that most magnetars are not manifested as radio pulsars.

On the other hand, it was shown (Usov, 2002) that the splitting of $\parallel$-polarized photons (i.e., those with the electric vector located in the plane containing the external magnetic field and the wave vector) below the pair production threshold is strictly forbidden in arbitrary magnetic fields. Solving the system of kinetic equations for splitting photons and taking into account their polarization, it was shown that the photon splitting, which was earlier considered as a suppression factor for the secondary electron–positron plasma generation, is not suppressed at all (Istomin and Sobyanin, 2007). Moreover, the plasma density in the magnetar magnetosphere can be even higher than that in the magnetosphere of a pulsar with a weak magnetic field. Thus, some light can be shed on the recent discovery of the pulsed radio emission from several magnetars (Malofeev et al., 2007).

But, in general, the new qualitative phenomena that could be helpful in the observation of the quantum effects in the superstrong magnetic field were not found, and the earlier obtained results were only refined in the computations.

2.3.4 General Relativity Effects

We consider the GR effects which, unlike the quantizing magnetic field effects, can, undoubtedly, greatly affect the particle generation process in the vicinity of radio pulsars. It turned out that in the model of free particle escape from the neutron star surface, the GR effects must be of vital importance. Recall that the gravitational potential φ_g on the pulsar surface is rather large

$$\varepsilon_g = \frac{2|\varphi_g|}{c^2} \approx \frac{2GM}{Rc^2} \sim 0.2, \tag{2.62}$$

and any computations whose accuracy is better than 20% must be carried out, with account taken of the relativistic effects. However, in the nonfree particle escape models, taking account of these effects does not ensure substantial corrections, because the qualitative structure of the electrodynamic equations does not change. On the other hand, in the free particle escape model in Eq. (2.44), besides the small geometric factor ε_A (2.38), the purely relativistic factor ε_g appears, which is associated with the frame-dragging (Lense–Thirring) effect (Thorne et al., 1986). For most radio pulsars with $P \sim 1$ s, the relativistic correction ε_g turns out to be, at least in order of magnitude, larger than ε_A so that the GR effects are to be taken into consideration.

Indeed, as was already mentioned, in the Arons model, the occurrence of longitudinal electric field in the gap region is due to the difference in the plasma charge

density ρ_e from the GJ charge density ρ_{GJ} (2.39). In the general relativistic case, Eq. (2.44) is to be rewritten as (Thorne et al., 1986)

$$\frac{d}{dh}\left(\frac{1}{\alpha}E_{\parallel}\right) = 4\pi(\rho_e - \rho_{GJ}), \tag{2.63}$$

and the GJ density has the form (see Sect. 3.2.5 for details)

$$\rho_{GJ} = -\frac{1}{8\pi^2}\nabla_k\left(\frac{\Omega-\omega}{\alpha c}\nabla^k\Psi\right). \tag{2.64}$$

Here again α is the lapse function, ω is the Lense–Thirring angular velocity, and Ψ is a magnetic flux. Within the necessary accuracy, they can be written as

$$\alpha^2 = 1 - \frac{r_g}{r}, \tag{2.65}$$

$$\omega = \Omega\frac{r_g I_r}{Mr^3}, \tag{2.66}$$

$$\Psi = \frac{1}{2}B_0R^3\frac{\sin^2\theta_m}{r}, \tag{2.67}$$

where B_0 is the magnetic field at the neutron star pole and I_r is its moment of inertia. In the linear order with respect to the small values ε_A and ε_g, we now have

$$\rho_{GJ} = -\frac{(\Omega-\omega)B\cos\theta_b}{2\pi c\alpha}, \tag{2.68}$$

where θ_b is again an angle between the magnetic field line and the rotation axis. On the other hand, the expression for the charge density of the relativistic plasma has the form

$$\rho_e = C(\Psi)\frac{B}{\alpha}, \tag{2.69}$$

where, as before, $C(\Psi)$ is constant along the magnetic field lines. As a result, the GJ charge density (2.68), besides the factor B/α identical to the density ρ_e (2.69), as well as the geometric factor $\cos\theta_b$, also contains the factor $(\Omega-\omega)$, which changes by the dependence of $\omega(r)$ on r. As a result, for $\sin\chi > \varepsilon_A$ and $\cos\chi > \varepsilon_A$, the constant A_a in Eq. (2.53) has the form (Muslimov and Tsygan, 1990; Beskin, 1990; Muslimov and Tsygan, 1992)

$$A_a = \frac{3}{2}\frac{\Omega B_0}{cR}\left[4\frac{\omega}{\Omega}\cos\chi + \theta_m\cos\varphi_m\sin\chi + O(\varepsilon_g^2) + \cdots\right]. \tag{2.70}$$

As we see, taking account of the GR effects leads to the additional term, proportional to $\omega/\Omega \sim \varepsilon_g$. According to (2.70), for $4\,\omega/\Omega > \varepsilon_A\tan\chi$, the major

contribution to A_a is made by the gravitational term. For the homogeneous density of the star when on its surface

$$\frac{\omega}{\Omega} = \frac{2}{5}\varepsilon_{\rm g}, \tag{2.71}$$

this condition can be rewritten as

$$P > 10^{-3}\,{\rm s}\left(\frac{R}{10^6\,{\rm cm}}\right)^2\left(\frac{M}{M_\odot}\right)^{-2}. \tag{2.72}$$

Hence, the GR effects are of vital importance for all observed pulsars. The most important consequence of expression (2.70) is that all open field lines prove "preferable" (Beskin, 1990), because the first term in (2.70) proves positive. Thus, allowance for the GR effects qualitatively changes the conclusions of the first version of the Arons model. The stationary generation becomes possible over the entire polar cap surface.

2.3.5 Particle Generation in the Magnetosphere

We discuss how all the above physical processes affect the particle generation in the vicinity of the neutron star surface. We first consider the effects of the superstrong magnetic field $B > 10^{14}$ G characteristic of magnetars. As was noted, only for these magnetic fields, the pronounced effects of the quantizing magnetic field should be expected (Baring and Harding, 1997; Shaviv et al., 1999). First of all, it was obvious long ago that the strong magnetic field must suppress the secondary plasma generation process. First, with the fields larger than 10^{13} G, a secondary electron–positron pair is to be produced at the lower Landau level, which results in the suppression of the synchrotron radiation (Beskin, 1982; Daugherty and Harding, 1983). Second, the nontrivial vacuum permeability in the vicinity of the generation threshold at the zero Landau level with the transverse photon momentum close to $2m_{\rm e}c$ can give rise to the deflection of the γ-quanta along the magnetic field. As a result, instead of two free particles, their bound state is generated, viz., positronium (Shabad and Usov, 1985, 1986). Third, as was mentioned, the photon splitting process $\gamma \to \gamma + \gamma$ becomes significant, which results in a decrease in their energy and the suppression (though incomplete) of the secondary particle generation (Baring and Harding, 1998). However, most radio pulsars have insufficiently large magnetic fields for these effects to be detected.

On the other hand, for ordinary radio pulsars, the interaction process of primary particles accelerated in the gap, with X-ray photons radiated by the heated neutron star surface, may appear substantial; Kardashev et al. (1984) first pointed to the importance of inverse Compton (IC) scattering in the particle generation region. As it turned out, the hard γ-quanta generated by this interaction have enough energy to produce electron–positron pairs and, hence, affect the inner gap structure (Cheng

et al., 1986; Hirotani and Shibata, 2001). Finally, as was already noted, the value of the work function φ_w also substantially affects the electric field structure.

Nevertheless, in this part of the theory, new important results have recently been obtained. In particular, one should mention A. Harding and A. Muslimov (1998, 2002) who studied both the GR effects and the process of (the nonresonance and resonance) IC scattering of X-ray photons emitted by the neutron star surface. It is interesting to note that in this model, the acceleration region may not be adjacent to the neutron star surface, but it is as if suspended over the magnetic poles of the pulsar. However, as was noted, for a comprehensive analysis, it is necessary to take into account the kinetic effects, as it was first done by Gurevich and Istomin (1985), for the acceleration region in vicinity of the neutron star surface within the nonfree particle escape model (see also Hirotani and Shibata, 2001). Recall that analysis of the kinetic effects is needed, in particular, for the determination of particle backflow, which, in turn, is directly associated with the problem of constructing the plasma generation region.

In conclusion, we emphasize that the general properties of the secondary electron–positron plasma outflowing from the magnetosphere appeared, as a whole, to be low-sensitive to the details of the acceleration region structure. For most models (Ruderman and Sutherland, 1975; Daugherty and Harding, 1982; Gurevich and Istomin, 1985), both the density and the energy spectra of the outflowing plasma appear rather universal. Therefore, it is safe to say that the plasma flowing along the open field lines in the pulsar magnetosphere consists of a beam of primary particles with energy $\varepsilon \approx 10^7$ MeV and density close to the GJ density n_{GJ} and also of the secondary electron–positron component. Its energy spectrum, within adequate accuracy, has the power form

$$N(\varepsilon_e) \propto \varepsilon_e^{-2}, \tag{2.73}$$

and the energies are enclosed in the range from $\varepsilon_{min} \sim 100$ MeV to $\varepsilon_{max} \sim 10^4$–$10^5$ MeV (true, if we suppose the presence of a strong nondipole component near the magnetic poles, the minimum energies can be reduced to 10 MeV and even 3 MeV). Note that the minimum energy ε_{min} directly follows from the estimate (2.31), where for most low-energy particles we should take $l_\gamma = R$, because for longer free paths the decrease in the magnetic field with distance from the neutron star surface is substantial. The total secondary plasma density, as the numerous calculations show, is to be 10^3–10^4 times greater than the GJ density:

$$\lambda = \frac{n_e}{n_{GJ}} \sim 10^3 - 10^4. \tag{2.74}$$

Exactly this model was studied in a great number of papers devoted to the pulsar radio emission theory. It is important that the electron and positron distribution functions must be shifted from one another [this was already shown in Ruderman and Sutherland (1975)]. Only in this case, the outflowing plasma charge density coincides with the GJ charge density.

2.3.6 "Hollow Cone" Model

As was noted, there is no common viewpoint on the nature of the pulsar coherent radio emission now. Nevertheless, it turned out that the basic observed properties of the radio emission can be interpreted by the above particle generation pattern. It is the so-called hollow cone model (Radhakrishnan and Cooke, 1969), which was proposed already at the end of the 1960s and perfectly accounted for the basic geometric properties of the radio emission. Indeed, as was shown, the secondary particle generation is impossible in the rectilinear magnetic field when, first, the intensity of the curvature radiation is low and, second, the photons emitted by relativistic particles propagate at small angles to the magnetic field. Therefore, as shown in Fig. 2.6, in the central regions of the open magnetic field lines, a decrease in secondary plasma density should be expected.

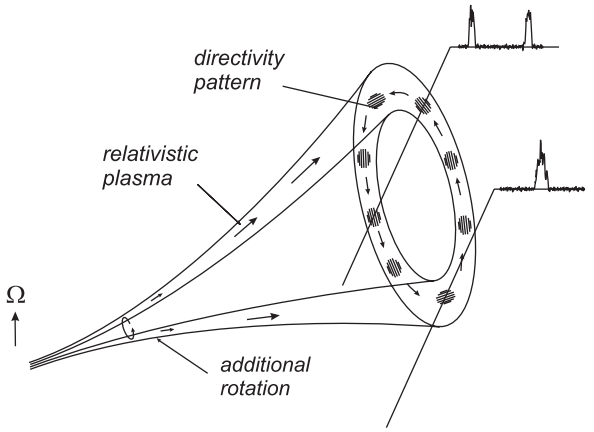

Fig. 2.6 The hollow cone model. If the intensity of the radio emission is directly connected with the outflowing plasma density, in the center of the directivity pattern there must be a decrease in the radio emission. Therefore, we should expect a single mean profile in pulsars whose line of sight intersects the directivity pattern far from its center and the double profile for the central passage. The plasma rotation around the magnetic axis leads to the observed subpulse drift

If we make a rather reasonable assumption that the radio emission must be directly connected with the outflowing plasma density, there must be a decrease in the radio emission intensity in the center of the directivity pattern. Therefore, without going into details (actually, the mean profiles have a rather complex structure (Rankin, 1983, 1990; Lyne and Graham-Smith, 1998)), we should expect a single (one-hump) mean profile in pulsars in which the line of sight intersects the directivity pattern far from its center and the double (two-hump) profile for the central passage. It is exactly what is observed in reality (Beskin et al., 1993; Lyne and Graham-Smith, 1998).

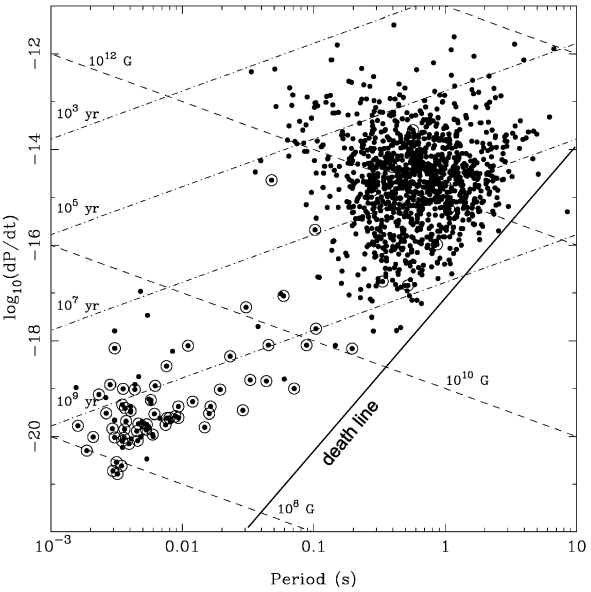

Fig. 2.7 Pulsar distribution in the P–$\dot{P}$ diagram. *Encircled dots* indicate radio pulsars in binary systems. *Dashed lines* indicate magnetic field B_0 evaluated by magnetodipole formula (2.5), *dashed and dotted lines* indicate dynamical age τ_D (Seiradakis and Wielebinski, 2004). The *death line* corresponds to the relation $H = R_0$

As a result, it was possible to explain all the basic properties of the pulsar radio emission such as

- the death line in the P–$\dot{P}$ diagram (see Fig. 2.7);
- the statistical distribution of pulsars with single and double mean profiles (double profiles are mainly observed in pulsars in the vicinity of the death line when particles can be generated only in a thin ring in the vicinity of the polar cap boundary) (Beskin et al., 1993);
- the characteristic S-shaped change in the position angle of the linear polarization along the mean profile (Radhakrishnan and Cooke, 1969) (as shown in Fig. 2.8, the complete change in the position angle is close to 180° if the line of sight

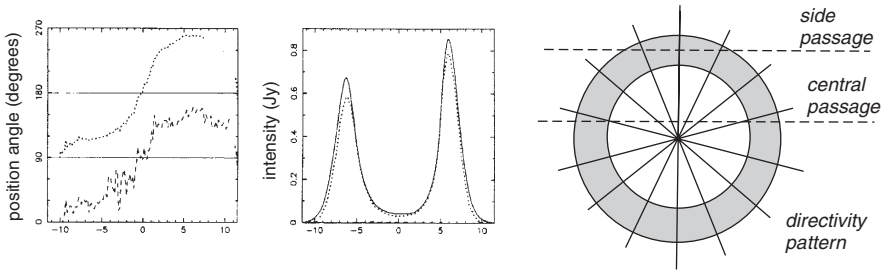

Fig. 2.8 The change in the position angle (*left panel*) of two linear polarizations along the double mean profile, which is naturally connected with the change in the magnetic field orientation (*right panel, radial lines*) in the picture plane. With the central passage of the directivity pattern, the change in the position angle is close to 180° (with side passage, it is much less)

intersects the directivity pattern in the vicinity of its center and the small change in the periphery passage); and also

- the radio window width $W_{\rm d}$ and even its statistical dependence on the pulsar period (Rankin, 1990; Beskin et al., 1993).

The latter circumstance is based on the assumption that the generation of radio emission in all pulsars occurs roughly at the same distance $r_{\rm rad}$ from the neutron star. We thus have for the width of the directivity pattern $W_{\rm d}$

$$W_{\rm d} \approx \left(\frac{\Omega r_{\rm rad}}{c}\right)^{1/2} \approx 10^{\circ} P^{-1/2} \left(\frac{r_{\rm rad}}{10R}\right)^{1/2}, \tag{2.75}$$

i.e., $W_{\rm d} \propto P^{-1/2}$, which is in agreement with the observations.

As to the death line, it is natural to connect it with the termination of the secondary plasma generation in the vicinity of the magnetic poles. Indeed, as was mentioned, the radio emission must be generated by the secondary electron–positron plasma produced in neutron star polar regions. Therefore, the condition

$$H(P, B) = R_0(P) \tag{2.76}$$

(i.e., $\psi = \psi_{\max}$) can be regarded as an "ignition condition" dividing the active and passive ranges of parameters when the neutron star does not manifest itself as a radio pulsar. In the nonfree particle escape model, relation (2.76) can be rewritten as (Ruderman and Sutherland, 1975; Beskin et al., 1984)

$$P_{\max} \approx 1\text{s} \left(\frac{B_0}{10^{12}\,\text{G}}\right)^{8/15} \approx 1\text{–}3\,\text{s}. \tag{2.77}$$

This condition is usually represented as a "death line" in the P–$\dot{P}$ diagram. This satisfactory agreement can, unconditionally, be regarded as the confirmation of the pattern discussed here. For the free particle escape model, because of the much smaller values of the accelerating potential, the limit period must be smaller:

$$P_{\max} = 0.1 - 0.3\,\text{s}. \tag{2.78}$$

The expectations that $P_{\max}$ can be increased by taking account the GR effects were not realized (Arons, 1998). Here there are still different solutions, for example, a dipole displacement from the neutron star center (Arons, 1998) or the existence of a rather strong nondipole magnetic field near the neutron star surface (Gil and Melikidze, 2002; Asséo and Khechinashvili, 2002; Kantor and Tsygan, 2003), which results in a decrease in the curvature of the magnetic field lines $R_{\rm c}$ and, hence, in an increase in the particle generation efficiency. Nevertheless, as we see, the free particle escape models encounter certain difficulties.

Note also that for the nonfree particle escape models, it is convenient to introduce the dimensionless parameter Q

$$Q = 2\left(\frac{P}{1\,s}\right)^{11/10}\left(\frac{\dot{P}}{10^{-15}}\right)^{-4/10}, \tag{2.79}$$

determined, as we see, directly from the observations. It turns out to be an extremely convenient parameter characterizing the main characteristics of radio pulsars (Beskin et al., 1984; Taylor and Stinebring, 1986; Rankin, 1990). For example, the ratios of the inner radius of the hollow cone near the star surface $r_{\rm in}$ and the inner gap height H to the polar cap radius R_0 are written as

$$\frac{r_{\rm in}}{R_0} \approx Q^{7/9}, \tag{2.80}$$

$$\frac{H}{R_0} \approx Q. \tag{2.81}$$

Therefore, the pulsars with $Q > 1$, in which the directivity pattern is a rather narrow cone, mostly have a double mean profile of the radio emission. It is in these pulsars that various irregularities, such as the full radio emission termination (nulling), mode switching, are detected. Conversely, the pulsars with $Q \ll 1$ ($r_{\rm in} \ll R_0$) are characterized by stable radio emission, and their mean profiles are mostly of a single type.

Finally, some properties of radio pulsars (for example, subpulse drift) indirectly confirm the existence of the potential drop and the particle acceleration over the magnetic poles of the neutron star (Ruderman and Sutherland, 1975). Indeed, if in the vicinity of the pulsar surface there is a longitudinal electric field region on the open field lines, an additional potential difference develops between the central and periphery domains over the acceleration region so that the additional electric field is directed to or from the magnetic axis (see Fig. 2.9). As a result, besides the general motion around the rotation axis, the additional electric drift results in the plasma

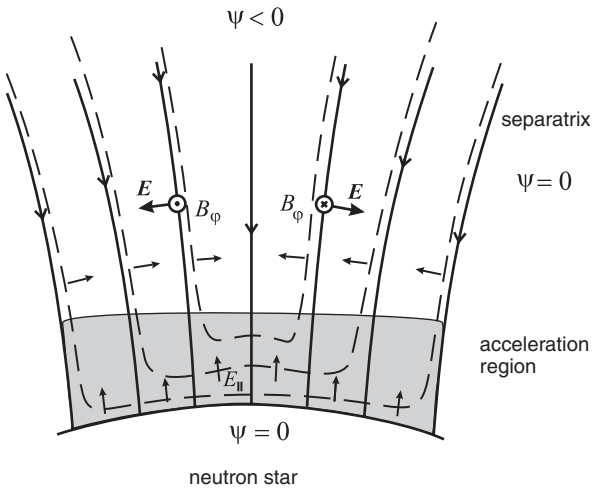

Fig. 2.9 Equipotential surfaces $\psi = \text{const}$ (*dashed lines*) in the region of the open field lines. The potential drop in the acceleration region gives rise to an additional potential difference between the magnetic surfaces. The electric drift produced by the additional electric field (*fine arrows*) results in an additional plasma rotation around the magnetic axis

rotation around the magnetic axis, which, in turn, can be observed as the regular drift of radiating regions within the mean pulse (see Fig. 2.6). About 200 radio pulsars with drifting subpulses are known now (Lyne and Graham-Smith, 1998; Weltevrede et al., 2007).

2.3.7 Secondary Plasma Generation—"Outer Gap"

Finally, we should point to another particle generation mechanism that can occur already far from the neutron star. As seen from Fig. 2.3, on some open field lines, where $\mathbf{\Omega} \cdot \mathbf{B} = 0$, the charge density, according to (2.39), changes the sign. Clearly, the charge-separated plasma outflowing from the star could not ensure the fulfillment of the condition $\rho_e = \rho_{GJ}$. Therefore, the hypothesis for the existence of an "outer gap" in the vicinity of the line ρ_{GJ}=0 was put forward, in which the emerging longitudinal electric field also produces the secondary plasma. However, since, because of a weak magnetic field, the one-photon conversion becomes impossible, the main particle generation mechanism is the two-photon conversion process $\gamma + \gamma \rightarrow e^+ + e^-$ (Cheng et al., 1986). At present, the thorough computations of cascade processes in the outer gap were carried out and their aim was to explain the high-energy radiation of radio pulsars (Chiang and Romani, 1994; Zhang and Cheng, 1997; Cheng et al., 2000; Hirotani and Shibata, 2001). The chain of processes is the following:

1. The occurrence of the longitudinal electric field, because the condition $\rho_e = \rho_{GJ}$ cannot be satisfied.
2. The acceleration of primary particles.
3. The emission of curvature photons.
4. The IC scattering of thermal X-ray photons emitted from the neutron star surface.
5. The secondary particles generated by the collision of high-energy IC γ-quanta with soft X-ray photons.

Certainly, in the real conditions, plasma outflowing from the magnetosphere contains particles of both signs so that, in principle, the condition $\rho_e = \rho_{GJ}$ could be satisfied by slightly changing the longitudinal particle velocities. However, this problem, which requires, generally speaking, kinetic analysis, has not been solved yet (see, e.g., Lyubarskii, 1995).

2.4 Pulsar Equation

2.4.1 Force-Free Approximation. The Magnetization Parameter

Let us return to our main subject and place a force-free limit to the GS equation. For this approximation to be used, it is necessary that

1. the plasma energy density $\epsilon_{\rm part}$ is much smaller than the energy density of the electromagnetic field $\epsilon_{\rm em}$;
2. the amount of plasma is enough to screen the longitudinal electric field $E_\parallel$.

The force-free approximation must be valid in the radio pulsar magnetosphere with large margin, because the plasma filling the magnetosphere is secondary with respect to the magnetic field. Following Michel (1969), for a quantitative estimate, one can introduce the magnetization parameter

$$\sigma = \frac{e\Omega\Psi_{\rm tot}}{4\lambda m_{\rm e}c^3}, \tag{2.82}$$

where $\Psi_{\rm tot}$ is the total magnetic flux and $\lambda = n/n_{\rm GJ}$ (2.74) is the multiplicity of particle generation. One should, however, stress that in Michel (1969), the case of the monopole magnetic field was considered for simplicity. Therefore, we must be careful when determining this value for concrete astrophysical objects. In particular, for radio pulsars

$$\Psi_{\rm tot} \approx \pi B_0 R_0^2 \approx \pi B_0 R^2 \frac{\Omega R}{c}, \tag{2.83}$$

which corresponds to the magnetic flux only in the region of open field lines. Therefore, for the radio pulsar magnetosphere

$$\sigma = \frac{eB_0\Omega^2 R^3}{4\lambda m_{\rm e}c^4}. \tag{2.84}$$

As a result, the smallness condition of the particle contribution to the energy–momentum tensor $T^{\alpha\beta}_{\rm part} \ll T^{\alpha\beta}_{\rm em}$ up to the light cylinder can be written as

$$\sigma \gg \gamma_{\rm in}. \tag{2.85}$$

Here $\gamma_{\rm in} \sim 10^2$–$10^4$ is the characteristic Lorentz factor of the plasma near the star surface.

Problem 2.11 Using definitions (2.74) and (2.84), check that relation (2.85) really corresponds to the smallness condition of the particle contribution (up to the light cylinder!) for the component T^{00}, i.e., for the energy density.

The magnetization parameter is one of the key dimensionless parameters characterizing the relativistic plasma moving in the magnetic field. As we see, up to the factor $\gamma_{\rm in}$, it coincides with the ratio of the electromagnetic energy flux to the particle energy flux. In particular, the large value of σ shows that the main contribution to the energy flux in the interior regions of the magnetosphere is made by the electromagnetic flux. For the characteristic parameters of radio pulsar ($P{\sim}1$ s, $B_0{\sim}10^{12}$

G), we have $\sigma\sim10^4$–10^5, and only for the youngest ones ($P\sim0.1$ s, $B_0\sim10^{13}$ G) the value $\sigma\sim10^6$. Nevertheless, the condition $\sigma \gg \gamma_{\rm in}$ turns out to be satisfied. As to the screening of longitudinal electric field, this condition must also be satisfied with large margin by relation $\lambda \gg 1$ (2.74).

Thus, in the zero order with respect to the parameters σ^{-1} and λ^{-1}, the radio pulsar magnetosphere can actually be described by the force-free approximation. The force-free approximation implies that in the general equation—the energy–momentum conservation law $\nabla_\alpha T^{\alpha\beta} = 0$—we can now disregard the particle contribution. Using the explicit form of the energy–momentum tensor of the electromagnetic field (Landau and Lifshits, 1989)

$$T^{\alpha\beta}_{\rm em} = \begin{pmatrix} \dfrac{(E^2+B^2)}{8\pi} & \dfrac{c}{4\pi}\,\mathbf{E}\times\mathbf{B} \\ \dfrac{c}{4\pi}\,\mathbf{E}\times\mathbf{B} & -\dfrac{1}{4\pi}\,(E^iE^k + B^iB^k) + \dfrac{1}{8\pi}(E^2+B^2)\,\delta^{ik} \end{pmatrix}, \tag{2.86}$$

we obtain for the space components the known equation

$$\frac{1}{c}\mathbf{j}\times\mathbf{B} + \rho_{\rm e}\mathbf{E} = 0, \tag{2.87}$$

or

$$[\nabla\times\mathbf{B}]\times\mathbf{B} + (\nabla\cdot\mathbf{E})\,\mathbf{E} = 0. \tag{2.88}$$

Equation (2.87) in the nonrelativistic limit naturally reduces to zero of Ampére's force $\mathbf{F}_{\rm A} = \mathbf{j}\times\mathbf{B}/c$. Therefore, the approximation studied is called the force-free approximation.

2.4.2 Integrals of Motion

Recall now that we are, first of all, interested in axisymmetric stationary configurations. In this case, it is convenient to take, as an unknown variable, the magnetic flux function $\Psi(r,\theta)$. Strictly, it was just the method first successfully used by H. Grad (1960) and V.D. Shafranov (1958).

Thus, we write the magnetic field as

$$\mathbf{B} = \frac{\nabla\Psi\times\mathbf{e}_\varphi}{2\pi\varpi} - \frac{2I}{c\varpi}\mathbf{e}_\varphi, \tag{2.89}$$

dependent on two scalar functions $\Psi(r,\theta)$ and $I(r,\theta)$. Here the numerical coefficient in the first term is chosen so that the function $\Psi(r,\theta)$ coincides with the magnetic flux passing through the circle $r,\ \theta,\ 0<\varphi<2\pi$ (see Fig. 2.10).

Indeed, the definition of the magnetic flux function is quite analogous to that of the stream function $\Phi(r,\theta)$ (1.90) introduced in Sect. 2.4.2. Therefore, all the basic properties retain.

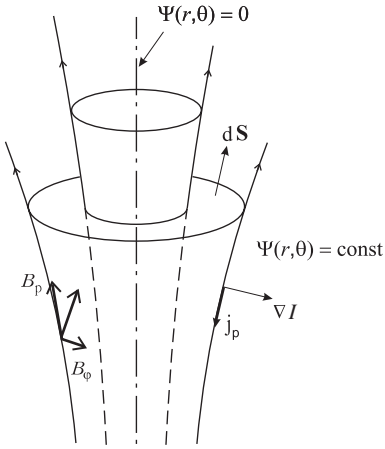

Fig. 2.10 Axisymmetric magnetic surfaces $\Psi(r,\theta) =$ const. For the case $\Psi > 0$, the GJ charge density $\rho_{GJ} < 0$. Therefore, in the vicinity of the north polar cap, I is positive and the current $\mathbf{j}_p$ is antiparallel to the magnetic field $\mathbf{B}$

- The condition $d\Psi = \mathbf{B} \cdot d\mathbf{S}$ is always satisfied ($d\mathbf{S}$—an area element). Therefore, the function $\Psi(r,\theta)$ has the meaning of a magnetic flux.
- The condition $\nabla \cdot \mathbf{B} = 0$ is satisfied automatically. Therefore, three magnetic field components are fully specified by two scalar functions $\Psi(r,\theta)$ and $I(r,\theta)$.
- The condition $\mathbf{B} \cdot \nabla\Psi = 0$ is also satisfied. Therefore, the lines $\Psi(r,\theta) =$ const prescribe the form of the magnetic surfaces.

As to $I(r,\theta)$, it is the total electric current passing through the same circle. We can easily verify this fact by the obvious relation $\int B_\varphi d\varphi = -(4\pi/\varpi c)I$. The minus sign in this expression and in the toroidal magnetic field expression (2.89) is chosen from the condition that the value I is positive for the electric current connected with the GJ charge density outflow. For the case $\Psi > 0$ shown in Fig. 2.10, the GJ charge density is negative, viz., $\rho_{GJ} < 0$ (and, conversely, $\rho_{GJ} > 0$ for $\Psi < 0$). Therefore, in the vicinity of the north polar cap, the current $\mathbf{j}_p$ is always antiparallel to the magnetic field $\mathbf{B}$. Having written the definition of the poloidal density of the electric current as

$$\mathbf{j}_p = -\frac{\nabla I \times \mathbf{e}_\varphi}{2\pi\varpi}, \tag{2.90}$$

we obtain the same set of properties as for the magnetic flux function.

- The condition $dI = -\mathbf{j} \cdot d\mathbf{S}$ is satisfied. Therefore, the function $I(r,\theta)$ has the meaning of the total electric current inflowing into the magnetosphere.
- The continuity condition $\nabla \cdot \mathbf{j} = 0$ is satisfied automatically (recall that we consider the stationary configurations only).
- The condition $\mathbf{j} \cdot \nabla I = 0$ is satisfied. Therefore, the lines $I(r,\theta) =$ const prescribe the form of the current surfaces in the magnetosphere.

Finally, the toroidal electric current can easily be determined from the φ-component of Maxwell's equation $\nabla \times \mathbf{B} = (4\pi/c)\mathbf{j}$. Thus, using the definition (2.89), we have

$$j_\varphi = -\frac{c}{8\pi^2 r \sin\theta}\left[\frac{\partial^2\Psi}{\partial r^2} + \frac{\sin\theta}{r^2}\frac{\partial}{\partial\theta}\left(\frac{1}{\sin\theta}\frac{\partial\Psi}{\partial\theta}\right)\right]. \tag{2.91}$$

As we see, in the definition of the toroidal current density j_φ, the known operator $\hat{\mathcal{L}} = \varpi^2\nabla_k\left(\varpi^{-2}\nabla^k\right)$ (1.119) written in the spherical coordinates is available again. On the other hand, when investigating the radio pulsar magnetosphere, as we will see, it is more convenient to use the cylindrical coordinates (ϖ, z). In this case, the expression for the toroidal current density looks like

$$j_\varphi = -\frac{c}{8\pi^2\varpi}\left[\nabla^2\Psi - \frac{2}{\varpi}\frac{\partial\Psi}{\partial\varpi}\right]. \tag{2.92}$$

We now proceed to the electric field definition. Naturally, it has three independent components in the general case. However,

1. Maxwell's equation $\nabla \times \mathbf{E} = 0$, in the axisymmetric case, yields the condition $E_\varphi = 0$;
2. the full screening assumption yields $E_\parallel = 0$.

Thus, it is convenient to write the electric field as

$$\mathbf{E} = -\frac{\Omega_\mathrm{F}}{2\pi c}\nabla\Psi, \tag{2.93}$$

i.e., express it in terms of one scalar function $\Omega_\mathrm{F}(r, \theta)$.

This expression yields the following important properties:

- The condition $\mathbf{E}\cdot\mathbf{B} = 0$ is satisfied automatically.
- From Maxwell's equation $\nabla \times \mathbf{E} = 0$, it follows that $\nabla\Omega_\mathrm{F} \times \nabla\Psi = 0$. In the axisymmetric case, where all the values depend only on two variables, this implies that

$$\Omega_\mathrm{F} = \Omega_\mathrm{F}(\Psi), \tag{2.94}$$

  i.e., the surfaces $\Omega_\mathrm{F}(r, \theta) = \text{const}$ are to coincide with the magnetic surfaces $\Psi(r, \theta) = \text{const}$.
- The drift velocity $\mathbf{U}_\mathrm{dr} = c\,\mathbf{E}\times\mathbf{B}/B^2$, as was mentioned, is now written as

$$\mathbf{U}_\mathrm{dr} = \boldsymbol{\Omega}_\mathrm{F}\times\mathbf{r} + j_\parallel\mathbf{B}, \tag{2.95}$$

  where again $j_\parallel$ is some scalar function. As we see, the introduced function Ω_F has the meaning of the angular velocity of particles moving in the magnetosphere. The condition (2.94) is the known Ferraro isorotation law (Ferraro, 1937; Alfven and Fälthammar, 1963) according to which the particle angular velocity is to be constant on the axisymmetric magnetic surfaces.

Finally, using definitions (2.89) and (2.90) for $\mathbf{B}$ and $\mathbf{j}_{\rm p}$, we can write the toroidal component of Eq. (2.88) as $[\nabla I \times \mathbf{e}_\varphi] \times [\nabla \Psi \times \mathbf{e}_\varphi] = \nabla I \times \nabla \Psi = 0$. Consequently, the total current inside the magnetic surface is also an integral of motion:

$$I = I(\Psi). \tag{2.96}$$

Problem 2.12 Show that in the force-free limit the total energy and angular momentum losses are now defined as

$$W_{\rm tot} = \frac{1}{c}\int E(\Psi){\rm d}\Psi, \qquad K_{\rm tot} = \frac{1}{c}\int L(\Psi){\rm d}\Psi, \tag{2.97}$$

where

$$E(\Psi) = \frac{\Omega_{\rm F} I}{2\pi}, \tag{2.98}$$

$$L(\Psi) = \frac{I}{2\pi}. \tag{2.99}$$

2.4.3 Grad–Shafranov Equation

We are now ready to formulate the GS equation describing the poloidal structure of the magnetic field. As in the hydrodynamical case, we write the poloidal component of Eq. (2.87) as

$$\frac{j_\varphi}{c}\nabla\Psi + \frac{B_\varphi}{c}\nabla I - \frac{\nabla\cdot\mathbf{E}}{4\pi}\frac{\Omega_{\rm F}}{2\pi\varpi}\nabla\Psi = 0. \tag{2.100}$$

This vector equation, under the condition $\nabla I = ({\rm d}I/{\rm d}\Psi)\nabla\Psi$ resulting from (2.96), can again be reduced to the scalar equation multiplied by $\nabla\Psi$. In the cylindrical coordinates, it has the form

$$-\left(1-\frac{\Omega_{\rm F}^2\varpi^2}{c^2}\right)\nabla^2\Psi + \frac{2}{\varpi}\frac{\partial\Psi}{\partial\varpi} - \frac{16\pi^2}{c^2}I\frac{{\rm d}I}{{\rm d}\Psi} + \frac{\varpi^2}{c^2}(\nabla\Psi)^2\,\Omega_{\rm F}\frac{{\rm d}\Omega_{\rm F}}{{\rm d}\Psi} = 0, \tag{2.101}$$

where ∇^2 is the Laplace operator. It is just the pulsar equation obtained in dozens of papers in the 1970s (see, e.g., Mestel (1973); Scharlemann and Wagoner (1973); Michel (1973a); Mestel and Wang (1979); the final version containing the latter term was deduced by Okamoto (1974)). The nonrelativistic version of the force-free GS equation is formulated in Appendix B.

The pulsar equation has the following properties:

- As any GS equation, it comprises only the stream function $\Psi(\varpi, z)$ and the invariants $\Omega_{\rm F}(\Psi)$ and $I(\Psi)$.
- On the other hand, the force-free equation does not contain any additional parameters associated with the plasma properties; therefore, it must not be supplemented with Bernoulli's equation.
- Equation (2.101) remains elliptic over the entire space where it is defined; this observation, as we will see, is very important. Indeed, the force-free equation (2.87) has meaning only if the condition $|\mathbf{E}| < |\mathbf{B}|$ is satisfied, whereas Eq. (2.101) can formally be extended to the nonphysical domain $|\mathbf{E}| > |\mathbf{B}|$.
- The differential operator

$$\hat{\mathcal{L}}_{\rm psr} = \left(1 - \frac{\Omega_{\rm F}^2 \varpi^2}{c^2}\right) \nabla^2 \Psi - \frac{2}{\varpi} \frac{\partial \Psi}{\partial \varpi} \tag{2.102}$$

  is linear in the derivatives Ψ; for $\Omega_{\rm F} = \text{const}$, all nonlinearity of the pulsar equation is only in the last two terms associated with the integrals of motion.
- The differential operator (2.102) does not explicitly contain the coordinate z.
- At small distances, as compared to the light cylinder radius $\varpi \ll R_{\rm L}$, the differential operator $\mathcal{L}_{\rm psr}$ coincides with $\hat{\mathcal{L}}$ (1.119).
- The equation contains one critical surface—the light cylinder $\varpi_{\rm L} = c/\Omega_{\rm F}$.
- For known flow structure (i.e., given $\Psi(\varpi, z)$, $\Omega_{\rm F}(\Psi)$, and $I(\Psi)$), the electric field and the toroidal component of the magnetic field are specified from the algebraic relations.
- According to the general formula $b = 2 + i - s'$ for the number of boundary conditions, we have $b = 3$, i.e., the problem requires three boundary conditions.

For example, within the analytical approach, it is convenient to take, as such boundary conditions, two integrals of motion $\Omega_{\rm F} = \Omega_{\rm F}(\Psi)$ and $I = I(\Psi)$, as well as the normal component of the magnetic field on the neutron star surface $r = R$ or, what is the same, the magnetic flux $\Psi = \Psi(R,\theta)$. Thus, for example, for the dipole magnetic field

$$\Psi(R, \theta) \approx |\mathbf{m}| \frac{\sin^2 \theta}{R}. \tag{2.103}$$

Here $\mathbf{m}$ is the magnetic moment of the neutron star. But in this case, it is not clear whether the solution can be extended to infinity. Therefore, in numerical simulations, one generally uses another set of boundary conditions, viz., the angular velocity $\Omega_{\rm F} = \Omega_{\rm F}(\Psi)$ and the magnetic flux Ψ both on the neutron star surface and "at infinity" (i.e., on the outer boundary of the computational domain). Then the current $I(\Psi)$ is to be determined from the solution.

It is very important that Eq. (2.101) contains two key values—the longitudinal current I and the angular rotational velocity $\Omega_{\rm F}$, the latter is directly associated with the voltage drop in the inner gap. Indeed, as shown in the following section, the

electric and magnetic fields for the arbitrary inclination angle χ must be connected by the relation

$$\mathbf{E} + \frac{\Omega \times \mathbf{r}}{c} \times \mathbf{B} = -\nabla\psi, \tag{2.104}$$

where ψ at small distances $\varpi \ll R_{\mathrm{L}}$ has the meaning of the electric potential in the rotating coordinate system. In particular, since in the interior of a perfectly conducting star $\mathbf{E}_{\mathrm{in}} + (\Omega \times \mathbf{r}/c) \times \mathbf{B}_{\mathrm{in}} = 0$, we have $\psi_{\mathrm{in}} = 0$. On the other hand, for the case of the zero longitudinal electric field $E_{\parallel} = 0$, we have $\mathbf{B} \cdot \nabla\psi = 0$. Thus, in the domain, where the condition $E_{\parallel} = 0$ is satisfied, the potential ψ must be constant on the magnetic surfaces

$$\psi = \psi(\Psi). \tag{2.105}$$

Hence, in the region of the closed magnetic field lines (i.e., the field lines not outgoing beyond the light cylinder), we simply have $\psi = 0$. On the other hand, in the region of the open field lines, which are separated from the neutron star by the longitudinal electric field region, the potential ψ is different from zero (see Fig. 2.9). Its value coincides with the electric potential drop in the particle generation region. The occurrence of the nonzero potential ψ in the region of the open field lines leads to additional plasma rotation around the magnetic axis, which is observed as a subpulse drift (see Fig. 2.6).

Indeed, using the definition of the electric field (2.93), we find that in the axisymmetric case the angular velocity Ω_{F} can be written as

$$\Omega_{\mathrm{F}} = \Omega + 2\pi c \frac{\mathrm{d}\psi}{\mathrm{d}\Psi}. \tag{2.106}$$

It is easy to verify that the derivative $\mathrm{d}\psi/\mathrm{d}\Psi$ is always negative, so the plasma angular velocity Ω_{F} is always smaller than the angular velocity of the neutron star Ω. The value $\psi(P, B_0)$ is determined by the concrete particle generation mechanism. In the following, it is convenient to introduce the dimensionless accelerating potential

$$\beta_0 = \frac{\psi(P, B_0)}{\psi_{\max}}, \tag{2.107}$$

where $\psi_{\max}$ (2.43) is the maximum potential drop in the acceleration region. As a result, the angular velocity Ω_{F} over the acceleration region, where the secondary plasma screens the longitudinal electric field (and, therefore, the GS equation method can be used), is simply determined by $\Omega_{\mathrm{F}} = (1 - \beta_0)\Omega$. As to the longitudinal currents, it is convenient to normalize them to the GJ current density $j_{\mathrm{GJ}} = c\rho_{\mathrm{GJ}}$. As a result, we can write

$$I(\Psi_{\mathrm{tot}}) = i_0 I_{\mathrm{GJ}}, \tag{2.108}$$

where

$$I_{\rm GJ} = \frac{B_0 \Omega^2 R^3}{2c} \tag{2.109}$$

is the characteristic total current across the polar cap surface.

2.4.4 Mathematical Intermezzo—Quasistationary Formalism

In this section, we call attention to some relations involving the quasistationary generalization of the above equations describing the magnetosphere of an inclined rotator. The assumption of quasistationarity implies that we consider the electromagnetic fields that depend on time t and angular coordinate φ only in $\varphi - \Omega t$ combination. Note that the condition for quasistationarity is wider than the condition for time independence of all values in the reference frame rotating with angular velocity Ω, because the quasistationarity condition can be extended beyond the light cylinder where the rotation with angular velocity Ω is impossible. In particular, the spherical wave (2.15), (2.16), (2.17), (2.18), (2.19), and (2.20) emitted by the rotating neutron star in vacuum satisfies the quasistationarity condition.

When the time dependence is available in all equations only in the $\varphi - \Omega t$ combination, all time derivatives can be replaced by derivatives with respect to the coordinates using the relations (Mestel, 1973)

$$\frac{\partial}{\partial t} Q = -\Omega \frac{\partial}{\partial \varphi} Q, \tag{2.110}$$

$$\frac{\partial}{\partial t} \mathbf{V} = -(\Omega \times \mathbf{r}, \nabla)\mathbf{V} + \Omega \times \mathbf{V} \tag{2.111}$$

for the arbitrary scalar $Q(\varpi, \varphi - \Omega t, z)$ and the vector $\mathbf{V}(\varpi, \varphi - \Omega t, z)$ fields. Using now the known vector relation $\nabla \times [\mathbf{U} \times \mathbf{V}] = -(\mathbf{U}\nabla)\mathbf{V} + (\mathbf{V}\nabla)\mathbf{U} + (\nabla \cdot \mathbf{V})\mathbf{U} - (\nabla \cdot \mathbf{U})\mathbf{V}$, we can rewrite the condition (2.111) as

$$\frac{1}{c} \frac{\partial}{\partial t} \mathbf{V} = \nabla \times [\boldsymbol{\beta}_{\rm R} \times \mathbf{V}] - (\nabla \cdot \mathbf{V})\boldsymbol{\beta}_{\rm R}. \tag{2.112}$$

Hereafter, by definition,

$$\boldsymbol{\beta}_{\rm R} = \frac{\Omega \times \mathbf{r}}{c} \tag{2.113}$$

is the corotation vector. As is easily checked, $\nabla \cdot \boldsymbol{\beta}_{\rm R} = 0$.

Problem 2.13 Check relations (2.110), (2.111), and (2.112).

Using relations (2.110), (2.111), and (2.112), we can rewrite Maxwell's equation as

$$\nabla \cdot \mathbf{E} = 4\pi\rho_{\mathrm{e}}, \tag{2.114}$$

$$\nabla \times \mathbf{E} = -\nabla \times [\boldsymbol{\beta}_{\mathrm{R}} \times \mathbf{B}], \tag{2.115}$$

$$\nabla \cdot \mathbf{B} = 0, \tag{2.116}$$

$$\nabla \times \mathbf{B} = \nabla \times [\boldsymbol{\beta}_{\mathrm{R}} \times \mathbf{E}] + \frac{4\pi}{c}\mathbf{j} - 4\pi\rho_{\mathrm{e}}\boldsymbol{\beta}_{\mathrm{R}}. \tag{2.117}$$

Equation (2.115) just yields relation $\mathbf{E} + \boldsymbol{\beta}_{\mathrm{R}} \times \mathbf{B} = -\nabla\psi$ (2.104), where

$$\psi = \Phi_{\mathrm{e}} - (\boldsymbol{\beta}_{\mathrm{R}} \cdot \mathbf{A}), \tag{2.118}$$

and Φ_{e} and $\mathbf{A}$ are, respectively, the scalar and vector potentials of the electromagnetic field.

If the $(4\pi/c)\mathbf{j} - 4\pi\rho_{\mathrm{e}}\boldsymbol{\beta}_{\mathrm{R}}$ combination in (2.117) is also zero (for example, this is the case for the vacuum approximation), this equation can be resolved as

$$\mathbf{B} - \boldsymbol{\beta}_{\mathrm{R}} \times \mathbf{E} = -\nabla h, \tag{2.119}$$

where $h(\varpi, \varphi - \Omega t, z)$ is an arbitrary scalar function. In this case, the electric and magnetic fields are expressed in terms of the potentials ψ and h as

$$\mathbf{E}_{\mathrm{p}} = \frac{1}{1 - \boldsymbol{\beta}_{\mathrm{R}}^2}\left(-\nabla\psi + \boldsymbol{\beta}_{\mathrm{R}} \times \nabla h\right), \tag{2.120}$$

$$E_{\varphi} = -\frac{1}{\varpi}\frac{\partial\psi}{\partial\varphi}, \tag{2.121}$$

$$\mathbf{B}_{\mathrm{p}} = \frac{1}{1 - \boldsymbol{\beta}_{\mathrm{R}}^2}\left(-\nabla h - \boldsymbol{\beta}_{\mathrm{R}} \times \nabla\psi\right), \tag{2.122}$$

$$B_{\varphi} = -\frac{1}{\varpi}\frac{\partial h}{\partial\varphi}. \tag{2.123}$$

Substituting these expressions in equations $\nabla \cdot \mathbf{E} = 0$ and $\nabla \cdot \mathbf{B} = 0$ valid for the vacuum case, we obtain the system of equations (Beskin et al., 1993)

$$\hat{\mathcal{L}}_2\psi - \frac{2}{1 - x_r^2}\frac{\partial h}{\partial z'} = 0, \tag{2.124}$$

$$\hat{\mathcal{L}}_2 h + \frac{2}{1 - x_r^2}\frac{\partial\psi}{\partial z'} = 0, \tag{2.125}$$

where $x_r = \Omega\varpi/c$, $z' = \Omega z/c$, and the operator $\hat{\mathcal{L}}_2$ is

$$\hat{\mathcal{L}}_2 = \frac{\partial^2}{\partial x_r^2} + \frac{1}{x_r}\frac{1+x_r^2}{1-x_r^2}\frac{\partial}{\partial x_r} + \frac{1-x_r^2}{x_r^2}\frac{\partial^2}{\partial \varphi^2} + \frac{\partial^2}{\partial z'^2}. \tag{2.126}$$

Problem 2.14 Check that the solutions to system (2.124) and (2.125) for the orthogonal rotator (i.e., if $\sin\chi = 1$)

$$h = |\mathbf{m}|\sin\theta\,\mathrm{Re}\left(\frac{1}{r^2} - \mathrm{i}\frac{\Omega}{c}\frac{1}{r} - \frac{\Omega^2}{c^2}\right)\exp\left(\mathrm{i}\frac{\Omega r}{c} + \mathrm{i}\varphi - \mathrm{i}\Omega t\right) \tag{2.127}$$

$$\psi = |\mathbf{m}|\sin\theta\cos\theta\,\mathrm{Re}\left(\frac{\Omega}{c}\frac{1}{r} - \mathrm{i}\frac{\Omega^2}{c^2}\right)\exp\left(\mathrm{i}\frac{\Omega r}{c} + \mathrm{i}\varphi - \mathrm{i}\Omega t\right) \tag{2.128}$$

exactly correspond to the electromagnetic fields (2.15), (2.16), (2.17), (2.18), (2.19), and (2.20) for the rotating magnetic dipole.

Within the quasistationary approximation, we can write the general equation for the magnetic field. Indeed, the condition for constancy of the total current I (2.96) on the magnetic surfaces can be regarded as a consequence of Eq. (2.95) for the drift velocity $\mathbf{U}_{\mathrm{dr}}$. Therefore, the electric current can also be represented as the expansion $\mathbf{j} = \rho_{\mathrm{e}}\,\Omega \times \mathbf{r} + i_{\parallel}\mathbf{B}$. Substituting this condition in the general equation (2.117), we readily see that $\nabla\cdot(i_{\parallel}\mathbf{B}) = 0$ and, hence, the function $i_{\parallel}$ must also be constant along the magnetic field lines, viz., $\mathbf{B}\cdot\nabla i_{\parallel} = 0$. In particular, if the longitudinal current is zero near the neutron star surface, it is to be zero in the entire magnetosphere. As a result, Eq. (2.117), with account taken of (2.104), can be rewritten as (Beskin et al., 1983)

$$\begin{aligned}\nabla\times\{(1-\boldsymbol{\beta}_{\mathrm{R}}^2)\mathbf{B} + \boldsymbol{\beta}_{\mathrm{R}}(\boldsymbol{\beta}_{\mathrm{R}}\cdot\mathbf{B}) + [\boldsymbol{\beta}_{\mathrm{R}}\times\nabla\psi]\} = \\ \frac{4\pi}{1-\boldsymbol{\beta}_{\mathrm{R}}^2 + \boldsymbol{\beta}_{\mathrm{R}}[\nabla\psi\times\mathbf{B}]/B^2}\left[\frac{i_{\parallel}}{c}\left((1-\boldsymbol{\beta}_{\mathrm{R}}^2)\mathbf{B} + [\boldsymbol{\beta}_{\mathrm{R}}\times\nabla\psi]\right)\right. \\ \left. + \frac{[\nabla\psi\times\mathbf{B}]}{B^2}\left(\frac{\Omega\cdot\mathbf{B}}{2\pi c} + \frac{1}{4\pi}(\nabla^2\psi - (\boldsymbol{\beta}_{\mathrm{R}}\nabla)(\boldsymbol{\beta}_{\mathrm{R}}\nabla\psi))\right)\right].\end{aligned} \tag{2.129}$$

Along with the equation $\nabla\cdot\mathbf{B} = 0$ (given the scalar functions $i_{\parallel}$ and ψ), it specifies the quasistationary magnetic field structure.

The quasistationary approximation is a natural generalization to axisymmetrical stationary configurations studied here. On the other hand, the possibility to use it seems unlikely. The point is that in the quasistationary case, it is impossible to introduce the analogue of the unique function Ψ describing the magnetic surfaces. As a result, one fails to reduce Maxwell's equations to a single scalar equation for the stream function by formalizing the constancy condition of the potential ψ and the current $i_{\parallel}$ along the given magnetic field line. Therefore, Eq. (2.129) was not essentially analyzed and its solutions were found only in the exceptional cases (Beskin

et al., 1983; Mestel et al., 1999), where it was actually reduced to the system of equations (2.124), (2.125) for the scalar functions ψ and h.

2.5 Energy Losses of Radio Pulsars

2.5.1 Current Loss Mechanism

Before proceeding to the discussion of the exact solutions to the pulsar equation, we consider the problem of the energy losses of the rotating neutron star. As was noted, in the vacuum approximation, the only mechanism resulting in the pulsar slowing down is a magnetodipole radiation. However, in the case of the plasma-filled magnetosphere, another slowing-down mechanism connected with the electric currents flowing in the magnetosphere occurs.

Indeed, the total current outflowing from the pulsar surface is to be zero. On the other hand, as was specially noted above, the charges of the same sign are to outflow from both magnetic poles (the charge densities ρ_{GJ} in the vicinity of the magnetic poles are identical). Therefore, an inverse current making up for the charge loss of the neutron star must inevitably flow along the separatrix dividing the open and closed magnetic field lines. As a result, the currents $\mathbf{J}_s$ that close the longitudinal currents in the magnetosphere flow over the pulsar surface (see Fig. 2.11). The ponderomotive action of these currents must result in the slowing down of the radio pulsar rotation (Beskin et al., 1993). It is important that this slowing-down mechanism occurs for the axisymmetric rotator when the magnetodipole losses are obviously zero. Actually, this mechanism was developed even in P. Goldreich and P. Julian's (1969) pioneer paper that was devoted to the axisymmetric magnetosphere.

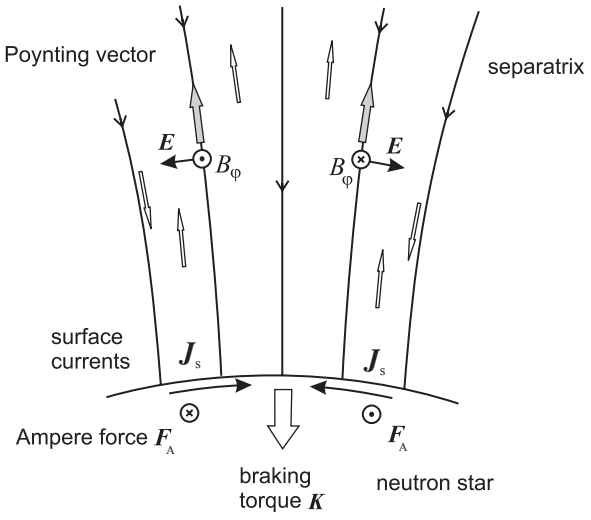

Fig. 2.11 Electric current structure (*contour arrows*) in the magnetic pole region of the neutron star. Ampére's force $\mathbf{F}_A$ connected with the surface current $\mathbf{J}_s$ generates the moment of force $\mathbf{K}$ resulting in the neutron star slowing down. For inclination angles χ not too close to 90°, the slowing-down moment $\mathbf{K}$ is antiparallel to the neutron star magnetic moment. The energy flux over the acceleration region is mainly connected with the Poynting vector (*shaded arrows*)

We first emphasize that if the energy losses of radio pulsars are really connected with the rotational kinetic energy loss of the neutron star, the total energy losses $W_{\rm tot} = -I_{\rm r}\Omega\dot{\Omega}$ and the angular momentum losses $K_{\rm tot} = -I_{\rm r}\dot{\Omega}$ should be connected by the relation

$$W_{\rm tot} = \Omega K_{\rm tot}. \tag{2.130}$$

Hence, the energy and the angular momentum for the outgoing radiation must satisfy the same condition.

To show that relation (2.130) really holds for the current losses, we write the energy losses as

$$W_{\rm tot} = -\Omega \cdot \mathbf{K}, \tag{2.131}$$

where

$$\mathbf{K} = \frac{1}{c}\int [\mathbf{r} \times [\mathbf{J}_{\rm s} \times \mathbf{B}]]{\rm d}S \tag{2.132}$$

is a slowing-down moment connected with Ampére's force of the current flowing on the surface. Here, for simplicity, we consider the axisymmetric case. The general relations are given in the following section.

It is easy to show that for $\chi = 0^{\circ}$, the slowing-down moment is exactly antiparallel to the neutron star angular velocity. The surface current $\mathbf{J}_{\rm s}$ must satisfy the continuity equation

$$\nabla_2 \mathbf{J}_{\rm s} = j_{\rm n}, \tag{2.133}$$

where ∇_2 is a two-dimensional differentiation operator and $j_{\rm n}$ is the normal component of the longitudinal current flowing in the magnetosphere. As a result, Eq. (2.133) can be rewritten as

$$\frac{1}{R\sin\theta}\frac{\rm d}{{\rm d}\theta}(\sin\theta J_\theta) = \frac{[\nabla I \times \mathbf{e}_\varphi]_n}{2\pi R\sin\theta}. \tag{2.134}$$

It yields

$$\mathbf{J}_{\rm s} = \frac{I}{2\pi R\sin\theta}\mathbf{e}_\theta. \tag{2.135}$$

Using formulae (2.131) and (2.132), we can write the total energy losses as

$$W_{\rm tot} = \frac{\Omega}{2\pi c}\int I(\Psi){\rm d}\Psi. \tag{2.136}$$

On the other hand, the total losses of the angular momentum $K_{\rm tot}$ (2.132) are rewritten as

$$K_{\rm tot} = \frac{1}{2\pi c}\int I(\Psi)\mathrm{d}\Psi. \tag{2.137}$$

As a result, relation (2.130), as was expected, turns out to be identically valid for the current losses.

Besides, we should point out that expression (2.136), as is seen, can be expanded into the sum of two terms

$$W_{\rm tot} = W_{\rm em} + W_{\rm part}. \tag{2.138}$$

Here the first term

$$W_{\rm em} = \frac{1}{2\pi c}\int \Omega_{\rm F}(\Psi)I(\Psi)\mathrm{d}\Psi, \tag{2.139}$$

according to definitions (2.89) and (2.93), is just the Poynting vector flux

$$W_{\rm em} = \frac{c}{4\pi}\int [\mathbf{E}\times\mathbf{B}]\mathrm{d}\mathbf{S}. \tag{2.140}$$

Therefore, $W_{\rm em}$ corresponds to the electromagnetic energy flux flowing away from the neutron star. As is expected, the electromagnetic energy losses are different from zero only in the presence of the longitudinal electric current generating the toroidal magnetic field. Note that the energy is transported at zero frequency; therefore, the electromagnetic field transporting this energy is not an electromagnetic wave in an ordinary sense.

On the other hand, the second term

$$W_{\rm part} = \frac{1}{2\pi c}\int I(\Psi)[\Omega - \Omega_{\rm F}(\Psi)]\mathrm{d}\Psi, \tag{2.141}$$

according to relation (2.106), can be rewritten as

$$W_{\rm part} = -\int \frac{\mathrm{d}\psi}{\mathrm{d}\Psi} I(\Psi)\,\mathrm{d}\Psi = -\int I(\Psi)\mathrm{d}\psi = \int \psi\mathrm{d}I = -\int \psi\mathbf{j}_{\rm e}\mathrm{d}\mathbf{S}. \tag{2.142}$$

Here, when integrating by parts, we used the zero condition of the potential ψ on the polar cap boundary. As we see, the losses $W_{\rm part}$ correspond to the energy gained by primary particles in the acceleration region.

Problem 2.15 Show that relation (2.138) holds for any inclination angle χ and, in particular, for any form of the polar cap.

(Hint: since the source of both the surface current $\mathbf{J}_s$ and the additional magnetic field $\mathbf{B}_T$ is the longitudinal current $i_\parallel \mathbf{B}$ flowing in the region of open field lines ($\nabla \cdot \mathbf{J}_s = i_\parallel B_n$, $\nabla \times \mathbf{B}_T = (4\pi/c) i_\parallel \mathbf{B}$), as is easily checked, they are connected by the simple relation

$$\mathbf{J}_s = -\frac{c}{4\pi}[\mathbf{B}_T \times \mathbf{n}]. \tag{2.143}$$

As a result, formulae (2.131) and (2.132) valid for any inclination angle χ can be identically rewritten as

$$W_{tot} = \frac{c}{4\pi} \int (\boldsymbol{\beta}_R \cdot \mathbf{B})(\mathbf{B} \cdot d\mathbf{S}). \tag{2.144}$$

Further, it is necessary to use relation (2.104) yielding the identity

$$[\mathbf{E} \times \mathbf{B}]d\mathbf{S} = (\boldsymbol{\beta}_R \cdot \mathbf{B})(\mathbf{B} \cdot d\mathbf{S}) + [\nabla\psi \times \mathbf{B}]d\mathbf{S} \tag{2.145}$$

and the condition $\psi = 0$ on the polar cap boundary.)

Thus, already from the analysis of the axisymmetric case, we can make a number of important conclusions.

1. The compatibility condition $W_{tot} = \Omega K_{tot}$ (2.130) cannot be obtained within the force-free approximation, because in this approximation there is no additional term W_{part} (2.141) corresponding to the energy of particles accelerated in the inner gap. Attempts to solve the loss problem by the force-free approximation, inevitably, lead to misunderstanding (Holloway, 1977; Shibata, 1994).
2. Under the condition $\psi \ll \psi_{max}$, of major importance in the total balance of current losses is the electromagnetic energy flux at zero frequency W_{em} (2.139). But for pulsars located near the "death line" in the P–$\dot{P}$ diagram (for which the condition $\psi \sim \psi_{max}$ is satisfied), the losses W_{part} correspond to the energy gained by primary particles in the acceleration region rather than to the energy of particles flowing along the open field lines. As was shown, a considerable part of the energy loss W_{part} is not used to generate particles but low-energy γ-quanta able to freely escape the neutron star magnetosphere. Therefore, the γ-quanta luminosity of radio pulsars located near the "death line" region is up to a few percent of the total losses $I_r \Omega \dot{\Omega}$. In these pulsars, the efficiency of the rotation energy processing in the high-energy radiation appears much larger than in the radio band. Consequently, the particle energy flux, at least, inside the light cylinder, appears much smaller than the flux W_{em} transported by the electromagnetic field. This fact just corresponds to the condition $\sigma \gg 1$ (2.82) valid for all radio pulsars.

3. On the other hand, for the slowing-down current mechanism discussed, the change in the angular moment $K_{\rm tot}$ is due to the electrodynamic losses (2.137). This must be the case as the angular momentum of photons $\mathcal{L}_{\rm ph}$ emitted in the vicinity of the star surface is much less than $\varepsilon_{\rm ph}/\Omega$. Therefore, the γ-quanta emitted in the vicinity of the neutron star surface cannot play a considerable role in the total balance of the angular momentum losses.

2.5.2 Slowing Down of Inclined and Orthogonal Rotators

We now discuss the problem of the energy losses of neutron stars for the arbitrary inclination angle χ. The necessity to do this is already obvious from an uncertainty in the expression for the energy losses of radio pulsars at the stage of the orthogonal rotator. The point is that the simple assumption based on the analysis of only the longitudinal currents results in a decrease in the factor $(\Omega R/c)^{1/2}$ as compared to the current losses of the axisymmetric rotator (Mestel et al., 1999). Indeed, let us estimate the energy losses by the Poynting vector flux through the light cylinder surface $R_{\rm L} = c/\Omega$

$$W_{\rm tot} = \frac{c}{4\pi}\int [\mathbf{E}\times\mathbf{B}]{\rm d}\mathbf{S} \sim cE(R_{\rm L})B_{\varphi}(R_{\rm L})R_{\rm L}^2. \tag{2.146}$$

The electric field in the vicinity of the light cylinder $E(R_{\rm L})$ is determined only by the value of the poloidal magnetic field $\mathbf{B}_{\rm p}$

$$E(R_{\rm L}) \approx \frac{\Omega R_{\rm L}}{c} B_{\rm p} \approx B_{\rm p}, \tag{2.147}$$

and according to the dependence $B \propto r^{-3}$ for the dipole magnetic field within the light cylinder, we have $B_{\rm p}(R_{\rm L}) \approx (\Omega R/c)^3 B_0$, where B_0 is a magnetic field on the neutron star surface. The toroidal magnetic field B_{φ} is connected with the longitudinal currents flowing in the magnetosphere. Therefore, the charge density of the orthogonal rotator within the polar cap $R_0 \sim (\Omega R/c)^{1/2}R$ is $\varepsilon_{\rm A} = (\Omega R/c)^{1/2}$ times less than that of the axisymmetric rotator. The toroidal magnetic field on the light cylinder can be estimated as

$$B_{\varphi}(R_{\rm L}) \approx \left(\frac{\Omega R}{c}\right)^{1/2} B_{\rm p}(R_{\rm L}), \tag{2.148}$$

which yields the additional factor $\varepsilon_{\rm A}$ in the expression for the energy losses. However, a comprehensive analysis shows that, in reality, a decrease in the factor must have the form $\varepsilon_{\rm A}^2 = (\Omega R/c)$, so that the total losses of the orthogonal rotator should be written as (Beskin et al., 1993; Beskin and Nokhrina, 2004)

$$W_{\rm tot}^{\rm orth} \approx \frac{B_0^2 \Omega^4 R^6}{c^3} \left(\frac{\Omega R}{c} \right). \tag{2.149}$$

To show this, we are to write the most general expression for the surface current $\mathbf{J}_{\rm s}$ in the presence of the strong magnetic field. It can be divided into two components, a parallel and a perpendicular one to the surface electric field $\mathbf{E}_{\rm s}$, i.e., we write the current $\mathbf{J}_{\rm s}$ as

$$\mathbf{J}_{\rm s} = \mathbf{J}_{\rm s}^{(1)} + \mathbf{J}_{\rm s}^{(2)}, \tag{2.150}$$

where

$$\mathbf{J}_{\rm s}^{(1)} = \Sigma_{||} \mathbf{E}_{\rm s}, \tag{2.151}$$

$$\mathbf{J}_{\rm s}^{(2)} = \Sigma_{\perp} \left[\frac{\mathbf{B}_{\rm n}}{B_{\rm n}} \times \mathbf{E}_{\rm s} \right]. \tag{2.152}$$

Here $\Sigma_{||}$ is the Pedersen conductivity and $\Sigma_{\perp}$ is the Hall conductivity. Suppose now that the pulsar surface conductivity perpendicular to the magnetic field is homogeneous and the field $\mathbf{E}_{\rm s}$ has the potential ξ'. Hence, relations (2.151) and (2.152) look like

$$\mathbf{J}_{\rm s}^{(1)} = \nabla \xi', \tag{2.153}$$

$$\mathbf{J}_{\rm s}^{(2)} = \frac{\Sigma_{\perp}}{\Sigma_{\parallel}} \left[\frac{\mathbf{B}_{\rm n}}{B_{\rm n}} \times \nabla \xi' \right]. \tag{2.154}$$

Note at once that since the magnetic field structure in the vicinity of the pulsar surface is symmetric about the plane passing through the vectors of the angular velocity and the magnetic moment of the neutron star, the surface current should have the same symmetry. Thus, the currents proportional to $\Sigma_{\perp}$ do not contribute to the energy losses of the neutron star.

As a result, Eq. (2.133) is now rewritten as

$$\nabla_2^2 \xi' = -i_{\parallel} B_0. \tag{2.155}$$

If we make in this equation the substitution $x_{\rm m} = \sin\theta_{\rm m}$ and introduce the dimensionless potential $\xi = 4\pi\xi'/B_0 R^2 \Omega$ and the current $i_0 = -4\pi i_{\parallel}/\Omega R^2$, we finally get

$$\left(1 - x_{\rm m}^2\right) \frac{\partial^2 \xi}{\partial x_{\rm m}^2} + \frac{1 - 2x_{\rm m}^2}{x_{\rm m}} \frac{\partial \xi}{\partial x_{\rm m}} + \frac{1}{x_{\rm m}^2} \frac{\partial^2 \xi}{\partial \varphi_{\rm m}^2} = i_0(x_{\rm m}, \varphi_{\rm m}). \tag{2.156}$$

Here again $\theta_{\rm m}$ and $\varphi_{\rm m}$ are spherical coordinates relative to the magnetic axis. Naturally, the solution to Eq. (2.156) substantially depends on the boundary conditions. As is shown below, this boundary condition is the assumption that beyond the polar

cap there are no surface currents associated with the bulk longitudinal current flowing in the magnetosphere. In this case, the boundary condition can be written as

$$\xi\,[x_0(\varphi_\mathrm{m}), \varphi_\mathrm{m}] = \mathrm{const}, \tag{2.157}$$

where the function $x_0(\varphi_\mathrm{m})$ prescribes the form of the polar cap.

We should emphasize that the main uncertainty is just in this assertion. Indeed, the absence of the longitudinal current in the region of the closed field lines $x_\mathrm{m} > x_0$, i.e., the fulfillment of the condition $i_0(x_\mathrm{m} > x_0, \varphi_\mathrm{m}) = 0$, does not imply that the gradient $\nabla\xi$ (and, hence, the surface current $\mathbf{J}_\mathrm{s}$) is also zero here. In the case of the inclined rotator, the longitudinal current closure can occur beyond the polar cap, where the equation for the potential ξ has the form $\nabla^2\xi = 0$. The solution to this equation is a set of multipole flows $\xi_n \approx A_n \cos^n \varphi_\mathrm{m}/x_\mathrm{m}^n$ whose amplitudes A_n could be quite arbitrary. The corresponding jump of the derivative of the potential ξ on the polar cap boundary fixes the value of the surface current flowing along the separatrix dividing the region of closed and open field lines (see Fig. 2.12). Otherwise, this implies that, besides the bulk current flowing along the open field lines, additional surface current must flow in the magnetosphere; the value of the current, at first sight, can be in no way associated with the value of the bulk current.

However, it is easy to show that, in reality, the closing surface currents cannot extend beyond the polar cap. If this were the case, the longitudinal currents would exist in the closed magnetosphere region (see Fig. 2.13). Indeed, as is evident from relations (2.151) and (2.152), the existence of the surface current $\mathbf{J}_\mathrm{s}$ must, inevitably, be accompanied by the occurrence of the surface electric field $\mathbf{E}_\mathrm{s}$, i.e., the electric potential difference between various points of the neutron star surface, which are

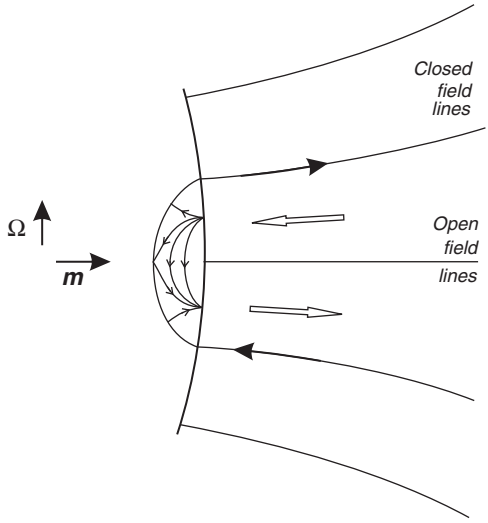

Fig. 2.12 The structure of electric currents flowing in the vicinity of the magnetic poles of the orthogonal rotator. The currents flowing along the separatrix (*bold arrows*) dividing the region of closed and open field lines are compatible with the bulk currents (*contour arrows*), so the closing surface currents (*fine arrows*) are totally concentrated within the polar cap

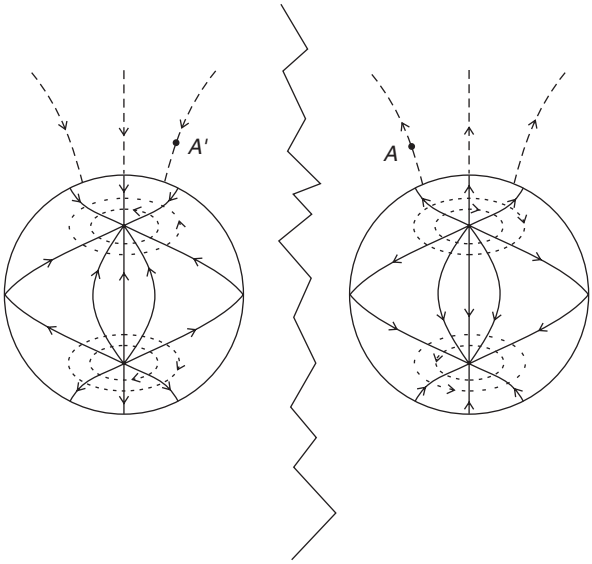

Fig. 2.13 Surface current structure (*fine lines*) and the toroidal magnetic field (*dotted lines*) for two magnetic poles of the orthogonal rotator. If the surface currents flew beyond the polar caps (*dashed lines*), this would give rise to a potential difference between the points A and A' connected by the closed magnetic field line. The surface current structure corresponds to the solution (2.159)

connected by the closed magnetic field lines. But this contradicts the assumption of the absence of longitudinal currents in the closed magnetosphere. Consequently, the current flowing along the separatrix must be compatible with the bulk currents flowing within the open field line region so that the closing surface currents may be totally concentrated within the polar cap. This just leads to the boundary condition (2.157).

On the other hand, for the arbitrary inclination angle χ the current i_0 can be written as a sum of the symmetric and antisymmetric components. It is natural to normalize the longitudinal current to the GJ current $j_{\rm GJ} = c\rho_{\rm GJ}$. Supposing the pulsar magnetic field to be a dipole one, we obtain for the GJ current with $x_{\rm m} \ll 1$

$$i_{\rm GJ}(x_{\rm m}, \varphi_{\rm m}) \approx \cos\chi + \frac{3}{2} x_{\rm m} \cos\varphi_{\rm m} \sin\chi . \tag{2.158}$$

Since within the polar cap $x_{\rm m} \sim \varepsilon_{\rm A} \ll 1$, we obtain $i_{\rm GJ} \sim 1$ for $\chi \simeq 0$ and $i_{\rm GJ} \sim \varepsilon_{\rm A}$ for $\chi \simeq 90^\circ$. In the following, we write the current i_0 as $i_0 = i_{\rm S} + i_{\rm A} x_{\rm m} \cos\varphi_{\rm m}$, where $i_{\rm S}$ and $i_{\rm A}$ are the amplitudes of the symmetric and antisymmetric longitudinal currents normalized to the corresponding components of the GJ current (2.158). In particular, for the GJ current, we have $i_{\rm S} = \cos\chi$ and $i_{\rm A} = (3/2)\sin\chi$. Thus, the solution to Eq. (2.156) is fully defined by the bulk longitudinal current i_0. For example, for $\chi = 90^\circ$ for the GJ current $i_0 = i_{\rm A} x_{\rm m} \cos\varphi_{\rm m}$ and for $x_0 = {\rm const}$, we have (Beskin et al., 1993)

$$\xi = i_{\rm A} \frac{x_{\rm m}(x_{\rm m}^2 - x_0^2)}{8} \cos\varphi_{\rm m}. \tag{2.159}$$

Problem 2.16 Show that in this case the total current $I_{\rm sep}$ flowing along the separatrix is 3/4 the total bulk current $I_{\rm bulk}$ flowing in the region of the open field lines:

$$\frac{I_{\rm sep}}{I_{\rm bulk}} = -\frac{3}{4}. \tag{2.160}$$

Further, we expand the slowing-down moment $\mathbf{K}$ (2.132) in terms of the vectors $\mathbf{e}_{\rm m}$, $\mathbf{n}_1$, and $\mathbf{n}_2$, where $\mathbf{e}_{\rm m} = \mathbf{m}/|\mathbf{m}|$, the unit vector $\mathbf{n}_1$ is perpendicular to the magnetic moment $\mathbf{m}$ and lies in the plane formed by the vectors Ω and $\mathbf{m}$ (and $\Omega \cdot \mathbf{n}_1 > 0$), and $\mathbf{n}_2 = \mathbf{e}_{\rm m} \times \mathbf{n}_1$

$$\mathbf{K} = K_{\parallel}\mathbf{e}_m + K_{\perp}\mathbf{n}_1 + K_{\dagger}\mathbf{n}_2. \tag{2.161}$$

As a result, we have (Beskin et al., 1993)

$$K_{\parallel} = -\frac{B_0^2 R^4 \Omega}{c} \int_0^{2\pi} \frac{{\rm d}\varphi_{\rm m}}{2\pi} \int_0^{x_0(\varphi_{\rm m})} {\rm d}x_{\rm m}\, x_{\rm m}^2 \sqrt{1 - x_{\rm m}^2}\, \frac{\partial \xi}{\partial x_{\rm m}}, \tag{2.162}$$

and $K_{\perp} = K_1 + K_2$, where

$$K_1 = \frac{B_0^2 R^4 \Omega}{c} \int_0^{2\pi} \frac{{\rm d}\varphi_{\rm m}}{2\pi} \int_0^{x_0(\varphi_{\rm m})} {\rm d}x_{\rm m} \left(x_{\rm m} \cos\varphi_{\rm m} \frac{\partial \xi}{\partial x_{\rm m}} - \sin\varphi_{\rm m} \frac{\partial \xi}{\partial \varphi_{\rm m}} \right), \tag{2.163}$$

$$K_2 = \frac{B_0^2 R^4 \Omega}{c} \int_0^{2\pi} \frac{{\rm d}\varphi_{\rm m}}{2\pi} \int_0^{x_0(\varphi_{\rm m})} {\rm d}x_{\rm m}\, x_{\rm m}^3 \cos\varphi_{\rm m} \frac{\partial \xi}{\partial x_{\rm m}}, \tag{2.164}$$

and $K_{\dagger}$, as we will see, does not enter the Euler equations at all. Here we also took into account that both magnetic poles contribute to the slowing-down moment.

Since integration over $x_{\rm m}$ in (2.163) and (2.164) is taken to the polar cap boundary $x_0(\varphi_{\rm m}) \sim \varepsilon_{\rm A}$, as an estimate, we could take $K_2 \sim \varepsilon_{\rm A}^2 K_1$, i.e., $K_2 \ll K_1$. However, as is readily checked, when the boundary condition (2.157) is satisfied, the integrand in (2.163) is a complete derivative with respect to $\varphi_{\rm m}$:

$$\int_0^{x_0(\varphi_{\rm m})} {\rm d}x_{\rm m} \left(x_{\rm m} \cos\varphi_{\rm m} \frac{\partial \xi}{\partial x_{\rm m}} - \sin\varphi_{\rm m} \frac{\partial \xi}{\partial \varphi_{\rm m}} \right) =$$
$$\frac{\partial}{\partial \varphi_{\rm m}} \left[-\int_0^{x_0(\varphi_{\rm m})} {\rm d}x_{\rm m}\, \xi \sin\varphi_{\rm m} + \xi\,(x_0, \varphi_{\rm m})\, x_0(\varphi_{\rm m}) \sin\varphi_{\rm m} \right]. \tag{2.165}$$

Therefore, the contribution K_1 appears identically equal to zero. As a result, the expressions for $K_{\parallel}$ and $K_{\perp}$ have the form

$$K_{\parallel} = -\frac{B_0^2 \Omega^3 R^6}{c^3}\left[c_{\parallel} i_{\mathrm{S}} + \mu_{\parallel}\left(\frac{\Omega R}{c}\right)^{1/2} i_{\mathrm{A}}\right], \tag{2.166}$$

$$K_{\perp} = -\frac{B_0^2 \Omega^3 R^6}{c^3}\left[\mu_{\perp}\left(\frac{\Omega R}{c}\right)^{1/2} i_{\mathrm{S}} + c_{\perp}\left(\frac{\Omega R}{c}\right) i_{\mathrm{A}}\right], \tag{2.167}$$

where $c_{\parallel}$ and $c_{\perp}$ are factors of the order of unity dependent on the particular profile of the longitudinal current i_0 and the form of the polar cap. As to the coefficients $\mu_{\parallel}$ and $\mu_{\perp}$, they are associated with the polar cap axisymmetry and their contribution proves unessential. In particular, $\mu_{\parallel}(0) = \mu_{\perp}(0) = 0$ and $\mu_{\parallel}(90^{\circ}) = \mu_{\perp}(90^{\circ}) = 0$.

We can explain the unavailability of the leading term K_1 (2.163) for the energy losses. As was shown above, the energy losses of radio pulsars W_{tot} can be identically rewritten as (2.144)

$$W_{\mathrm{tot}} = \frac{c}{4\pi}\int (\boldsymbol{\beta}_{\mathrm{R}} \cdot \mathbf{B})(\mathbf{B} \cdot \mathrm{d}\mathbf{S}). \tag{2.168}$$

On the light cylinder, expression (2.168) coincides with the estimate (2.146) but can be used in the vicinity of the neutron star surface as well. It is easy to verify that the condition of the current closure within the polar cap (2.157) is equivalent to the condition of the complete screening of the magnetic field $\mathbf{B}_{\mathrm{T}}$, which is caused by the longitudinal currents flowing in the region of the open field lines. This fact is obvious for the axisymmetric rotator; however, it needs a substantial additional assumption for the angles $\chi \approx 90^{\circ}$. As shown in Fig. 2.13, the toroidal magnetic field specifying the value $(\boldsymbol{\beta}_{\mathrm{R}} \cdot \mathbf{B})$ must not extend beyond the polar cap. As a result, in the zero approximation, the mean value of the scalar product $(\boldsymbol{\beta}_{\mathrm{R}} \cdot \mathbf{B})$ in the region of open field lines turns out to be zero and the energy loss itself is determined by the small corrections $\sim \varepsilon_{\mathrm{A}}^2$ associated with the curvature of the neutron star surface. Clearly, the pattern must be the same on the light cylinder. In other words, for the orthogonal rotator, the mean value of the toroidal magnetic field of order $B_{\varphi}(R_{\mathrm{L}}) \sim i_0 B_{\mathrm{p}}(R_{\mathrm{L}})$ is to be zero on the light cylinder. This establishes the difference in the estimates of the energy losses for the orthogonal rotator.

Writing the Euler equations, we can find the change in the angular velocity $\dot{\Omega}$ and the inclination angle $\dot{\chi}$ of the pulsar:

$$I_{\mathrm{r}}\frac{\mathrm{d}\Omega}{\mathrm{d}t} = K_{\parallel}\cos\chi + K_{\perp}\sin\chi, \tag{2.169}$$

$$I_{\mathrm{r}}\Omega\frac{\mathrm{d}\chi}{\mathrm{d}t} = K_{\perp}\cos\chi - K_{\parallel}\sin\chi. \tag{2.170}$$

Here we, for simplicity, suppose that the neutron star is spherically symmetric, and its moment of inertia I_{r} is thus independent of the orientation of the rotation axis. As a result, for angles χ not too close to 90°, so that $\cos\chi > \varepsilon_{\mathrm{A}}^2$ (i.e., when the symmetric currents are of major importance), we find

$$\frac{\mathrm{d}\Omega}{\mathrm{d}t} = -c_{\parallel}\frac{B_0^2\Omega^3R^6}{I_{\mathrm{r}}c^3}i_{\mathrm{S}}\cos\chi, \tag{2.171}$$

$$\frac{\mathrm{d}\chi}{\mathrm{d}t} = \quad c_{\parallel}\frac{B_0^2\Omega^2R^6}{I_{\mathrm{r}}c^3}i_{\mathrm{S}}\sin\chi. \tag{2.172}$$

We readily see that Eqs. (2.171) and (2.172) yield the conservation of the invariant

$$\mathcal{I}_{\mathrm{cur}} = \Omega\sin\chi, \tag{2.173}$$

different from (2.22). This is because, as was mentioned, the slowing-down moment **K** (2.132) for the symmetric currents is opposite to the magnetic dipole **m**, so the projection of the angular velocity Ω onto the axis perpendicular to **m** is an integral of motion. For the orthogonal rotator $\chi \approx 90^\circ$, where $\cos\chi < \varepsilon_{\mathrm{A}}^2$, we get

$$\frac{\mathrm{d}\Omega}{\mathrm{d}t} = -c_{\perp}\frac{B_0^2\Omega^4R^7}{I_{\mathrm{r}}c^4}i_{\mathrm{A}}. \tag{2.174}$$

Because of the dependence $i_{\mathrm{S}} \approx \cos\chi$, the contribution of the symmetric current can be disregarded here. The comparison of relations (2.171) and (2.174) shows that the energy release of pulsars at the orthogonal rotator stage (and for GJ current $i_{\mathrm{A}} \approx 1$) is $\Omega R/c$ times less than that of axisymmetric pulsars.

To sum up, we can make the general conclusions:

1. For inclination angles $\chi < 90^\circ$, the slowing-down moment **K** (2.132) is antiparallel to the magnetic moment of the neutron star **m**. Therefore, for the current losses the invariant value is

$$\Omega\sin\chi = \mathrm{const}. \tag{2.175}$$

   This conclusion directly follows from the analysis of the Euler equations, viz., the projection of the angular velocity onto the direction perpendicular to the applied moment of forces is an invariant of motion (Landau and Lifshits, 1976). Consequently, unlike the magnetodipole losses, the inclination angle must increase with time. According to the invariant (2.173), the characteristic time of the change in the inclination angle χ ($\tau_\chi = \chi/2\dot{\chi}$) coincides with the dynamical age of the pulsar $\tau_{\mathrm{D}} = P/2\dot{P}$

$$\tau_{\mathrm{D}} \approx \frac{I_{\mathrm{r}}c^3}{2B_0^2\Omega^2R^6} \approx 10\,\mathrm{mln\,years}\left(\frac{P}{1\,s}\right)^2\left(\frac{B_0}{10^{12}\,\mathrm{G}}\right)^{-2}. \tag{2.176}$$

2. The current losses W_{tot} can be rewritten as $W_{\mathrm{tot}} = VI$. Here

$$V \sim EL \sim \left(B_0\frac{\Omega R_0}{c}\right)R_0 \tag{2.177}$$

is the characteristic potential drop within the polar cap and I is the total current circulating in the magnetosphere. Using now the definition $i_0 = I/I_{\rm GJ}$ and the fact that for χ not too close to 90°, we can take $V \approx \psi_{\max}$ to obtain

$$W_{\rm tot} = c_{\parallel} \frac{B_0^2 \Omega^4 R^6}{c^3} i_0 \cos\chi . \tag{2.178}$$

The coefficient $c_{\parallel} \sim 1$, as seen from relation (2.164), depends on the longitudinal current profile. One should stress here that, besides the factor $\cos\chi$ connected with the scalar product in (2.131), the substantial dependence of the current losses $W_{\rm tot}$ on the inclination angle is in the factor $i_0 \approx i_{\rm S}$. The point is that in the definition of the dimensionless current, there is the GJ current for the axisymmetric case, whereas for nonzero χ the GJ charge density in the vicinity of the magnetic poles substantially depends on the angle χ, viz., $\rho_{\rm GJ} \approx -(\Omega \cdot \mathbf{B})/2\pi c \propto \cos\chi$. Therefore, it is logical to expect that for the inclined rotator the dimensionless current i_0 is bounded from above

$$i_0^{(\max)}(\chi) \sim \cos\chi . \tag{2.179}$$

As a result, the current losses decrease as the angle χ increases, at least, as $\cos^2\chi$.

3. As to radio pulsars, in which the inclination angle χ is close to 90°, for the antisymmetric longitudinal currents $i_{\rm A}$ the energy losses can be written as

$$W_{\rm tot} = c_{\perp} \frac{B_0^2 \Omega^4 R^6}{c^3} \left(\frac{\Omega R}{c}\right) i_{\rm A}. \tag{2.180}$$

Here the coefficient $c_{\perp} \sim 1$ already depends not only on the antisymmetric longitudinal current profile but also on the form of the polar cap. Consequently, the current losses for the orthogonal rotator (and for $i_{\rm A} \sim 1$) turn out to be $(\Omega R/c)$ times less than in the axisymmetric case. Certainly, if the current density can be much larger than the local GJ current $\rho_{\rm GJ,90}c$, then $i_{\rm A} \gg 1$, the energy losses can be large enough. We discuss this possibility in Sect. 2.6.3.

Problem 2.17 Show that for the constant current density $i_{\rm S} = \text{const}$ within the polar cap (Beskin et al., 1993)

$$c_{\parallel} = \frac{f_*^2}{4}, \tag{2.181}$$

where f_* is the dimensionless area of the polar cap: $S = f_* \pi (\Omega R/c) R^2$.

Problem 2.18 Using relation (2.159), show that for the orthogonal rotator

$$c_{\perp} = \frac{f_*^3}{64}. \tag{2.182}$$

Thus, the important conclusion is that for currents $I \sim I_{\rm GJ}$ (i.e., for $i_0 \sim 1$) characteristic of the radio pulsar magnetosphere, the current losses (2.178) in this expression coincide with the magnetodipole losses (2.5). On the other hand, the current and magnetodipole losses have a number of considerable differences.

- The magnetodipole losses (2.5) are absent in the axisymmetric case, whereas the current losses are maximal for $\chi = 0^\circ$.
- The magnetodipole losses result in a decrease in the inclination angle with time ($\Omega \cos\chi = \text{const}$), whereas for the current losses the angle χ, on the contrary, is to increase ($\Omega \sin\chi = \text{const}$) approaching 90°. However, in both cases, the evolution of the angle χ is in the range of parameters, where the energy losses of the neutron star become minimal.
- For the magnetodipole losses, the braking index $n_{\rm br}$ is larger than three (see (2.24)), whereas for the current losses, it can be less than three (see Beskin et al. (1993) for details).
- The magnetodipole losses are universal i.e., they are independent of the additional parameters. On the other hand, the current losses (2.178) are proportional to the electric current i_0 circulating in the magnetosphere.

Otherwise, the difference between the current and magnetodipole losses is rather substantial. Theoretically, this brings up the question of the relative role of these two slowing-down mechanisms in the total balance of the energy losses. The answer to this question can be given only together with the solution to the complete problem of the neutron star magnetosphere. On the other hand, one should note that for most radio pulsars the dimensionless current is $i_0 \sim 1$, so that the simplest magnetodipole formula (2.5) yields, in the large, a reliable estimate for the total energy losses of the rotating neutron star. As a result, both the magnetodipole and the current losses give similar results when analyzing the statistical characteristics of radio pulsars (Michel, 1991; Beskin et al., 1993). The direct determination of the sign of the derivative $\dot{\chi}$ different for the two slowing-down mechanisms is now beyond the sensitivities of the present-day receivers. Therefore, up to now, the observations do not allow one to choose between these two slowing-down mechanisms (see Appendix C as well).

2.6 Magnetosphere Structure

2.6.1 Exact Solutions

We again return to our main topic and consider the structure of the radio pulsar magnetosphere. It was shown that in the zero order with respect to the small parameters

σ^{-1} and λ^{-1}, the magnetosphere structure can be described by the force-free equation (2.101). As was noted, this equation contains only one singular surface and, therefore, needs three boundary conditions. As such boundary conditions, one can take the values of the invariants $\Omega_{\rm F}(\Psi)$ and $I(\Psi)$, as well as the normal component of the magnetic field on the neutron star surface (or, what is the same, the stream function $\Psi(R,\theta)$ on its surface).

Equation (2.101) is of a nonlinear type. However, unlike the hydrodynamical GS equation version, the whole nonlinearity is now associated with the integrals of motion. In particular, in the absence of the longitudinal current and for the constant angular velocity $\Omega_{\rm F}(\Psi)=\Omega$, it becomes linear

$$-\left(1-\frac{\Omega^2\varpi^2}{c^2}\right)\nabla^2\Psi+\frac{2}{\varpi}\frac{\partial\Psi}{\partial\varpi}=0. \tag{2.183}$$

On the other hand, unlike the hydrodynamical case, for the constant value of the angular velocity $\Omega_{\rm F}$, the location of the singular surface $\Omega_{\rm F}\varpi/c=1$ is known beforehand. Since Eq. (2.183) does not explicitly comprise the cylindrical coordinate z, its solution can be sought by the method of separation of variables (Michel, 1973a; Mestel and Wang, 1979)

$$\Psi(\varpi,z)=\frac{|\mathbf{m}|}{R_{\rm L}}\int_0^\infty R_\lambda(\varpi)\cos(\lambda z)\,{\rm d}\lambda. \tag{2.184}$$

These properties made it possible to obtain the solution to Eq. (2.101) for a number of the simplest cases.

2.6.1.1 Axisymmetric Magnetosphere with the Zero Longitudinal Current for the Dipole Magnetic Field of the Neutron Star

In the absence of the longitudinal currents, the only currents in the magnetosphere are corotation currents $\Omega_{\rm F}\varpi\rho_{\rm GJ}\mathbf{e}_\varphi$. Recall that we assume here $\Omega_{\rm F}=$ const. Therefore, the range of applicability of Eq. (2.183) extends only to the light cylinder which coincides with the light surface. Substituting expansion (2.184) in Eq. (2.183), we obtain for the radial function $R_\lambda(x_r)$ (Michel, 1973a; Mestel and Wang, 1979)

$$\frac{{\rm d}^2R_\lambda(x_r)}{{\rm d}^2x_r}-\frac{(1+x_r^2)}{x_r(1-x_r^2)}\frac{{\rm d}R_\lambda(x_r)}{{\rm d}x_r}-\lambda^2R_\lambda(x_r)=0. \tag{2.185}$$

Hereafter, we again use the dimensionless variables $x_r=\Omega\varpi/c$ and $z'=\Omega z/c$.

The boundary conditions for Eq. (2.185) are

1. the dipole magnetic field in the vicinity of the star surface $\mathbf{B}=[3(\mathbf{nm})\mathbf{n}-\mathbf{m}]/r^3$, i.e.,

$$\Psi(x_r,z')=\frac{|\mathbf{m}|}{R_{\rm L}}\frac{x_r^2}{(x_r^2+z'^2)^{3/2}} \tag{2.186}$$

for $x_r\to 0$ and $z'\to 0$;

2. the absence of a singularity on the light cylinder $x_r = 1$.

According to the known expansion

$$\frac{x_r^2}{(x_r^2 + z'^2)^{3/2}} = \frac{2}{\pi} \int_0^\infty \lambda x_r \, K_1(\lambda x_r) \cos(\lambda z') \, \mathrm{d}\lambda, \tag{2.187}$$

where $K_1(x)$ is the Macdonald function of the first order, the first condition implies that for $x_r \to 0$ the relation

$$R_\lambda(x_r) \to \frac{2}{\pi} \lambda x_r \, K_1(\lambda x_r) \tag{2.188}$$

must hold. As we see, the situation is absolutely equivalent to the hydrodynamical limit when one of the boundary conditions for the ordinary differential equation is connected with a field source and the second one corresponds to the absence of a singularity on the critical surface.

Problem 2.19 Show that the solution to Eq. (2.185) can be constructed in the form of the series

$$R_\lambda(x_r) = \mathcal{D}(\lambda) \sum_{n=0}^{\infty} a_n (1 - x_r^2)^n, \tag{2.189}$$

where the expansion coefficients a_n satisfy the recurrent relations

$$a_0 = 1, \quad a_1 = 0, \quad a_{n+1} = \frac{4n^2}{4(n+1)^2} \, a_n + \frac{\lambda^2}{4(n+1)^2} \, a_{n-1}. \tag{2.190}$$

The value $\mathcal{D}(\lambda)$ can be determined from the boundary condition (2.188) near the neutron star surface. Indeed, using the asymptotic behavior $K_1(x) = x^{-1}$ for $x \to 0$, we get

$$\mathcal{D}(\lambda)^{-1} = \frac{\pi}{2} \sum_{n=0}^{\infty} a_n. \tag{2.191}$$

Figure 2.14 shows the magnetic field structure obtained from the solution to Eq. (2.183) (Michel, 1973a). As was expected, the dipole magnetic field is disturbed only in the vicinity of the light cylinder; at small distances the magnetic field remains dipole. Note also that the magnetic field on the light cylinder appears orthogonal to its surface. This fact can be directly checked by definition (2.89) in the form of expansion (2.189)—the z-component of the magnetic field on the light cylinder $B_z(x_r = 1)$ turns out to be automatically equal to zero. This is, by the way, the solution to the singularity problem in expression (2.41)—the charge density remains finite on the light cylinder. At the equator of the light cylinder ($\varpi = R_\mathrm{L}$, $z = 0$), the magnetic field is zero. Finally, it turned out that the total

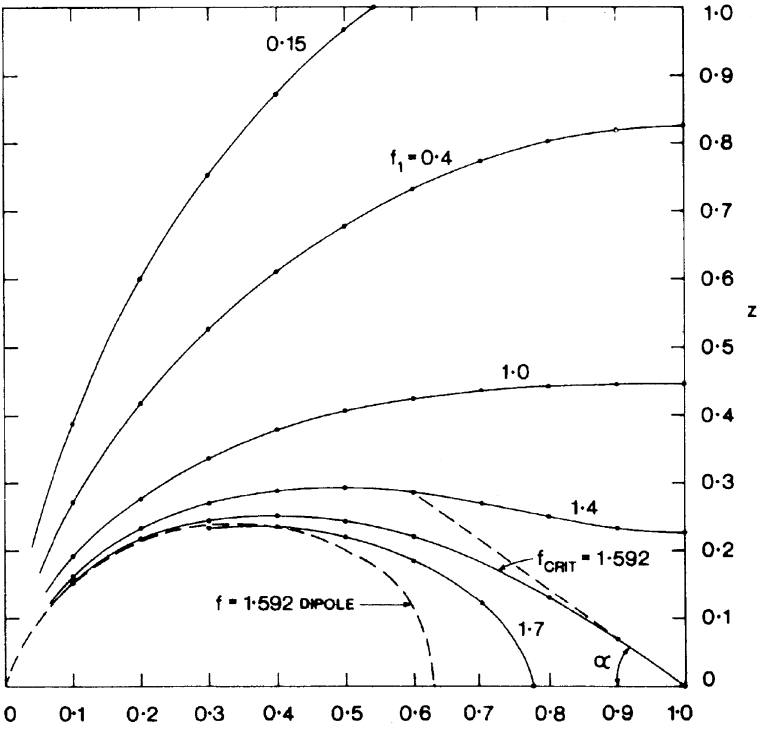

Fig. 2.14 Magnetic field structure for the zero longitudinal current and the accelerating potential ($i_0 = 0$, $\beta_0 = 0$) for the dipole axisymmetric magnetic field of the neutron star (Michel, 1973a). The numbers indicate the values of the dimensionless magnetic field function f ($\Psi = \pi B_0 R^2 (\Omega R/c) f$) (Reproduced by permission of the AAS, Fig. 1 from Michel, F.C.: Rotating magnetosphere: a simple relativistic model. ApJ **180**, 207–226 (1973))

magnetic flux crossing the light cylinder is about 1.592 times larger than that in the vacuum case. This result implies that the area of the polar cap increases in the same proportion (Michel, 1973a)

$$S_{\rm cap} \approx 1.592\,\pi R_0^2. \tag{2.192}$$

As to the toroidal magnetic field, since the longitudinal electric currents are absent, it is identically equal to zero in the whole magnetosphere.

Problem 2.20 Having written the expression for the magnetic flux through the light cylinder surface, show that the coefficient $f_* \approx 1.592$ (so-called Michel number) is connected with the function $\mathcal{D}(\lambda)$ by the relation

$$f_* = \int_0^\infty \mathcal{D}(\lambda)\mathrm{d}\lambda. \tag{2.193}$$

It is also interesting to note that when receding from the equatorial plane, within the light cylinder, the electric and magnetic fields decrease exponentially fast rather than by a power law: $B \propto \exp(-pz/R_{\mathrm{L}})$, where $p \approx 3.0$. This property is associated with the structure of expansion (2.184) and the existence of the pole of the function R_λ for $\lambda = ip$ (Beskin et al., 1993). This fast decrease in the fields is possible because the magnetic moment of the corotation currents almost fully screens the magnetic moment of the neutron star.

Further, the electric field on the light cylinder is compared in magnitude with the magnetic one, but its direction is along the rotation axis of the neutron star. Since the normal component of the electric field vanishes on the light cylinder, one can conclude that the total charge of the neutron star and the magnetosphere turns out to be zero. Otherwise, part of the charge Q_* (2.12) located, in the vacuum case, on the neutron star surface passes into the pulsar magnetosphere. On the other hand, the equality of the electric and magnetic fields on the light cylinder shows that for the zero longitudinal current the light cylinder coincides with the light surface. Therefore, the constructed solution cannot be extended beyond the light cylinder, though, formally, the pulsar equation does not have any singularities here.

2.6.1.2 Axisymmetric Magnetosphere with the Zero Longitudinal Current for the Monopole Magnetic Field

At first sight, there is no sense to consider this case, because the monopole magnetic field does not occur in reality. However, as we see in the following, the analysis of the rotating monopole magnetosphere proves very fruitful, especially, for the case of the black hole magnetosphere.

The solution of the problem for the monopole magnetic field is analogous to the previous one (Michel, 1973a). There is a difference only in boundary condition 1 on the star surface and, hence, only in the explicit form of the function $\mathcal{D}(\lambda)$. As a result, as for the dipole magnetic field, the magnetic field on the light cylinder appears orthogonal to its surface and also decreases exponentially with distance from the equatorial plane, and at small distances from the star the monopole field perturbations prove small (see Fig. 2.15). On the other hand, as in the previous example, the electric field on the light cylinder is compared with the magnetic one and, therefore, the solution of the pulsar equation cannot be extended beyond the light cylinder.

2.6.1.3 Magnetosphere with the Zero Longitudinal Current for the Inclined Rotator

The exact solution for the zero longitudinal currents (and in the absence of the accelerating potential $\psi = 0$) can be constructed at an arbitrary inclination angle of χ (Beskin et al., 1983). This becomes possible because for $i_\parallel = 0$ and $\psi = 0$ the quasistationary GS equation (2.129) also becomes linear

$$\nabla \times \left[(1 - \boldsymbol{\beta}_{\mathrm{R}}^2)\mathbf{B} + \boldsymbol{\beta}_{\mathrm{R}}(\boldsymbol{\beta}_{\mathrm{R}} \cdot \mathbf{B})\right] = 0. \tag{2.194}$$

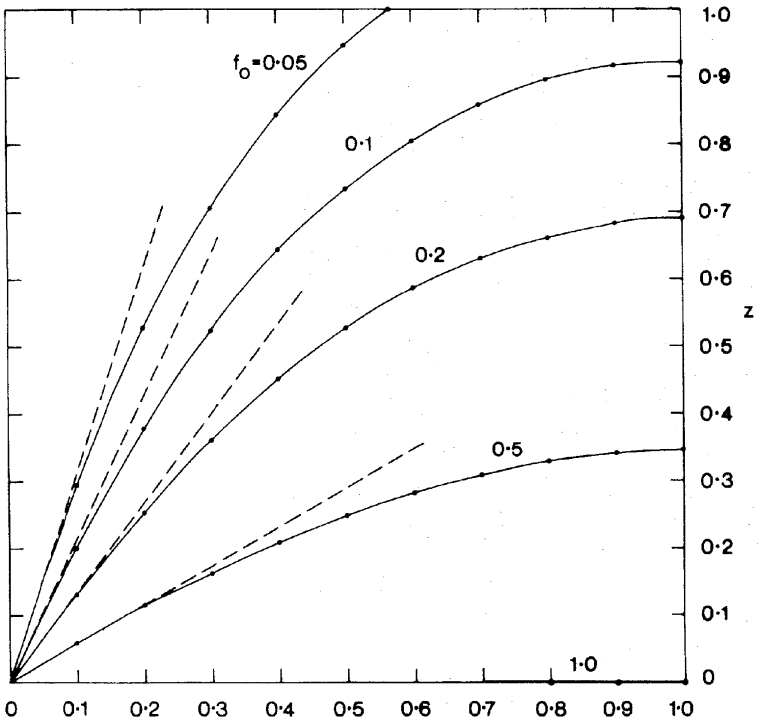

Fig. 2.15 Magnetic field structure for the zero longitudinal current and the accelerating potential ($i_0 = 0$, $\beta_0 = 0$) for the monopole magnetic field of the compact object (Michel, 1973a) [Reproduced by permission of the AAS, Fig. 2 from Michel, F.C.: Rotating magnetosphere: a simple relativistic model. ApJ **180**, 207–226 (1973)]

The solution to Eq. (2.194) [so-called Mestel equation (Mestel, 1973)] can be written as

$$(1 - \boldsymbol{\beta}_{\mathrm{R}}^2)\mathbf{B} + \boldsymbol{\beta}_{\mathrm{R}}(\boldsymbol{\beta}_{\mathrm{R}} \cdot \mathbf{B}) = -\nabla h, \tag{2.195}$$

while, for the zero accelerating potential ψ, Maxwell's equation $\nabla \cdot \mathbf{B} = 0$ looks like $\hat{\mathcal{L}}_2 h = 0$:

$$\frac{\partial^2 h}{\partial x_r^2} + \frac{(1 + x_r^2)}{x_r(1 - x_r^2)} \frac{\partial h}{\partial x_r} + \frac{(1 - x_r^2)}{x_r^2} \frac{\partial^2 h}{\partial \varphi^2} + \frac{\partial^2 h}{\partial z'^2} = 0. \tag{2.196}$$

On the other hand, the electric field for $\psi = 0$ can be found from the condition $\mathbf{E} + \boldsymbol{\beta}_{\mathrm{R}} \times \mathbf{B} = 0$, because relation (2.104) must hold for any quasistationary configurations. Therefore, the electric and magnetic fields can again be specified by equalities (2.120), (2.121), (2.122), and (2.123) in which we must take $\psi = 0$

$$\mathbf{E}_{\rm p} = \frac{[\boldsymbol{\beta}_{\rm R} \times \nabla h]}{1 - \boldsymbol{\beta}_{\rm R}^2}, \tag{2.197}$$

$$E_\varphi = 0, \tag{2.198}$$

$$\mathbf{B}_{\rm p} = -\frac{\nabla h}{1 - \boldsymbol{\beta}_{\rm R}^2}, \tag{2.199}$$

$$B_\varphi = -\frac{1}{\varpi}\frac{\partial h}{\partial \varphi}. \tag{2.200}$$

To construct the solution to Eq. (2.196), we see that in the studied linear case, the magnetic field of the neutron star can be expanded into axisymmetric and orthogonal parts. In other words, the potential $h(x_r, \varphi - \Omega t, z')$ can be represented as

$$h(x_r, \varphi - \Omega t, z') = h_0(x_r, z') \cos\chi + h_1(x_r, z')\ \cos(\varphi - \Omega t) \sin\chi, \tag{2.201}$$

and now the potentials $h_0(x_r, z')$ and $h_1(x_r, z')$ satisfy the equations

$$\frac{\partial^2 h_0}{\partial x_r^2} + \frac{(1 + x_r^2)}{x_r(1 - x_r^2)}\frac{\partial h_0}{\partial x_r} + \frac{\partial^2 h_0}{\partial z'^2} = 0, \tag{2.202}$$

$$\frac{\partial^2 h_1}{\partial x_r^2} + \frac{(1 + x_r^2)}{x_r(1 - x_r^2)}\frac{\partial h_1}{\partial x_r} + \frac{\partial^2 h_1}{\partial z'^2} - \frac{(1 - x_r^2)}{x_r^2} h_1 = 0. \tag{2.203}$$

Therefore, as in the case of the axisymmetric rotator, the solution to Eqs. (2.202) and (2.203) can be found in the form

$$h_0(x_r, z') = \frac{|\mathbf{m}|}{R_{\rm L}^2}\int_0^\infty R_\lambda^{(0)}(x_r) \sin(\lambda z')\, {\rm d}\lambda, \tag{2.204}$$

$$h_1(x_r, z') = \frac{|\mathbf{m}|}{R_{\rm L}^2}\int_0^\infty R_\lambda^{(1)}(x_r) \cos(\lambda z')\, {\rm d}\lambda, \tag{2.205}$$

where the radial functions $R_\lambda^{(0)}(x_r)$ and $R_\lambda^{(1)}(x_r)$ must satisfy the equations

$$\frac{{\rm d}^2 R_\lambda^{(0)}(x_r)}{{\rm d}^2 x_r} + \frac{(1 + x_r^2)}{x_r(1 - x_r^2)}\frac{{\rm d}R_\lambda^{(0)}(x_r)}{{\rm d}x_r} - \lambda^2 R_\lambda^{(0)}(x_r) = 0, \tag{2.206}$$

$$\frac{{\rm d}^2 R_\lambda^{(1)}(x_r)}{{\rm d}^2 x_r} + \frac{(1 + x_r^2)}{x_r(1 - x_r^2)}\frac{{\rm d}R_\lambda^{(1)}(x_r)}{{\rm d}x_r} - \left(\lambda^2 + \frac{1 - x_r^2}{x_r^2}\right) R_\lambda^{(1)}(x_r) = 0. \tag{2.207}$$

The boundary conditions for Eqs. (2.206) and (2.207), as before, are

1. the dipole magnetic field $\mathbf{B} = [3(\mathbf{nm})\mathbf{n} - \mathbf{m}]/r^3$ in the vicinity of the star surface, i.e.,

$$h_0(x_r, z') \to \frac{|\mathbf{m}|}{R_{\rm L}^2} \frac{z'}{(x_r^2 + z'^2)^{3/2}}, \tag{2.208}$$

$$h_1(x_r, z') \to \frac{|\mathbf{m}|}{R_{\rm L}^2} \frac{x_r}{(x_r^2 + z'^2)^{3/2}}, \tag{2.209}$$

for $x_r \to 0$ and $z' \to 0$;

2. the absence of a singularity on the light cylinder $x_r = 1$:

$$\left.\frac{{\rm d}R_\lambda^{(0)}}{{\rm d}x_r}\right|_{x_r=1} = 0, \tag{2.210}$$

$$\left.\frac{{\rm d}R_\lambda^{(1)}}{{\rm d}x_r}\right|_{x_r=1} = 0. \tag{2.211}$$

Using expansion (2.187) again, we find that for $x_r \to 0$, the following relations must hold:

$$R_\lambda^{(0)}(x_r) \to \frac{2}{\pi}\lambda K_0(\lambda x_r), \tag{2.212}$$

$$R_\lambda^{(1)}(x_r) \to \frac{2}{\pi}\lambda K_1(\lambda x_r). \tag{2.213}$$

Here $K_0(x)$ and $K_1(x)$ are the Macdonald functions of zero and the first order.

Besides (and it is very important), it is also necessary that the magnetic field should decrease at infinity along the rotation axis for $z \to \infty$. The necessity to introduce an "additional" boundary condition is that the magnetic field line extending to infinity along the rotation axis does not intersect the light cylinder and, hence, there is no additional regularity condition for it. When this condition is not satisfied, we have the nonphysical solution (Endean, 1983)

$$h_{\rm E}(x_r, \varphi, z', t) = h_*[x_r J_0(x_r) - J_1(x_r)]\cos(\varphi - \Omega t) \tag{2.214}$$

(h_*—an arbitrary constant) independent of z and, hence, not decreasing at infinity.

Problem 2.21 Show that the solution to Eqs. (2.206) and (2.207) can be constructed in the form of the formal series (Beskin et al., 1983; Mestel et al., 1999)

$$R_\lambda^{(0)}(x_r) = \mathcal{D}_0(\lambda)\sum_{n=2}^{\infty} b_n(1 - x_r^2)^n, \tag{2.215}$$

$$R_\lambda^{(1)}(x_r) = \mathcal{D}_1(\lambda)\sum_{n=2}^{\infty} c_n(1 - x_r^2)^n, \tag{2.216}$$

where the expansion coefficients b_n and c_n satisfy the recurrent relations

$$b_{n+1} = \frac{n}{n+1} b_n + \frac{\lambda^2}{4(n^2-1)} b_{n-1}, \tag{2.217}$$

$$c_{n+1} = \frac{n(2n-3)}{n^2-1} c_n - \frac{4(n-1)(n-2)-\lambda^2}{4(n^2-1)} c_{n-1} - \frac{\lambda^2-1}{4(n^2-1)} c_{n-2}, \tag{2.218}$$

where $b_0 = b_1 = c_0 = c_1 = 0$ and $b_2 = c_2 = 1$.

Problem 2.22 Using the asymptotic behavior $K_0(x) \to -\ln x$ and $K_1(x) \to x^{-1}$ for $x \to 0$, show that

$$\mathcal{D}_0(\lambda)^{-1} = -\frac{\pi}{2\lambda} \lim_{x_r \to 0} \frac{1}{\ln x_r} \sum_{n=2}^{\infty} b_n (1 - x_r^2)^n, \tag{2.219}$$

$$\mathcal{D}_1(\lambda)^{-1} = \frac{\pi}{2} \lim_{x_r \to 0} x_r \sum_{n=2}^{\infty} c_n (1 - x_r^2)^n. \tag{2.220}$$

Problem 2.23 Using definitions (2.197), (2.198), (2.199), and (2.200) and (2.215) and (2.216), show that the magnetic field and the charge density on the light cylinder are defined as

$$B_\varpi(R_\mathrm{L}, \varphi', z') = \tag{2.221}$$
$$4\frac{|\mathbf{m}|}{R_\mathrm{L}^3} \left[\cos\chi \int_0^\infty \mathcal{D}_0(\lambda) \sin(\lambda z') \mathrm{d}\lambda + \sin\chi \cos\varphi' \int_0^\infty \mathcal{D}_1(\lambda) \cos(\lambda z') \mathrm{d}\lambda \right],$$

$$\rho_\mathrm{e}(R_\mathrm{L}, \varphi', z') = \tag{2.222}$$
$$\frac{\Omega |\mathbf{m}|}{2\pi c R_\mathrm{L}^3} \left[\cos\chi \int_0^\infty \mathcal{D}_0(\lambda) \lambda \cos(\lambda z') \mathrm{d}\lambda - \sin\chi \cos\varphi' \int_0^\infty \mathcal{D}_1(\lambda) \lambda \sin(\lambda z') \mathrm{d}\lambda \right],$$

where $\varphi' = \varphi - \Omega t$.

Problem 2.24 Show that in the axisymmetric case the singular solution independent of z has a singularity on the light cylinder and, hence, must be abandoned automatically.

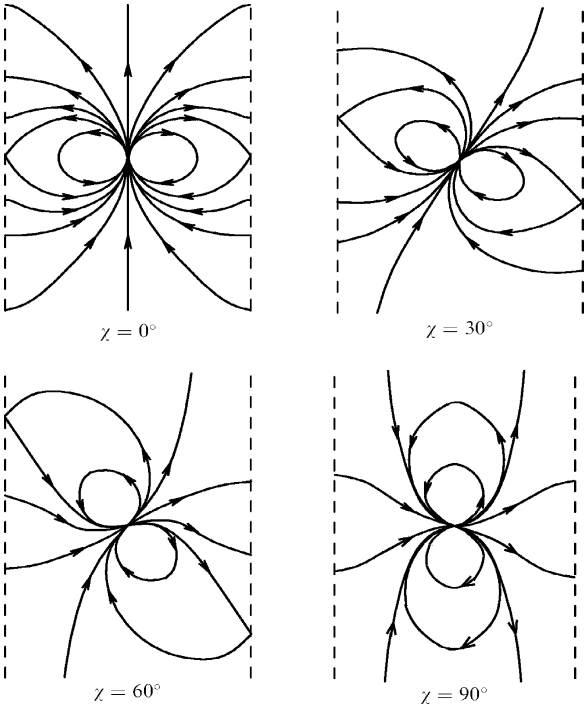

Fig. 2.16 Magnetic field structure for the zero longitudinal current and the accelerating potential ($i_0 = 0$, $\beta_0 = 0$) for the inclined dipole magnetic field of the neutron star (Beskin et al., 1983)

As shown in Fig. 2.16, for the case of the inclined rotator, the basic properties valid for the axisymmetric magnetosphere fully retain. In the absence of the longitudinal currents, the boundary of the region of applicability is the light cylinder, where the corotation currents begin to distort the dipole magnetic field. The magnetic field itself becomes orthogonal to the light cylinder here. On the other hand, the electric and magnetic fields exponentially decrease with distance from the equatorial plane. Finally, the total electric charge in the magnetosphere is zero.

Relations (2.215) and (2.216) allow us to get the complete information concerning the magnetosphere structure. Thus, Table 2.2 gives the values of the magnetic field (in $|\mathbf{m}|/R_{\rm L}^3$ units) and the charge density (in $\Omega B/2\pi c$ units) on the light cylinder for four different inclination angles χ. Besides, Fig. 2.17 shows the change in the polar cap form as the inclination angle χ increases. Its area varies from $1.592\,\pi R_0^2$ for $\chi = 0^\circ$ to $1.96\,\pi R_0^2$ for $\chi = 90^\circ$.

Problem 2.25 Using the nonphysical solution (2.214), show that the dimensionless area of the polar cap surface $f_*(90) \approx 1.96$ for $\chi = 90^\circ$ is expressed in terms of the Bessel functions J_0 and J_1

$$f_*(90) = \frac{2}{\pi[J_0(1) - J_1(1)]}. \tag{2.223}$$

Table 2.2 The magnetic field B_x (2.221) and the charge density ρ_e (2.222) on the light cylinder at different inclination angles of χ

	$\chi = 0^\circ$		$\chi = 30^\circ$		$\chi = 60^\circ$		$\chi = 90^\circ$	
z/R_L	B_x	ρ_e	B_x	ρ_e	B_x	ρ_e	B_x	ρ_e
1.5	0.16	−0.13	0.17	−0.14	0.12	−0.11	0.05	−0.05
1.4	0.22	−0.17	0.23	−0.19	0.18	−0.16	0.07	−0.08
1.3	0.30	−0.23	0.32	−0.26	0.25	−0.22	0.11	−0.12
1.2	0.41	−0.30	0.44	−0.35	0.36	−0.31	0.18	−0.19
1.1	0.54	−0.38	0.61	−0.48	0.51	−0.44	0.27	−0.29
1.0	0.71	−0.48	0.83	−0.63	0.72	−0.61	0.41	−0.43
0.9	0.93	−0.58	1.11	−0.81	1.00	−0.84	0.62	−0.63
0.8	1.17	−0.65	1.48	−1.02	1.39	−1.11	0.93	−0.90
0.7	1.44	−0.67	1.93	−1.20	1.89	−1.41	1.36	−1.24
0.6	1.70	−0.59	2.43	−1.32	2.52	−1.70	1.93	−1.62
0.5	1.89	−0.35	2.96	−1.30	3.24	−1.90	2.65	−1.99
0.4	1.95	0.08	3.44	−1.05	4.01	−1.90	3.50	−2.23
0.3	1.81	0.67	3.77	−0.53	4.72	−1.59	4.41	−2.22
0.2	1.41	1.31	3.84	0.22	5.23	−0.92	5.23	−1.82
0.1	0.78	1.82	3.58	1.06	5.42	0.01	5.81	−1.04
0.0	0.00	2.01	3.01	1.74	5.22	1.01	6.02	0.00
−0.1	−0.78	1.82	2.23	2.09	4.64	1.81	5.81	1.04
−0.2	−1.41	1.31	1.39	2.05	3.82	2.23	5.23	1.82
−0.3	−1.81	0.67	0.64	1.69	2.91	2.25	4.41	2.22
−0.4	−1.95	0.08	0.06	1.18	2.06	1.97	3.50	2.23
−0.5	−1.89	−0.35	−0.31	0.69	1.35	1.55	2.65	1.99
−0.6	−1.70	−0.59	−0.51	0.30	0.82	1.11	1.93	1.62
−0.7	−1.44	−0.67	−0.57	0.04	0.45	0.74	1.36	1.24
−0.8	−1.17	−0.65	−0.55	−0.11	0.22	0.46	0.93	0.90
−0.9	−0.92	−0.58	−0.49	−0.18	0.08	0.26	0.62	0.63
−1.0	−0.71	−0.48	−0.41	−0.20	0.00	0.14	0.41	0.43
−1.1	−0.54	−0.38	−0.33	−0.19	−0.04	0.06	0.27	0.29
−1.2	−0.41	−0.30	−0.26	−0.16	−0.05	0.02	0.18	0.19
−1.3	−0.30	−0.23	−0.20	−0.13	−0.05	−0.01	0.11	0.12
−1.4	−0.22	−0.17	−0.16	−0.11	−0.05	−0.01	0.07	0.08
−1.5	−0.16	−0.13	0.12	−0.08	−0.04	−0.01	0.05	0.05

(Hint: it is necessary to determine the Poynting vector flux through the light cylinder surface and the neutron star surface.)

On the other hand, from the analysis of the above solutions, we conclude that over the entire surface of the light cylinder, the toroidal magnetic field is zero though, unlike the axisymmetric case, it is not zero in the interior regions of the magnetosphere. Indeed, since expansions (2.215) and (2.216) begin with the second powers $(1 - x_r^2)$, definitions (2.199) and (2.200) show that at small distances from the light cylinder, the magnetic field components behave as

$$B_z \propto (1 - x_r^2), \quad B_\varphi \propto (1 - x_r^2)^2. \tag{2.224}$$

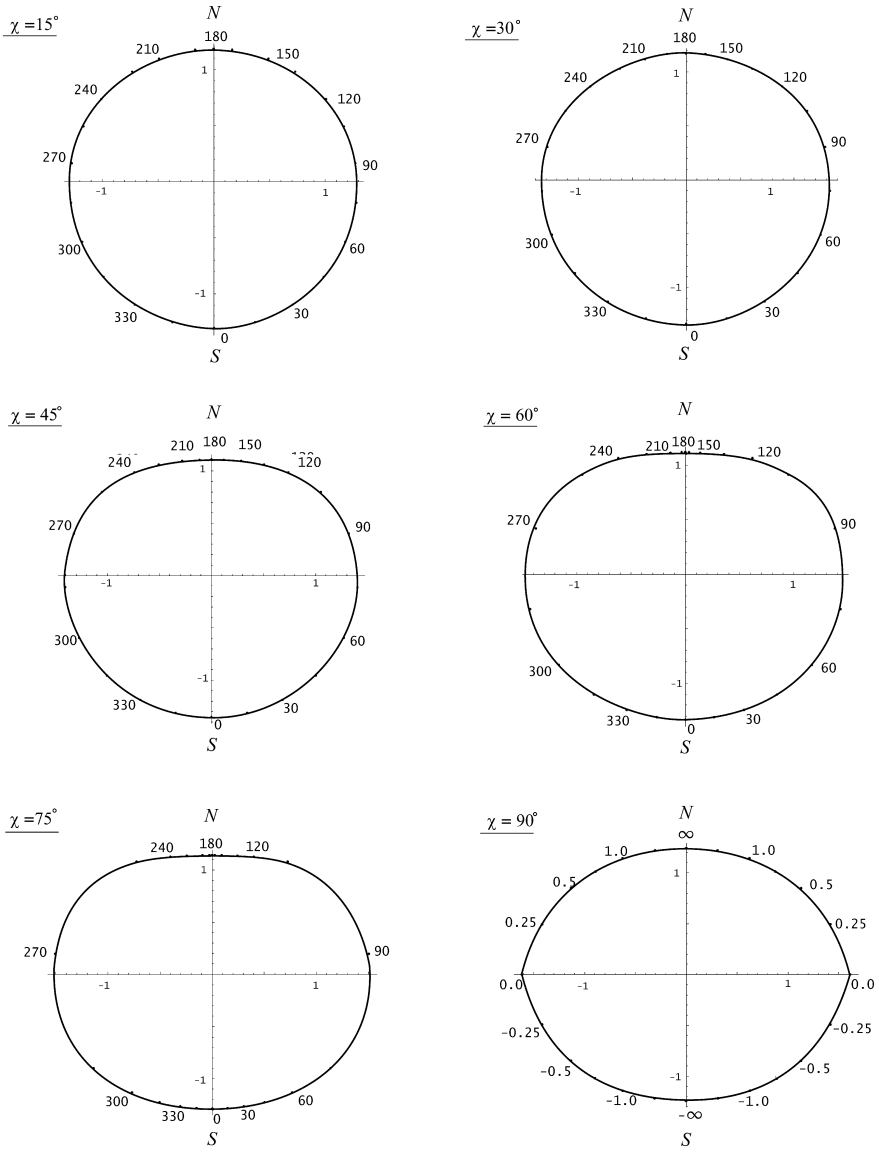

Fig. 2.17 The change in the polar cap form with increasing inclination angle χ. The numbers indicate the values of the angles φ (in degrees) and for $\chi = 90^\circ$ the values of z/R_L for which the field line coming out from the given point intersects the light cylinder

It is, at first sight, a purely mathematical property but, actually, is of fundamental importance and one of the key conclusions in this chapter. Therefore, the solution of the pulsar equation is thoroughly derived and given in the theorem:

Theorem 2.1 *In the absence of the longitudinal currents and the accelerating potential the Poynting vector flux through the surface of the light cylinder is zero. Otherwise, the corotation currents flowing in the magnetosphere completely screen the magnetodipole radiation of the neutron star. Therefore, in the case of the inclined rotator, all energy losses are connected with the longitudinal current circulating in the magnetosphere* (Beskin et al., 1983; Mestel et al., 1999).

One should note that the conclusion that there are no losses is, in no way, connected with the quasistationary approximation used here. Indeed, as was shown above, the magnetodipole radiation can be produced within this formalism. The point is that in the vacuum case we have two second-order equations (2.124) and (2.125) for the functions ψ and h, which can be rewritten as a single fourth-order equation for one of these values. Therefore, in the vacuum case, two independent solutions corresponding to retarded and advanced potentials are possible. The choice of only the retarded potentials involves an additional physical assumption in the absence of the confluence energy flux from infinity. In the case of the plasma-filled magnetosphere, Eq. (2.196) has the unique solution in the form of a standing wave that does not transport energy to infinity.

2.6.1.4 Axisymmetric Magnetosphere with a Nonzero Longitudinal Current for the Monopole Magnetic Field

F.C. Michel found another remarkable analytical solution for the monopole magnetic field of the star (Michel, 1973b). It turned out that for the special choice of the longitudinal current

$$I(\Psi) = I_{\rm M} = \frac{\Omega_{\rm F}}{4\pi}\left(2\Psi - \frac{\Psi^2}{\Psi_0}\right) \tag{2.225}$$

and for $\Omega_{\rm F} = \text{const}$, the monopole magnetic field

$$\Psi(r,\theta) = \Psi_0(1-\cos\theta) \tag{2.226}$$

is the exact solution to the pulsar equation (2.101), beyond the light cylinder as well. Otherwise, for the current $I = I_{\rm M}$ (2.225), the effects of the longitudinal currents and the corotation currents are fully compensated. It is easy to check that the current I takes the form $I(\theta) = I_{\rm M}^{(\rm A)}\sin^2\theta$, where

$$I_{\rm M}^{(\rm A)} = \frac{\Omega_{\rm F}\Psi_0}{4\pi}, \tag{2.227}$$

which, actually, corresponds to the GJ current density. As is evident from relations (2.225) and (2.226), in the Michel solution the electric field $\mathbf{E}$ having only the

θ-component is equal in magnitude to the toroidal component of the magnetic field

$$B_\varphi = E_\theta = -B_0 \left(\frac{\Omega R}{c}\right) \frac{R}{r} \sin\theta, \tag{2.228}$$

which at distances larger than the light cylinder radius becomes larger than the poloidal magnetic field $B_\mathrm{p} = B_0(R/r)^2$. On the other hand, in this solution the full magnetic field remains larger than the electric one everywhere, which makes the light surface extend to infinity.

As was already noted, the Michel solution, in spite of its artificial character, is of great importance in the black hole magnetosphere theory. Therefore, we return to this solution in the next chapter. We note here that the Michel solution proves useful for the radio pulsar magnetosphere theory as well, because this structure of the magnetic field can be realized beyond the light cylinder in the pulsar wind region. Therefore, we should emphasize at once that under the real conditions we, of course, deal with the so-called split monopole

$$\Psi(r,\theta) = \Psi_0(1 - \cos\theta), \quad \theta < \pi/2, \tag{2.229}$$

$$\Psi(r,\theta) = \Psi_0(1 + \cos\theta), \quad \theta > \pi/2, \tag{2.230}$$

rather than with a monopole when the magnetic flux converges in the lower hemisphere and diverges in the upper one, as shown in Fig. 2.18. In other words, for this solution to exist it is necessary to introduce the current sheet in the equatorial plane dividing the convergent and divergent magnetic fluxes. One should remember that in this geometry topologically equivalent to the dipole magnetic field both in the northern and in the southern parts of the magnetosphere, there is a charge outflow of the same sign. Therefore, the poloidal surface currents closing the bulk currents and ensuring the electric current conservation must flow along the sheet. This sheet is possible in the presence of the accretion disk in which the studied force-free approximation becomes inapplicable.

Problem 2.26 Show by direct substitution in Eq. (2.101) that the monopole magnetic field remains an exact solution for the arbitrary profile of the angular velocity $\Omega_\mathrm{F}(\Psi)$ if the electric current is still connected with it by the relation (Blandford and Znajek, 1977; Beskin et al., 1992a)

$$4\pi I(\Psi) = \Omega_\mathrm{F}(\Psi) \left(2\Psi - \frac{\Psi^2}{\Psi_0}\right). \tag{2.231}$$

Later Bogovalov (2001) demonstrated that in the force-free approximation (when massless charged particles can move radially with the velocity of light), the inclined split monopole field

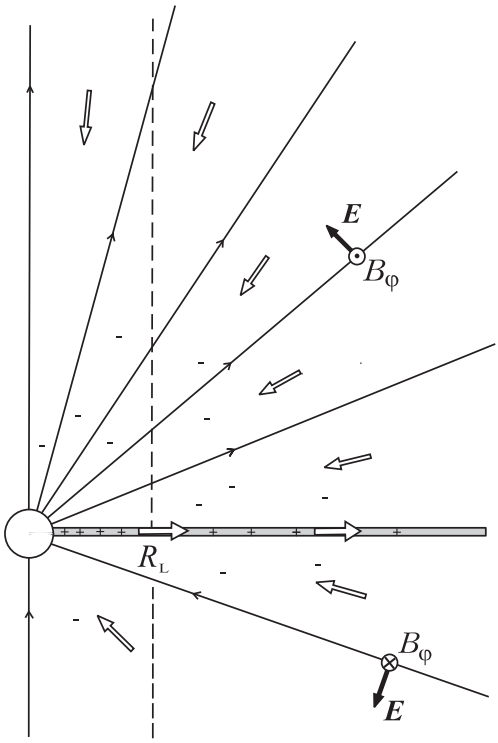

Fig. 2.18 The Michel monopole solution in which the electric field E_θ is exactly equal to the toroidal magnetic field B_φ. In the real conditions, this solution can be realized in the presence of the conducting disk in the equatorial plane along which the electric current closure occurs (*contour arrows*)

$$\Psi(r,\theta,\varphi,t) = \Psi_0(1-\cos\theta), \quad \theta < \pi/2 - \chi\cos(\varphi - \Omega t + \Omega r/c), \quad (2.232)$$

$$\Psi(r,\theta,\varphi,t) = \Psi_0(1+\cos\theta), \quad \theta > \pi/2 - \chi\cos(\varphi - \Omega t + \Omega r/c), \quad (2.233)$$

is the solution of the problem as well. In this case, within the cones $\theta < \pi/2 - \chi$, $\pi - \theta < \pi/2 - \chi$ near the rotation axis, the electromagnetic field is not time dependent, while in the equatorial region the electromagnetic fields change the sign at the instant the processing current sheet intersects the given point.

2.6.1.5 Axisymmetric Magnetosphere with a Nonzero Longitudinal Current for the Parabolic Magnetic Field

It turned out that the exact solution can be constructed by the "nonphysical" parabolic field $\Psi \propto r(1-\cos\theta)$ (1.127) shown in Fig. 2.19 (Blandford, 1976). Certainly, this structure of the magnetic field can again be realized only in the presence of the conducting disk so that the magnetic field lines in the lower and upper hemispheres specularly repeat one another. The jump of the tangential component of the magnetic field is connected with the electric currents flowing within the disk. One should stress at once that in the studied solution only the form of the magnetic

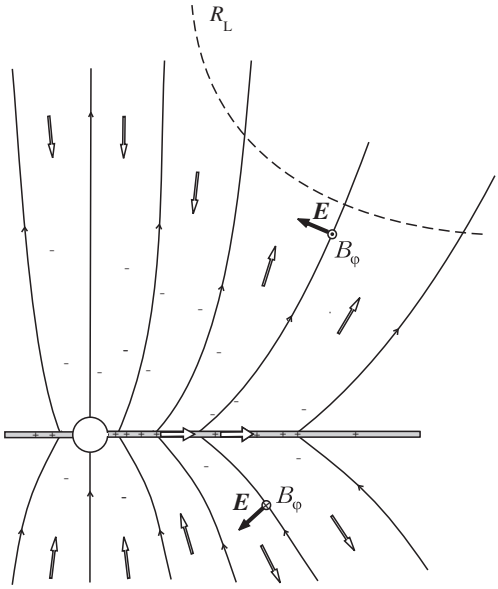

Fig. 2.19 The parabolic structure of the magnetic field and the longitudinal currents for the "nonphysical" solution (2.237). The angular velocity $\Omega_F(\Psi)$ is determined by the rotational velocity of the disk. Therefore, according to (2.235), the longitudinal current closes at the finite values of the magnetic flux Ψ. *Dashed line* indicates the light cylinder

surfaces coincides with the vacuum magnetic field. The density of the magnetic field lines should differ from that of the magnetic field in vacuum. Otherwise, the magnetic flux $\Psi(r,\theta)$ should have the form $\Psi(r,\theta)=\Psi(X)$, where for $\theta<\pi/2$

$$X = r(1-\cos\theta). \tag{2.234}$$

As in the previous case, this structure of the magnetic field can occur only if there is a certain connection between the angular velocity Ω_F and the current I, viz., when the following relation holds:

$$I(\Psi) = \frac{\mathcal{C}\Omega_F(X)X}{2\left[1+\dfrac{\Omega_F^2(X)X^2}{c^2}\right]^{1/2}}, \tag{2.235}$$

where $\mathcal{C}$ is an integration constant. In this case, the magnetic flux can be found from the condition

$$\frac{\mathrm{d}\Psi}{\mathrm{d}X} = \frac{\pi\mathcal{C}}{\left[1+\dfrac{\Omega_F^2(X)X^2}{c^2}\right]^{1/2}}. \tag{2.236}$$

As we see, here the solution also exists for any profile $\Omega_F(X)$. In particular, for the constant angular velocity, it has the form (Lee and Park, 2004)

$$\Psi(r,\theta)=\frac{\pi\mathcal{C}c}{\Omega_{\rm F}}\ln\left[\frac{\Omega_{\rm F}X}{c}+\sqrt{1+\frac{\Omega_{\rm F}^2X^2}{c^2}}\right]. \tag{2.237}$$

We should emphasize that though the above solution is formally valid for any value $\Omega_{\rm F}(X)X/c$, in reality, only the configurations in which

$$\frac{\Omega_{\rm F}(X)X}{c}<1 \tag{2.238}$$

can be realized. The point is that, as shown in Fig. 2.19, all magnetic surfaces must intersect the region of the accretion disk that must determine the value of the angular velocity $\Omega_{\rm F}$. But the accretion disk cannot rotate with the velocity larger than the velocity of light. Since in the equatorial plane $X=\varpi$, the condition (2.238) is to be satisfied over the entire space. As a result, the magnetic field structure does not differ too much from the vacuum solution.

On the other hand, for a fast decrease in the angular velocity $\Omega_{\rm F}(\Psi)$ with increasing Ψ, so that $\Omega_{\rm F}(\Psi)\varpi/c\to 0$, the longitudinal current, according to (2.235), is concentrated only in the region $\Omega_{\rm F}(0)X/c\sim 1$, so that the characteristic magnetic flux, within which the current closure occurs, can be estimated as

$$\Psi_0=\frac{\pi\mathcal{C}c}{\Omega_{\rm F}(0)}. \tag{2.239}$$

This relation defines the connection between the integration constant $\mathcal{C}$ and the flow Ψ_0 involved, for example, in the definition of the magnetization parameter σ (2.82).

The "nonphysical" solution was not as known as the Michel monopole solution though it, in many respects, much better describes the structure of the magnetized wind outflowing from compact objects. In particular, it adequately models the jet formation process. On the other hand, one should remember that for the existence of the magnetic field decreasing with distance as r^{-1} (and it is exactly how the magnetic field corresponding to the potential $X=r(1-\cos\theta)$ is constructed), the toroidal currents flowing in the equatorial plane are needed. In the absence of these currents, the parabolic magnetic field cannot be realized.

Problem 2.27 Show that for the parabolic solution, as in the Michel monopole solution, at large distances $r\to\infty$ the electric field is compared in magnitude with the magnetic one so that $B_{\rm p}\ll B_\varphi$ and $B_\varphi\approx|\mathbf{E}|$, where

$$B_\varphi = -\frac{\mathcal{C}\Omega_\mathrm{F}}{c\left[1+\dfrac{\Omega_\mathrm{F}^2(X)X^2}{c^2}\right]^{1/2}}\frac{(1-\cos\theta)}{\sin\theta}, \tag{2.240}$$

$$|\mathbf{E}| = \frac{\mathcal{C}\Omega_\mathrm{F}}{c\left[1+\dfrac{\Omega_\mathrm{F}^2(X)X^2}{c^2}\right]^{1/2}}\left(\frac{1-\cos\theta}{2}\right)^{1/2}. \tag{2.241}$$

2.6.1.6 Perturbation of the Monopole Magnetic Field

In conclusion, we consider another model problem of the small perturbation of the Michel monopole solution (Beskin et al., 1998). As was already mentioned, Eq. (2.101) needs three boundary conditions. We suppose that the angular velocity $\Omega_\mathrm{F} = \mathrm{const}$ remains the same as in the Michel solution. As to the longitudinal current $I(R,\theta)$, it is assumed to differ little from the Michel current (2.228)

$$I(R,\theta) = I_\mathrm{M}(\theta) + l(\theta) = I_\mathrm{M}^{(\mathrm{A})}\sin^2\theta + l(\theta), \tag{2.242}$$

so that $l(\theta) \ll I_\mathrm{M}^{(\mathrm{A})}$. Since the perturbations are assumed to be small, relation (2.242) defines the value of the current as a function of the stream function Ψ.

Writing now the solution to Eq. (2.101) as $\Psi(r,\theta) = \Psi_0[1-\cos\theta+\varepsilon f(r,\theta)]$, we obtain in the first order with respect to the small parameter $\varepsilon = l/I_\mathrm{M}^{(\mathrm{A})}$

$$\varepsilon(1-x^2\sin^2\theta)\frac{\partial^2 f}{\partial x^2} + \varepsilon(1-x^2\sin^2\theta)\frac{\sin\theta}{x^2}\frac{\partial}{\partial\theta}\left(\frac{1}{\sin\theta}\frac{\partial f}{\partial\theta}\right) - 2\varepsilon x\sin^2\theta\frac{\partial f}{\partial r}$$
$$-2\varepsilon\sin\theta\cos\theta\frac{\partial f}{\partial\theta} + 2\varepsilon(3\cos^2\theta-1)f = -\frac{1}{I_\mathrm{M}^{(\mathrm{A})}\sin\theta}\frac{\mathrm{d}}{\mathrm{d}\theta}(l\sin^2\theta). \tag{2.243}$$

Here $x = \Omega_\mathrm{F} r/c$. Equation (2.243), as was expected, has a singularity on the light cylinder $x\sin\theta = 1$.

In the general case, the solution to Eq. (2.243) is extremely cumbersome. However, for the special choice of the perturbation

$$l(\theta) = \varepsilon_* I_\mathrm{M}^{(\mathrm{A})}\sin^2\theta, \tag{2.244}$$

where $|\varepsilon_*| = \mathrm{const} \ll 1$, the analytical solution can be found. It has the form

$$\Psi(r,\theta) = \Psi_0\left[1-\cos\theta+\varepsilon_*\left(\frac{\Omega_\mathrm{F} r}{c}\right)^2\sin^2\theta\cos\theta\right]. \tag{2.245}$$

The solution (2.245) shows that for $I < I_{\rm M}$ ($\varepsilon_* < 0$), the magnetic field lines are concentrated near the equator ($\delta\Psi < 0$ for $\theta < \pi/2$). In this case, the light surface is located at finite distance from the light cylinder. It has the form of a cylinder with the radius

$$\varpi_{\rm C} = |2\varepsilon_*|^{-1/4} R_{\rm L}, \tag{2.246}$$

on which the monopole field perturbation can still be considered to be small. Accordingly, for $I > I_{\rm M}$ ($\varepsilon_* > 0$), the magnetic field lines turn to the rotation axis ($\delta\Psi > 0$ for $\theta < \pi/2$), and the light surface is reached only at infinity.

Problem 2.28 Find relation (2.246).

The above exact solutions of the pulsar equation lead to the following general conclusions:

1. The solution to the force-free equation (2.101) can be constructed only within the light surface $|\mathbf{E}| = |\mathbf{B}|$, which, for the zero longitudinal currents, coincides with the light cylinder $\varpi = c/\Omega_{\rm F}$. Beyond the light surface, the electric field becomes larger than the magnetic one, which results in violation of the frozen-in condition $\mathbf{E} + \mathbf{v} \times \mathbf{B}/c = 0$. In the general case, the light surface does not coincide with the light cylinder but is located at larger distances. As we will see, the presence or the absence of the light surface is of crucial importance for the discussion of the particle acceleration problem (within the force-free approximation the particle Lorentz factor on the light surface, formally, is infinite).
2. In the case of zero longitudinal currents, regardless of the inclination angle χ, the magnetic field on the light cylinder must be perpendicular to its surface (Henriksen and Norton, 1975; Beskin et al., 1983). This mathematical result leads to the most important physical conclusion—the Poynting vector does not have a normal component here and, hence, the electromagnetic energy flux through the light cylinder surface is zero. Consequently, in the absence of the longitudinal currents, the secondary plasma filling the magnetosphere must fully screen the magnetodipole radiation of the neutron star (Beskin et al., 1983; Mestel et al., 1999). Therefore, all the energy losses of the rotating neutron star are to be associated with the ponderomotive action of the surface currents closing the longitudinal currents flowing in the magnetosphere. Thus, formula (2.178) fully defines the slowing down of radio pulsars.
3. In the absence of the longitudinal currents, the magnetic field lines are concentrated in the vicinity of the equator. Otherwise, the toroidal currents $\mathbf{j} = \rho_{\rm GJ}\, \boldsymbol{\Omega} \times \mathbf{r}$ connected with the corotation of the GJ charge density $\rho_{\rm GJ}$ do not collimate the magnetic field lines but, on the contrary, make them diverge and concentrate near the equator. As a result, the magnetic field along the rotation axis decreases exponentially fast rather than by the power law.

2.6.2 Magnetosphere Structure with Longitudinal Currents

We proceed to the key part of this chapter, viz., to the discussion of the magnetosphere structure in the presence of the longitudinal current I and the accelerating potential ψ. The importance of this problem is obvious—as was shown above, the energy losses of radio pulsars are fully specified by the longitudinal electric currents circulating in the magnetosphere. Therefore, the question of the value of the longitudinal currents (and, hence, the presence or the absence of the light surface) is the key one the neutron star magnetosphere theory is to answer.

At the same time, there are two important circumstances. First, as was already noted, within the force-free approximation, the longitudinal current is a free parameter. Second, and it was also mentioned, the particle acceleration problem cannot be solved within this approximation. Therefore, we can analyze a limited set of problems only. A more comprehensive analysis is made in Chap. 5 on the basis of the full magnetohydrodynamic version of the GS equation.

On the other hand, in the presence of the longitudinal current even in the force-free approximation, Eq. (2.129) becomes essentially nonlinear. It is not surprising, therefore, that in most papers the analysis of only the axisymmetric magnetosphere was made. Indeed, since the total current within the polar cap is to be zero, expression $I\,\mathrm{d}I/\mathrm{d}\Psi$ cannot be a linear function Ψ on all open field lines. Except for the Michel and Blandford remarkable solutions (Michel, 1973b; Blandford, 1976), only some analytical solutions were obtained (Beskin et al., 1983; Lyubarskii, 1990; Sulkanen and Lovelace, 1990; Fendt et al., 1995; Beskin and Malyshkin, 1998). Therefore, the problem of construction of magnetosphere with nonzero longitudinal currents is still to be solved. As to the case of an inclined rotator, there are only preliminary results here (Mestel and Wang, 1982; Bogovalov, 1999, 2001).

Technically, the reason is that Eq. (2.101) contains a critical surface—a light cylinder, the passage of which requires the expansion of the solution into eigenfunctions that have no singularity on this surface. Exactly this method of solution was described above when analyzing the magnetosphere with zero longitudinal current. Therefore, in most cases, the similar problem was solved only analytically, which, in turn, could be done only for a certain class of functions $I(\Psi)$, viz., when the current density is constant in the whole region of open magnetic field lines (i.e., when $I(\Psi) = k\Psi$), and the current closure occurs along the separatrix dividing the open and closed field lines. In this statement, Eq. (2.101) appears linear in the region of not only closed but also open magnetic field lines, and the main problem reduces to matching the solutions in these two regions. It is in this direction that the main results of the magnetosphere structure with longitudinal electric field were obtained.

Consider now the analytical method for constructing the solution in more detail, since it allows us to formulate the main problems that arise when trying to construct the self-consistent model of the magnetosphere of radio pulsars containing longitudinal currents. Thus, we consider the axisymmetric force-free magnetosphere of the rotating neutron star. As was already mentioned, with the special choice of the longitudinal current I and the potential ψ, Eq. (2.101) can be reduced to a linear one. This is possible if we take the values of $\Omega_{\mathrm{F}}(\Psi)$ and $I(\Psi)$ in the form

$$\Omega_{\rm F}(\Psi) = \Omega(1-\beta_0), \tag{2.247}$$

$$I(\Psi) = \frac{\Omega}{2\pi} i_0 \Psi, \tag{2.248}$$

where i_0 and β_0 are constant. Recall that their physical meaning is defined by relations (2.107) and (2.108).

The pulsar equation in the region of open field lines in the dimensionless variables $x_r = \Omega\varpi/c$, $z' = \Omega z/c$ takes the form

$$-\nabla^2\Psi\left[1 - x_r^2(1-\beta_0)^2\right] + \frac{2}{x_r}\frac{\partial\Psi}{\partial x_r} - 4i_0^2\Psi = 0. \tag{2.249}$$

In the region of closed field lines, where, as was already noted, the potential $\psi = 0$ (i.e., $\beta_0 = 0$), we simply have

$$-\nabla^2\Psi\left(1 - x_r^2\right) + \frac{2}{x_r}\frac{\partial\Psi}{\partial x_r} = 0. \tag{2.250}$$

As a result, all nonlinearity is enclosed in a thin transition layer in the vicinity of the separatrix, the very position of which must be found from the solution. Note that, unlike the case of the zero longitudinal current, the zero point of the magnetic field must not necessarily lie on the light cylinder surface $x_r = 1$.

Problem 2.29 Show that, in this case, the solution to Eq. (2.249) that has no singularity on the surface $x_r = (1-\beta_0)^{-1}$ can be constructed in the form of the series (Beskin et al., 1983)

$$R_\lambda(x_1) = \mathcal{D}(\lambda)\sum_{n=0}^{\infty} a_n(1-x_1^2)^n, \tag{2.251}$$

where $x_1 = (1-\beta_0)x_r$, $\alpha_1 = 4i_0^2/(1-\beta_0)^2$, and the expansion coefficients a_n satisfy the recurrent relations

$$a_0 = 1, \quad a_1 = -\frac{\alpha_1}{4}, \quad a_{n+1} = \frac{4n^2-\alpha_1}{4(n+1)^2}\,a_n + \frac{\alpha_1+\lambda^2}{4(n+1)^2}\,a_{n-1}. \tag{2.252}$$

Here $\mathcal{D}(\lambda)^{-1} = (\pi/2)(1-\beta_0)^{-1}\sum_{n=0}^{\infty} a_n$.

We now specify the boundary conditions for the system of equations (2.249) and (2.250). In the region of open field lines, Eq. (2.249), according to (1.64), requires three boundary conditions. These conditions are, first of all, the values i_0 and β_0 determined on the star surface. The third boundary condition is not only the value of the stream function $\Psi(R,\theta)$ on the star surface (2.103) but also the value of the

function Ψ on the surface of the separatrix $z'_*(x_r)$ dividing the region of the open and closed magnetospheres (Okamoto, 1974)

$$\Psi^{(1)}\big|_{z'=z'_*(x_r)} = \Psi^{(2)}\big|_{z'=z'_*(x_r)}. \tag{2.253}$$

Finally, the regularity condition (2.211) on the light cylinder $x_r = x_\mathrm{L}$ is written as

$$\frac{2}{x_r}\frac{\partial\Psi}{\partial x_r}\bigg|_{x_r=(1-\beta_0)^{-1}} - 4i_0^2\Psi\big|_{x_r=(1-\beta_0)^{-1}} = 0. \tag{2.254}$$

Clearly, in the presence of the longitudinal current (i.e., for $B_\varphi \neq 0$), the light surface no longer coincides with the light cylinder. Relation (2.254) also shows that in the studied statement of the problem, the magnetic field lines on the light cylinder must be directed from the equator ($B_z > 0$ for $\Omega \cdot \mathbf{m} > 0$).

As to the region of closed field lines, which, in the general case, does not reach the light cylinder, exactly the conditions of matching the regions of closed and open field lines must act as additional boundary conditions for it. These conditions should be, first of all, the coincidence of the location of the separatrix field line $z' = z'_*(x_r)$ for both the regions (2.253) and, besides, the continuity of the value $\mathbf{B}^2 - \mathbf{E}^2$:

$$\{\mathbf{B}^2 - \mathbf{E}^2\} = 0. \tag{2.255}$$

The latter condition is easy to deduce by integrating the force-free equation written as $(\nabla\cdot\mathbf{E})\mathbf{E}+[\nabla\times\mathbf{B}]\times\mathbf{B} = 0$ over a thin transition layer (Okamoto, 1974; Lyubarskii, 1990). It is important that the condition (2.255) is obtained if the curvature of the magnetic field lines is disregarded and, therefore, cannot be used in the vicinity of singular points.

Problem 2.30 Find the condition (2.255) for the Cartesian coordinate system in which the transition layer coincides with the xy-plane (Lyubarskii, 1990).

We can now mention the main papers concerned with the force-free magnetosphere of radio pulsars (in which, in particular, the system of equations (2.249) and (2.250) was analyzed) for the real dipole field of the neutron star.

1. In Beskin et al. (1983), the case $i_0 \neq 0$, $\beta_0 \neq 0$ was studied. Only relation (2.253) was used; the equilibrium condition (2.255) was not taken into account. Besides, the region of closed field lines was supposed to remain the same as in the absence of the longitudinal current.
2. In Lyubarskii (1990), for $\beta_0 = 0$, both the equilibrium conditions (2.253) and (2.255) were taken into account. Incidentally, the additional assumption was that the last open field line, as in the Michel monopole solution, coincides with the equator beyond the light cylinder. Finally, in the paper, the absence of an inverse

current along the separatrix was implicitly assumed, which substantially changed the magnetic field structure in the vicinity of the zero point.

3. In Sulkanen and Lovelace (1990), for $\beta_0 = 0$, the case of the strong longitudinal current $i_0 > 1$ was studied. As was expected, with these longitudinal currents, the magnetic surface collimates to the rotation axis. The equilibrium conditions with the region of closed field lines were not used at all. As a result, there occurred a region, in which the poloidal magnetic field is absent, between the regions of open and closed field lines.
4. In Beskin and Malyshkin (1998), both the two equilibrium conditions and the perturbation of the region of closed field lines were taken into account. It was also shown that the zero point can be located inside the light cylinder: $x_r^{(*)} < 1$. However, the magnetic field structure in the equatorial region beyond the zero point was not discussed in the paper.

Figure 2.20 shows, as an example, the structure of the magnetic surfaces for the nonzero longitudinal current i_0 and the accelerating potential β_0 obtained numerically by solving Eqs. (2.249) and (2.250) (Beskin and Malyshkin, 1998). It was shown that the solution of the problem cannot be constructed for any values of i_0 and β_0. The point is that, for certain parameters i_0, β_0, the solution to Eq. (2.249) in the region of open field lines shows that the zero line of the magnetic field is located beyond the light cylinder $x_{\rm L} = 1$. Clearly, in this case, the solution cannot be matched to the closed magnetosphere region because the solution with $i_0 = 0$ cannot be extended to the region $x_r > 1$. As shown in Fig. 2.21, on the plane of the parameters $i_0 - \beta_0$, the forbidden region corresponds to rather small values of i_0.

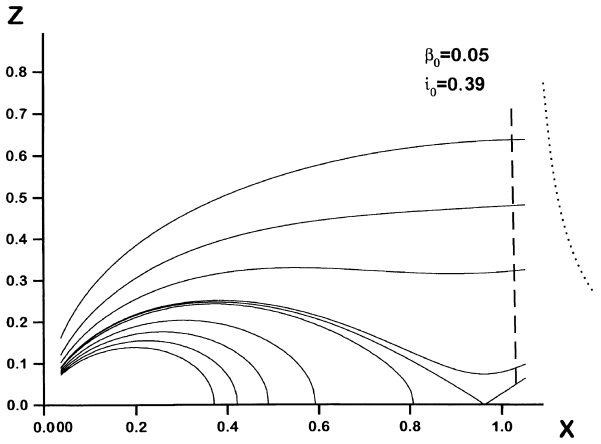

Fig. 2.20 The magnetosphere structure of the axisymmetric rotator for $i_0 = 0.39$ and $\beta_0 = 0.05$. The values of i_0 and β_0 do not correspond to "Ohm's law" (2.256) and, therefore, the zero point is within the "light cylinder" $x_r = 1$. The real light cylinder (*dashed line*) is at a distance of $x_r = 1/(1 - \beta_0)$ from the rotation axis. The *dotted line* indicates the light surface (in this paper, its location was not established) (Beskin and Malyshkin, 1998)

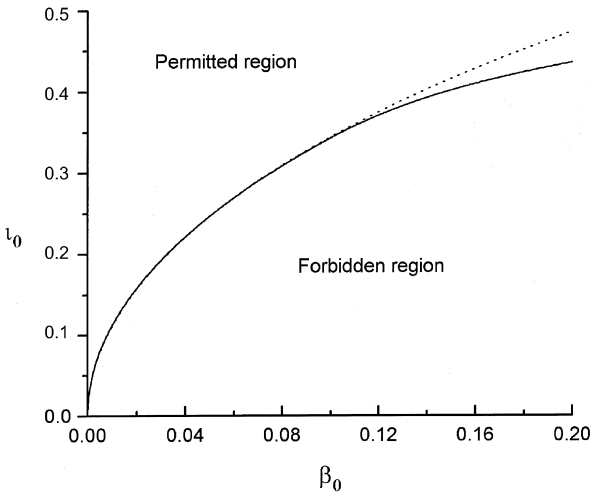

Fig. 2.21 The range of parameters i_0–β_0, for which the construction of the solution is possible. The *dotted line* indicates "Ohm's law" (2.256) (Beskin and Malyshkin, 1998)

Thus, the important conclusion is that the existence in the neutron star magnetosphere of the closed magnetic field lines that do not intersect the light cylinder can impose a certain constraint on the longitudinal currents circulating in the magnetosphere. The thorough computations show that the total energy of the electromagnetic field proves minimal exactly in the vicinity of the boundary line $\beta_0 = \beta_0(i_0)$, when, by the way, the zero point of the magnetic field lies in the vicinity of the light cylinder (Beskin and Malyshkin, 1998). Consequently, we can suppose that the equilibrium of the radio pulsar magnetosphere is realized only for a certain connection between the accelerating potential $\psi(P, B_0)$ and the longitudinal current I.

The existence of this "Ohm's law" (Beskin et al., 1983) is certainly a very important conclusion. Indeed, as was shown, it is the longitudinal currents that specify the energy losses of a rotating neutron star. Consequently, if there is a connection between the longitudinal current and the accelerating potential, the energy losses of the neutron star are fully determined by the concrete particle generation mechanism near the pulsar surface. Note that the compatibility relation prescribing nonlinear "Ohm's law" can be derived directly from the pulsar equation. Indeed, supposing that the field line $\Psi = \Psi_*$ corresponding to the solution of Eq. (2.249) in the open magnetosphere region passes in the vicinity of the zero point (where $B_z \propto (\partial\Psi/\partial x_r) = 0$) located on the light cylinder (where $x_r = 1$), we have directly from (2.249)

$$\beta_0(i_0) = 1 - \left(1 - \frac{i_0^2}{i_{\max}^2}\right)^{1/2}, \tag{2.256}$$

where $i_{\max} = \sqrt{(\nabla^2\Psi)_*/4\Psi_*} \approx 0.79$. As seen from Fig. 2.21, the analytical estimate (2.256) is in good agreement with the numerical computations. Relation (2.256), in the large, remains valid for the inclined rotator (Beskin et al., 1993).

On the other hand, as shown in Fig. 2.21, relation (2.256) actually yields only the lower bound for the longitudinal current. Accordingly, the conclusion of the small value of the longitudinal current was not confirmed independently in other papers. Therefore, the question of the value of the longitudinal current remains open. What can be stated with assurance is that the longitudinal current circulating in the radio pulsar magnetosphere does not, evidently, exceed the GJ current. Thus, the problem of the exact value of the energy losses $W_{\rm tot}$ and the existence of the light surface, on which, as we will see, the extra acceleration of particles is possible, remains unsolved. However, for most applications, the estimate $I \approx I_{\rm GJ}$ appears adequate, so that relation (2.5) is a good approximation to $W_{\rm tot}$. In any event, the problem of the value of the longitudinal current cannot be fully solved by the force-free approximation.

As was already noted, the analytical approach is restricted by the choice of the homogeneous longitudinal current density ($I(\Psi) = k\Psi$). Only a quarter of a century later, after the pulsar equation was formulated, Contopoulos et al. (1999) first studied the system of equations (2.249) and (2.250) numerically. In particular, they succeeded in (by an iterative procedure) passing the singularity on the light cylinder for the arbitrary current $I(\Psi)$. For the case $\beta_0 = 0$, the additional assumption that the last open field line coincides with the equator was also made there (see Fig. 2.22). It is not surprising, therefore, that the longitudinal current (which in the presence of the additional condition is no longer a free parameter) appeared close to

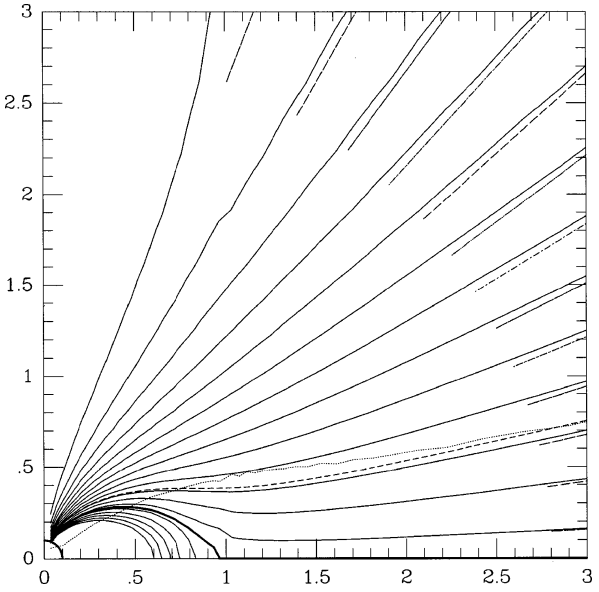

Fig. 2.22 The magnetosphere structure in the model (Contopoulos et al., 1999). The additional assumption that the last open field line coincides with the equator was made (Reproduced by permission of the AAS, Fig. 3 from Contopoulos, I., Kazanas, D., Fendt, C.: The axisymmetric pulsar magnetosphere. ApJ **511**, 351–558 (1999))

the current $I_{\rm M}$ (2.225) for the Michel monopole solution which does not correspond to the GJ current density $j_{\rm GJ} = \rho_{\rm GJ}c \approx$ const. At the same time, the equilibrium condition (2.255) was not taken into account in the paper. This statement of the problem was later discussed in Ogura and Kojima (2003), Goodwin et al. (2004), Gruzinov (2005), Contopoulos (2005), Komissarov (2006), McKinney (2006a), and Timokhin (2006), and, in a number of papers, the case, in which the zero point of the magnetic field can be located within the light cylinder, was also analyzed.

Let us briefly enumerate the main difficulties the force-free magnetosphere theory encounters. First of all, it turned out that the analytical solution method discussed above does not, actually, allow us to uniquely specify the magnetic field structure. The point is that the dipole magnetic field in the vicinity of the neutron star corresponds to the high harmonics λ in expansion (2.184), whereas the visible magnetic field structure on scales comparable with those of the light cylinder is specified by the small values of λ. As a result, the solution

$$\Psi(\varpi, z) = \frac{|\mathbf{m}|}{R_{\rm L}} \int_0^\infty Q(\lambda) R_\lambda(\varpi) \cos \lambda z \mathrm{d}\lambda, \tag{2.257}$$

where $Q(\lambda) \to 1$ for $\lambda \to \infty$, still corresponds to the dipole magnetic field for $\mathbf{r} \to 0$. This is because on the background of the large dipole magnetic field near the neutron star surface, one fails to control the harmonics with the small value of λ, which is crucial at large distances from the star.

The problem of the magnetic field structure in the equatorial region beyond the zero point is not solved either. As was mentioned, in most papers it was supposed in the example of the solar wind that a current sheet is to develop here, which separates the oppositely directed flows of the magnetic field (see Fig. 2.22) (Lyubarskii, 1990; Contopoulos et al., 1999; Uzdensky, 2003; Goodwin et al., 2004). It was, generally, believed that the inverse current is enclosed in an infinitely thin sheet and, therefore, the toroidal magnetic field B_φ does not disappear up to the separatrix surface. However, as was shown (Beskin and Malyshkin, 1998; Uzdensky, 2003), allowance for the width finiteness of the sheet with the inverse current (i.e., allowance for the continuity of B_φ) can appreciably change the main conclusions of the magnetic field structure in the vicinity of the separatrix. In particular, it is obvious that if the toroidal magnetic field B_φ is zero in the equatorial plane, the light surface $|\mathbf{E}| = |\mathbf{B}|$ must pass through the point $\varpi = c/\Omega$, $z = 0$ on the light cylinder surface (see Uzdensky (2003) for details). This problem does not arise for the solar wind since the Earth is within the light cylinder.

On the other hand, one should note that this topology is not the only possibility. Indeed, as is seen from the form of Eq. (2.250), at the zero point (i.e., at the point at which $\partial\Psi/\partial x_r = 0$), either the condition $(\nabla^2\Psi)_* = 0$ or the condition $x_r^2 = 1$ is to be satisfied. Therefore, for rather large longitudinal currents when the zero point is located within the light cylinder, the condition $(\nabla^2\Psi)_* = 0$ is to be satisfied. This implies that the angle between the separatrices is 90°. There is the same angle for the vacuum case. Therefore, this zero point can be matched to the outer region that is not connected by the magnetic field lines with the neutron star surface, for example,

with the chain of magnetic islands located in the equatorial plane (see Fig. 3.12b). Only in the limiting case, in which the zero point lies on the light cylinder $x_r = 1$ (as, for example, is the case for the solution with the zero longitudinal current), the value $(\nabla^2\Psi)_*$ remains finite at the zero point (the angle between the separatrices, as shown in Fig. 2.14, is 70°).

Finally, one should remember that most of the solutions, which influence our viewpoint on the radio pulsar magnetosphere structure, referred to the axisymmetric case. For the inclined rotator, quite new effects can occur, which completely change the entire pattern involved. Unfortunately, in this region (except for the case of the above zero longitudinal current) no reliable results that would allow us to confidently judge the magnetosphere properties of the inclined rotator were obtained (Mestel and Wang 1982; Bogovalov 1999, 2001; Spitkovsky, 2006).

Nevertheless, let us try to point out the general properties following from the analysis of Eq. (2.101) describing the force-free neutron star magnetosphere.

1. In the case of zero longitudinal currents independent of the inclination angle χ, the secondary plasma filling the magnetosphere fully screens the magnetodipole radiation (Beskin et al., 1983; Mestel et al., 1999). Therefore, the energy losses of the rotating radio pulsar can be caused only by the ponderomotive action of the surface currents closing the longitudinal currents flowing in the pulsar magnetosphere. Consequently, formula (2.178) fully defines the slowing down of radio pulsars.
2. When the longitudinal current coincides with the Michel current $I_{\rm M}$, the full compensation of two opposite processes occurs, viz., the decollimation connected with the toroidal current and the collimation due to the longitudinal currents. As a result, the monopole magnetic field, which is an exact vacuum solution, turns out to be an exact solution to Eq. (2.101) in the presence of plasma. Certainly, the exact value of the critical current depends on the concrete geometry of the poloidal magnetic field. However, we can confidently state that $j_{\rm cr} \approx \rho_{\rm GJ} c$.
3. For $j_\parallel > j_{\rm cr}$, the light surface (which, in the general case, does not coincide with the light cylinder) extends to infinity. This implies that for sufficiently large longitudinal currents the solution can be really extended to infinity. The magnetic surfaces are collimated to the rotation axis (Sulkanen and Lovelace, 1990).
4. If there are any physical constraints from above on the value of the longitudinal current so that $j_\parallel < j_{\rm cr}$, the magnetosphere has a "natural boundary"—the light surface. In this case, the complete problem comprising the outer regions cannot be solved within one-fluid magnetic hydrodynamics because, in this case, multiple flow regions occur.

2.6.3 Magnetosphere Models

As was mentioned, the pulsar wind problem is impossible to solve by the force-free approximation. Therefore, we briefly discuss here only the common features of the most developed models of the radio pulsar magnetosphere. The particle acceleration problems are discussed in Chap. 5.

Recall first that the existence of the light surface depends on the value of the longitudinal current. The point is that, as was noted, the presence of light surface at a finite distance from the neutron star must result in the efficient particle acceleration in the pulsar wind. In particular, in the nonfree particle escape models (in which the electric current in the plasma generation region can be arbitrary), the longitudinal current i_0 is to be determined from relation (2.256). For sufficiently small values of the potential drop $\beta_0 < 1$, the longitudinal current should also be small. This implies that the light surface, on which the additional particle acceleration, inevitably, occurs, should be at a finite distance from the neutron star. Certainly, the existence of the light surface leads to the substantial complication of the theory—in fact, not a single, at least, somewhat reliable result of the plasma behavior beyond the light surface has been obtained yet.

Besides, one should not think that the existence of the light surface can be realized only within the model of the nonfree particle escape from the neutron star surface. Indeed, as is evident from the example of the force-free approximation, the light surface extends to infinity only for rather large values of the longitudinal current. As shown in Chap. 4, this conclusion remains valid for the MHD flows as well. Therefore, for any additional constraints from above on the value of the longitudinal electric current, the occurrence of the light surface at a finite distance from the pulsar can be expected. However, within the particle generation model with free particle escape from the star surface, the value of the longitudinal electric current $4\pi I(\Psi) = 2\Omega_{\rm F}\Psi$ ($j_\parallel = j_{\rm GJ}$) is fixed and, what is especially important, substantially differs from the Michel current $4\pi I_{\rm M} = \Omega_{\rm F}(2\Psi - \Psi^2/\Psi_0)$. Therefore, it is not improbable that in the real dipole geometry of the pulsar magnetic field this current is not strong enough for a continuous (in particular, transonic) plasma outflow to exist up to large distances as compared to the light cylinder radius. In any case (and it is very important), in the numerically obtained solutions, the value of the longitudinal current $I(\Psi)$ is smaller than that of the limit current $I_{\rm M}$ (2.225) corresponding to the Michel monopole solution. Therefore, the light surface for this solution can be at a finite distance from the neutron star (see, e.g., Ogura and Kojima, 2003). Certainly, the exact proof of this fact invites further investigation.

Indeed, the analysis of the axisymmetric magnetosphere produced up to now did not clarify this point. As was demonstrated, exact analytical solutions (having the longitudinal current $j_\parallel \approx$ const within open magnetic field lines) contain the light surface at a finite distance. But their behavior is irrational near the equatorial plane outside the light cylinder. On the other hand, the numerical calculations postulating the existence of the current sheet outside the light cylinder demand the presence of the longitudinal current $I \approx I_{\rm M}$, which is inconsistent with any particle generation mechanism ($j_\parallel \to 0$ near the separatrix).

The above arguments for the existence of the light surface were brought forward for the axisymmetric magnetosphere. It turned out that in the case of the inclined rotator, the situation is much more obvious. Indeed, for the orthogonal rotator the GJ charge density in the vicinity of the magnetic pole should be $\varepsilon_{\rm A} = (\Omega R/c)^{1/2}$ times less than that in the axisymmetric magnetosphere. Accordingly, one can expect that the longitudinal current flowing along the open field lines is weaker in the same

proportions. Then in the vicinity of the light cylinder, the toroidal magnetic field appears much smaller than the poloidal magnetic field. On the other hand, as we saw in the example of the Michel solution, for the light surface to extend to infinity, it is necessary that the toroidal magnetic field on the light cylinder be of the order of the poloidal field. Therefore, if the longitudinal current $j_\parallel$, in reality, is not $\varepsilon_{\mathrm{A}}^{-1/2}$ times higher than $\rho_{\mathrm{GJ},90}c$, where $\rho_{\mathrm{GJ},90}$ is the mean charge density on the polar cap for $\chi \sim 90^\circ$ (and for ordinary pulsars this factor is 10^2), the light surface for the orthogonal rotator must, inevitably, be in the immediate vicinity of the light cylinder.

Thus, the presence or the absence of the light surface must be the basic element when constructing the radio pulsar magnetosphere model. Therefore, we will try to classify the magnetosphere models with this in mind. *The first class* of models suggests the presence of the light surface in the vicinity of the light cylinder, which can be realized for rather weak longitudinal currents flowing in the magnetosphere (Beskin et al., 1983; Chiueh et al., 1998). Within this approach, it is supposed that

- the energy losses of the rotating neutron star are fully defined by the current losses;
- the small value of the longitudinal current $i_0 < 1$ results in the occurrence of the light surface;
- in the vicinity of the light surface almost the total electromagnetic flux is transferred to the particle energy flux;
- accordingly, the full closure of the longitudinal current circulating in the magnetosphere really occurs here (see Fig. 2.23).

The problems of the particle acceleration in the vicinity of the light surface are beyond the scope of our discussion. Therefore, we only point to the main features of this process. In the simplest cylindrical geometry when solving the two-fluid hydrodynamical equations (describing exactly the difference in the electron and positron motion), it was shown (Beskin et al., 1983) that a considerable part of the energy carried within the light surface by the electromagnetic field in the thin transition layer

$$\Delta r \sim \lambda^{-1} R_{\mathrm{L}} \tag{2.258}$$

in the vicinity of the light surface is transferred to the particle energy flux ($\lambda \sim 10^4$ is the multiplicity parameter). Here, as shown in Fig. 2.23, the total closure of the longitudinal current circulating in the magnetosphere really occurs. As a result, the high efficiency of the particle acceleration has its logical explanation.

Note, however, that the presence of the light surface leads to a considerable complication of the whole problem of the neutron star magnetosphere structure. In this case, it is possible to somewhat reliably describe only the interior regions of the magnetosphere. The problems of the future destiny of the accelerated particles, the energy transport at large distances, and also the current closure are still to be solved. As was noted, these problems are beyond the scope of one-fluid hydrodynamics; evidently, they cannot be solved at all within the analytical approach.

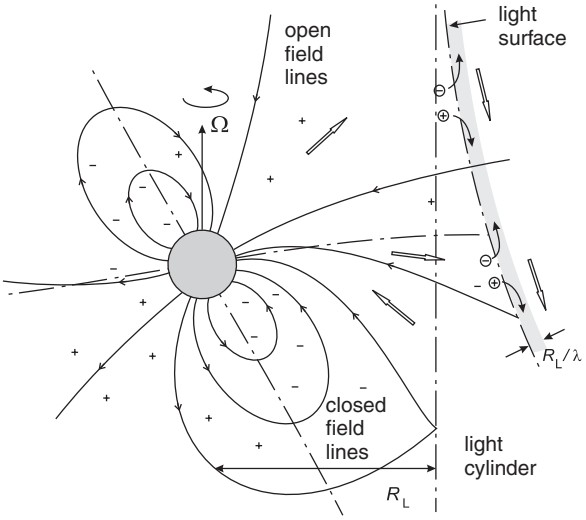

Fig. 2.23 Magnetosphere structure in the model by Beskin et al. (1993). If there are some physical constraints on the value of the longitudinal current (*contour arrows*) so that $j_\parallel < j_{\rm cr}$, the magnetosphere has a "natural boundary"—the light surface $|\mathbf{E}| = |\mathbf{B}|$, where the frozen-in condition becomes inapplicable. Therefore, electrons and positrons begin to accelerate in different directions along the electric field and a strong poloidal electric current is generated. As a result, in the thin layer $\Delta r \approx R_{\rm L}/\lambda$, the full closure of the electric current really occurs and the particle energy flux becomes comparable with the total energy flux

The analogous result was later obtained on the basis of the solutions of the two-fluid hydrodynamical equations for more realistic geometry when the poloidal magnetic field is close to the monopole one (Beskin and Rafikov, 2000). It was shown that all results obtained for the cylindrical case remain valid for the more realistic two-dimensional geometry. In particular, it was confirmed that the particles can be accelerated up to energy

$$\varepsilon_{\rm e} \sim eB_0R\frac{1}{\lambda}\left(\frac{\Omega R}{c}\right)^2 \sim 10^4\,{\rm MeV}\left(\frac{\lambda}{10^3}\right)^{-1}\left(\frac{B_0}{10^{12}{\rm G}}\right)\left(\frac{P}{1{\rm s}}\right)^{-2}, \qquad (2.259)$$

but not more than 10^6 MeV, when the radiation friction effects become appreciable. However, as in the one-dimensional case, the problem of constructing the solution beyond the light surface remains unsolved.

The second class of models also suggests the existence of the "dissipation domain" in the vicinity of the light cylinder (see Fig. 2.24). However, only the insignificant energy transfer from the electromagnetic field to particles is postulated here (Mestel and Shibata, 1994; Mestel, 1999). Otherwise, within this model, it is assumed that

- the longitudinal current is close to the critical current ($i_0 \approx 1$);
- in the vicinity of the light surface, only a small amount of the electromagnetic energy flux is transferred to the particle energy flux;

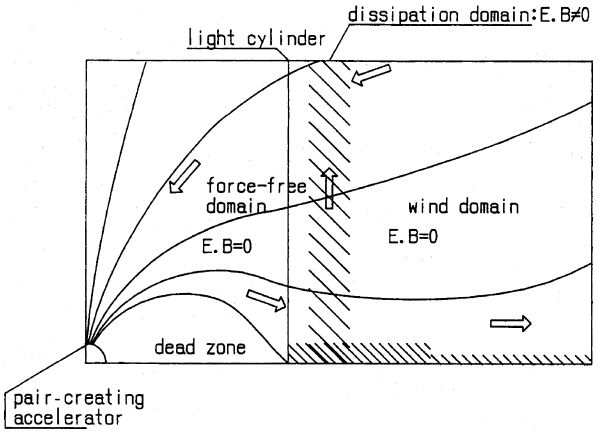

Fig. 2.24 The magnetosphere structure in the Mestel model (Mestel and Shibata, 1994). The existence of the particle acceleration region in the vicinity of the light surface is also supposed. However, only a small change in the longitudinal current (*contour arrows*) is assumed, whereas the potential drop along the magnetic field lines (and, hence, the change in the angular velocity Ω_F) was assumed to be significant but insufficient for the particle energy to change appreciably. Therefore, at large distances from the neutron star, the main energy flux is still connected with the Poynting flux

- accordingly, there is only the partial closure of the longitudinal currents circulating in the magnetosphere;
- at large distances from the neutron star, the main energy flux is still connected with the Poynting flux.

Note that in this model the properties of the transition layer were only postulated. In particular, it was assumed that in the transition layer only a small change in the longitudinal current occurs, whereas the relative change in the electric potential along the magnetic field lines (and, hence, the change in the angular velocity Ω_F) was assumed to be significant. As a result, the light surface again extended to infinity. Therefore, at large distances from the neutron star, the main energy flux was still connected with the Poynting flux.

One should stress that the basic property of the transition layer studied—the large change in the angular velocity Ω_F with a relatively small longitudinal current—is in contradiction with the properties of the acceleration region in the vicinity of the light surface. As the analysis of the two-fluid MHD equations showed (Beskin et al., 1983; Beskin and Rafikov, 2000), it is the longitudinal current rather than the electric potential that should change most rapidly in the direction perpendicular to the transition layer.

This result can be readily explained. The point is that in the vicinity of the light surface, as was already mentioned, the particle energy formally tends to infinity. As a result, the frozen-in equation is violated, which requires transition to the more exact two-fluid equations. Physically, the result is that electrons and positrons begin to accelerate in different directions along the electric field. Consequently, a strong

poloidal electric current occurs, which is generated by the entire electron–positron density $\lambda|\rho_{GJ}|/|e|$. This poloidal current results in an abrupt decrease in the toroidal magnetic field, i.e., in a decrease in the Poynting flux. As to the electric potential, its change in the layer is specified by the electric charge density proportional to the difference in the electron and positron densities only. Since in the radio pulsar magnetosphere the particle density is many orders of magnitude higher than the GJ density $n_{GJ} = |\rho_{GJ}|/|e|$, the relative change in the layer current must considerably exceed the change in the electric potential. Actually, the availability of the factor $1/\lambda$ in expression (2.258) is exactly associated with this event.

Finally, *the third class* includes models in which the light surface is absent (Lyubarskii, 1990; Bogovalov, 1997b; Contopoulos et al., 1999). Otherwise, it is assumed here that

- the longitudinal current is larger than the critical current ($i_0 > 1$);
- the light surface extends to infinity;
- the longitudinal current is closed at large distances from the light cylinder;
- at large distances from the neutron star the main energy flux is still connected with the Poynting flux.

This class of models has presently been studied quite thoroughly, though mainly for the axisymmetric case only (Goodwin et al., 2004; Gruzinov, 2005; Contopoulos, 2005; Komissarov, 2006; McKinney, 2006a; Timokhin, 2006). Only a few years ago, the new and rather fruitful efforts have been made in constructing the force-free model of the inclined rotator (Spitkovsky and Arons, 2003; Spitkovsky, 2006) (see Fig. 2.25). In particular, the existence of the surface currents flowing along the separatrix in the direction opposite to the bulk current in the region of open field lines was confirmed. It was also confirmed that for the existence of the outflowing

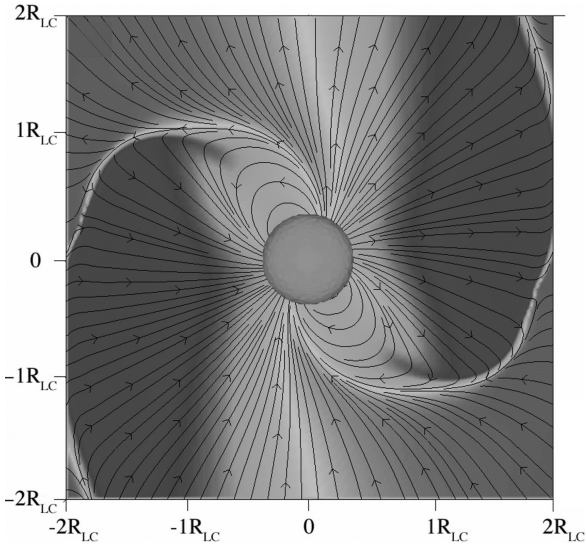

Fig. 2.25 The magnetosphere structure of the orthogonal rotator in which the light surface is absent (Spitkovsky, 2006). At large distances from the neutron star, the main energy flux is connected with the Poynting flux. Rotation axis is perpendicular to the figure plane [Reproduced by permission of the AAS, Fig. 2a from Spitkovsky, A.: Time-dependent force-free pulsar magnetospheres: axisymmetric and oblique rotators. ApJ **648**, L51–L54 (2006)]

wind, the longitudinal current density for the inclined rotator must be much larger than the local GJ one ($i_A \gg 1$). For this reason, it is not surprising that the energy losses even increase with the inclination angle χ

$$W_{\rm tot} = \frac{1}{4}\,\frac{B_0^2\Omega^4 R^6}{c^3}\left(1+\sin^2\chi\right). \tag{2.260}$$

On the other hand, since there is no restriction to the value of the longitudinal current, one fails to confirm or refute the hypothesis for the existence of the light surface in the vicinity of the light cylinder, where the efficient acceleration of particles is possible. Moreover, within this approach, it was impossible to effectively transfer the electromagnetic energy to the particle energy flux. This problem will be studied in more detail in Chap. 5.

2.7 Conclusion

As we see, the consistent theory of the radio pulsar magnetosphere is now still far from completion. One of the main problems is the insufficient potentialities of the analytical methods that fail, in the general case, to construct the solution even in the rather simple force-free approximation. Evidently, only a dozen papers dealing with this set of problems appeared in the 1990s. Attempts to formulate, in general form, the problem of the magnetosphere structure due to the particle motion in the self-consistent electromagnetic field were long beyond the available computating resources (Krause-Polstorff and Michel, 1984, 1985; Petri et al., 2002; Smith et al., 2001).

To sum up, the situation with the existence of the light surface in the pulsar magnetosphere remains unclear. The behavior of the exact analytical solutions corresponding to reasonable longitudinal currents $j_\parallel \approx$ const within the open magnetic field lines is irrational in the equatorial region outside the light cylinder. On the other hand, the numerical solutions postulating the reasonable quasispherical outflow at large distances are in disagreement with the longitudinal current that can be generated in the polar regions of the neutron star.

Thus, within the force-free approximation, it is impossible to determine the longitudinal current flowing in the magnetosphere and, hence, find the energy losses. Therefore, the force-free statement of the problem, inevitably, calls for the concretization of the medium properties on the boundary of the force-free region, be it infinity or the current sheet, which is to be included in the equatorial region in most models. As we will see, this flaw will be naturally eliminated in the full GS equation version, which takes into account that the particle mass is finite.

http://www.springer.com/978-3-642-01289-1

MHD Flows in Compact Astrophysical Objects
Accretion, Winds and Jets
Beskin, V.S.
2010, XVIII, 425 p., Hardcover
ISBN: 978-3-642-01289-1